



FACILITY FORM 802

N65 (ACCESSION NUMBER)	34910 (THRU)
104 (PAGES)	1 (CODE)
CR-54732 (NASA CR OR TMX OR AD NUMBER)	03 (CATEGORY)

# RESEARCH & DEVELOPMENT OF A HIGH CAPACITY NONAQUEOUS SECONDARY BATTERY

THIRD QUARTERLY REPORT

CONTRACT No. NAS 3-6017

prepared for

**NATIONAL AERONAUTICS AND SPACE ADMINISTRATION**

NET GROSS PRICE \$ \_\_\_\_\_

NET PRICE(S) \$ \_\_\_\_\_

Hard copy (HC) 1.00

Microfiche (MF) 75

**NASA**

**Lewis Research Center**

Space Power System Division

21000 Brookpark Road

Cleveland, Ohio

P.R. Mallory & Co. Inc.  
Laboratory for Physical Science  
Northwest Industrial Park  
Burlington, Massachusetts

## NOTICE

This report was prepared as an account of Government sponsored work. Neither the United States, nor the National Aeronautics and Space Administration (NASA), nor any person acting on behalf of NASA:

- A.) Makes any warranty or representation, expressed or implied, with respect to the accuracy, completeness, or usefulness of the information contained in this report, or that the use of any information, apparatus, method or process disclosed in this report may not infringe privately owned rights; or
- B.) Assumes any liabilities with respect to the use of, or for damages resulting from the use of any information, apparatus, method or process disclosed in this report.

As used above, "person acting on behalf of NASA" includes any employee or contractor of NASA, or employee of such contractor, to the extent that such employee or contractor of NASA, or employee of such contractor prepares, disseminates, or provides access to, any information pursuant to his employment or contract with NASA, or his employment with such contractor.

Requests for copies of this report should be referred to

National Aeronautics and Space Administration  
Office of Scientific and Technical Information  
Attention: AFSS-A  
Washington, D.C. 20546

COPY COPY

THIRD QUARTERLY REPORT

Research and Development of a High Capacity  
Nonaqueous Secondary Battery

April - June 1965

prepared for

NATIONAL AERONAUTICS AND SPACE ADMINISTRATION

August 31, 1965

CONTRACT NAS 3-6017

Technical Management  
Space Power Systems Division  
National Aeronautics and Space Administration  
Lewis Research Center, Cleveland, Ohio  
Mr. Robert B. King

P. R. Mallory & Co. Inc.  
Laboratory for Physical Science  
Northwest Industrial Park  
Burlington, Massachusetts

## TABLE OF CONTENTS

	<u>Page</u>
I. Introduction	1
A. Systems Selection	1
1. Theoretical	1
2. Experimental	1
3. Conclusions	2
B. Systems Development	3
C. Summary	4
II. Purification of Materials	5
II-A. Introduction	5
II-B. Purification by Distillation	5
II-C. Testing by Boiling Point Measurements	6
II-D. Testing by Vapor Phase Chromatography	7
II-E. Testing by Electrochemical Characterization	11
II-E-1. Electrochemical Characterization	11
II-E-2. Electrochemical Characterization: PC/LiBF <sub>4</sub>	12
II-E-3. Electrochemical Characterization: PC/LiI	23
II-E-4. Electrochemical Characterization: LiBr/PC	26
II-E-5. Electrochemical Characterization: PC/AgClO <sub>4</sub>	28
II-E-6. Electrochemical Characterization: PC/KI	33
II-E-7. Electrochemical Characterization: Morpholinium PF <sub>6</sub> /PC	36
II-E-8. Electrochemical Characterization: DMF/AgClO <sub>4</sub>	37
II-E-9. Electrochemical Characterization: LiCl/DMF, LiBF <sub>4</sub> /DMF	38
II-E-10. Electrochemical Characterization: Conclusions	42
II-F. Effect of Impurities: Molecular Sieve Treatment	44
II-G. Time Stability Tests	47

TABLE OF CONTENTS (Cont'd)

	<u>Page</u>
III. Screening Program	48
III-A. Chemical Compatibility	48
III-B. Electrochemical Reversibility	48
III-B-1. Electrochemical Reversibility: Anodes	48
III-B-2. Electrochemical Reversibility: Cathodes	61
III-C. Solubility Studies	79
III-D. Electrolyte Conductivity	80
III-E. Kinetic Studies	82
IV. Summary and Conclusions, Future Work	85
Appendix I: Hypothetical Cell Model	87
Appendix II: EMF Measurements in Propylene Carbonate	89
Appendix III: Cathode Support Structure	91

## LIST OF TABLES

	<u>Page</u>
1. V.P.C. Analysis of Unpurified Propylene Carbonate	8
2. V.P.C. Analysis of Propylene Carbonate for Water and Propylene Oxide	10
3. Lithium Anodic Utilization: Substrate Effects	55
4. Discharge of AgCl in Aqueous Solution	63
5. Discharge of AgCl in Propylene Carbonate	65
6. Discharge of AgCl in Propylene Carbonate (Electrode Capacity = $8.5 \text{ mA-hr cm}^{-2}$ )	65
7. Discharge of AgCl in BL, DMF, and AN	66
8. Discharge of $\text{AgNO}_3$ in Butyrolactone	67
9. Discharge of $\text{CuF}_2$ in Aqueous $\text{LiClO}_4$	70
10. Discharge of $\text{CuF}_2$ in Propylene Carbonate (1 M $\text{LiBF}_4$ )	71
11. Discharge of $\text{CuF}_2$ (Ag Additive) in Propylene Carbonate	74
12. Discharge of $\text{CuF}_2$ in Other Electrolytes	77
13. Solubility Studies	80
14. Equivalent Conductance in Propylene Carbonate	81

## LIST OF FIGURES

		<u>Page</u>
1.	Vapor Phase Chromatograph of Propylene Carbonate	9
2.	Potentiostatic Cathodization in Propylene Carbonate	14
3.	Polarization Curve for 0.01 M $\text{LiBF}_4$ - Propylene Carbonate	15
4.	Cathodic Chronopotentiometry in 0.01 M $\text{LiBF}_4$ - Propylene Carbonate	18
5.	Cathodic Chronopotentiometry in $\text{LiBF}_4$ - Propylene Carbonate	21
6.	Cathodic Chronopotentiometry in $\text{LiBF}_4$ - Propylene Carbonate	22
7.	Cathodic Chronopotentiometry in $\text{LiI}$ - Propylene Carbonate	25
8.	Cathodic Chronopotentiometry in $\text{LiBr}$ - Propylene Carbonate	27
9.	Cathodic-Anodic Cycling in $\text{LiBr}$ - Propylene Carbonate	29
10.	Cathodic-Anodic Cycling in $\text{LiBr}$ - Propylene Carbonate	30
11.	Cathodic Chronopotentiometry in $\text{AgClO}_4$ - Propylene Carbonate	31
12.	Cathodic Chronopotentiometry in $\text{KI}$ - Propylene Carbonate	35
13.	Cathodic Chronopotentiometry in $\text{LiBF}_4$ - Dimethylformamide	39
14.	Cathodic Chronopotentiometry in $\text{LiCl}$ - Dimethylformamide	41
15.	Cathodic Chronopotentiometry in $\text{LiBF}_4$ - Propylene Carbonate (Molecular Sieve Treatment)	46
16.	Anodic Discharge of Bulk Lithium in Propylene Carbonate	50
17.	Deposition of Lithium on Beryllium and Platinum	56
18.	Deposition of Lithium on Beryllium, Platinum, Aluminum and Copper	57

LIST OF FIGURES (Cont'd)

		<u>Page</u>
19.	Deposition of Lithium on Beryllium and Platinum	59
20.	Lithium Deposition on Beryllium and Platinum	60
21.	Discharge of $\text{CuF}_2$	69
22.	Discharge of $\text{CuF}_2$	72
23.	Discharge of $\text{CuF}_2$	73
24.	Discharge of $\text{CuF}_2$	75
25.	Discharge of $\text{CuF}_2$	76
26.	Experimental Electrode Configuration	92



## Research and Development of a High Capacity Nonaqueous Secondary Battery

### SUMMARY

We have begun an examination of the role of impurities in influencing the electrochemical behavior in nonaqueous electrolytes. The conditions of vacuum distillation of propylene carbonate, butyrolactone and dimethylformamide are reported. The results obtained with the gas chromatographic analysis of propylene carbonate are still tentative, but clearly a variety of impurities other than water are present and may influence electrochemical behavior. Molecular sieve treatment of propylene carbonate solutions of lithium salts is not satisfactory since exchange between the sodium ions in the sieve and lithium ions in the solution occurs.

The lack of general information concerning electrochemical behavior in nonaqueous electrolytes has led to the examination of a variety of propylene carbonate and dimethylformamide solutions. The cathodic reduction of lithium salts to form the metal deposit is not a straightforward process. It is expected that the development of a useful lithium secondary electrode will require more detailed basic research and we have anticipated some of the problems to be examined by studying cathodic behavior in various lithium salt solutions. The behavior is generally independent of the anion, but is markedly dependent on the nature of the substrate. Platinum, silver, aluminum, beryllium, cobalt, nickel, and copper substrates have been used in this work. Other solutes have been examined for comparison: silver perchlorate, potassium iodide, and morpholinium hexafluorophosphate solutions. Under the proper conditions as much as 95% efficiency for lithium deposition can be obtained. This is encouraging, and suggests that further study of lithium ion reduction in

particular and cathodic reduction in general will lead to a clear definition of the optimum conditions for a cyclable lithium electrode.

A primary objective of our work is the development of a cyclable cathode. The cyclability will doubtless be dependent on the electrolyte and we have begun a screening of electrolytes by simply studying the cathodic discharge of  $\text{CuF}_2$  in various electrolytes. For comparison, we have also studied the cathodic discharge of  $\text{AgCl}$  electrodes. There are marked and surprising differences in discharge efficiency in the various electrolytes. The causes for this are not known. The results indicate that of the four solvents, propylene carbonate, dimethylformamide, butyrolactone, and acetonitrile, propylene carbonate is the least satisfactory solvent, since discharges of both  $\text{CuF}_2$  and  $\text{AgCl}$  seem, in general, to be less efficient. The efficiency is also dependent on the nature of the solute and, in particular, potassium salt solutions allow only negligible discharge of both  $\text{CuF}_2$  and  $\text{AgCl}$ . The development of an efficiently dischargeable cathode is a prerequisite to the development of secondary electrodes and, we believe, a cathode which can discharge with stoichiometric, thermodynamic, and kinetic efficiency will be inherently cyclable. Therefore, we consider the investigation of cathodic discharge to be of continuing importance.

Research and Development of a High Capacity  
Nonaqueous Secondary Battery

ABSTRACT

34910

Electrochemical behavior in electrolytes employing as solvents, propylene carbonate, butyrolactone, dimethylformamide, and acetonitrile, has been examined. The cathodic reduction of silver chloride and cupric fluoride electrodes has been studied in these electrolytes. The cathodic behavior observed at constant current on various metal surfaces has been studied in propylene carbonate and dimethylformamide solutions of several salts with primary emphasis on lithium salts and on the ability to electrodeposit lithium. Results of preliminary gas chromatographic analysis of propylene carbonate are reported.



## I. INTRODUCTION

### A. Systems Selection

1. Theoretical. Lithium is theoretically the best anode for incorporation in high energy density cells.

A variety of cathodes with high theoretical energy density exist. Many of these can be eliminated as probably being impracticable for secondary cell operation. For example, it is doubtful that salts of a metal in the +3 or higher oxidation state can be reduced satisfactorily to the metal and subsequently re-oxidized on charge to the initial state. Other cathodes with high theoretical energy density exist in a physical form which is unsuitable for incorporation in practical cells. Realistically, one is left with the salts of metals in the +2 oxidation state. Of all such salts,  $\text{CuF}_2$  has the highest theoretical energy density.

The electrolyte serves such a complex function that there is no theoretical basis as yet for selecting suitable electrolytes. We do not believe conductivity is a primary criterion.

2. Experimental. In the best results obtained thus far lithium has been deposited from 0.1 M  $\text{LiBF}_4/\text{P.C.}$  solutions at  $1.26 \text{ mA cm}^{-2}$  on beryllium at  $2000 \text{ mC cm}^{-2}$  and subsequently re-anodized with over 90% efficiency. As reported in the Second Quarterly Report it was possible to deposit lithium at  $25 \text{ mA cm}^{-2}$  from 1 M  $\text{LiBF}_4/\text{P.C.}$  on platinum for  $6000 \text{ mC cm}^{-2}$  and subsequently discharge the deposit at  $10 \text{ mA cm}^{-2}$  with 78% efficiency. As discussed in the following section, we believe a desirable objective is an electrode with a capacity of  $36,000 \text{ mC cm}^{-2}$ , capable of operation at  $10 \text{ mA cm}^{-2}$ . The closest approach to this objective was described in the Second Quarterly Report, where the deposition of lithium from 1 M  $\text{LiBF}_4/\text{P.C.}$  on platinum at  $25 \text{ mA cm}^{-2}$  for  $30,000 \text{ mC cm}^{-2}$ , subsequent anodic discharge at  $20 \text{ mA cm}^{-2}$  with 47%

efficiency was reported. Such results are as encouraging as they are surprising.

No other anode has been reported to display equal or superior performance. We have not observed any deposition of aluminum, magnesium, or beryllium from the solvents under current consideration. Sodium and potassium, while they may be deposited, exhibit performance, so clearly inferior to that of lithium, that detailed studies have not been made.

Results on the  $\text{CuF}_2$  cathode are less encouraging. In the best results we have obtained, a  $\text{CuF}_2$ -acetylene black mix electrode with a theoretical capacity of  $30,000 \text{ mC cm}^{-2}$  was discharged at  $4.3 \text{ mA cm}^{-2}$  with 50% efficiency in  $\text{LiBF}_4/\text{B.L.}$  However, cyclability has not yet been observed with the  $\text{CuF}_2$  electrode. The fact that the discharge curves for  $\text{CuF}_2$  are usually quite flat, suggests that the reduction proceeds in a relatively straightforward manner, without mechanistic complications. We do believe that the  $\text{CuF}_2$  electrode is not inherently irreversible and that cyclability can and must be induced in some fashion.

3. Conclusions. Lithium remains the anode of choice. However, the behavior of the lithium electrode is not straightforward. The process occurring when a lithium salt solution is cathodized is not simply the one electron reduction of a lithium ion to the metal. Improvement in the performance of the lithium electrode will most efficiently come from a better understanding of the deposition process. This involves a good deal more general information about cathodic behavior in non-aqueous electrolytes. During this quarter we have attempted to approach this understanding by focusing attention on the effects of the electrode substrate and on the role of impurities. We do not believe satisfactory answers to the question of what happens when lithium is deposited will be found without much more intensive basic research and we have sought to anticipate such research by simply describing the phenomena as lucidly as

possible, without undue interpretation.

Cyclability should be inherent in cathodes which are reduced in a straightforward fashion. The conditions necessary for inducing cyclability are not yet clear, and the problem is confounded by the fact that there is yet no clear understanding of what happens even on initial discharge. Two important questions exist. First, how is the salt reduced? That is, what are the general mechanisms by which an insoluble salt may be cathodically reduced, and what are the specific phenomena attending reduction of the various salts of interest? Secondly, what happens to the anion (oxide, fluoride, etc.) on reduction? Is the anion trapped, through precipitation, within the porous cathode? We believe a clear understanding of the processes which obtain during reduction of cathode salts will almost automatically indicate the conditions necessary for inducing cyclability.

During this quarter we have simply concentrated on the discharge process. Discharges have been conducted on both  $\text{CuF}_2$  and  $\text{AgCl}$  in a variety of electrolytes.  $\text{AgCl}$  has been used as a type of reference system suitable for the investigation of cathode salt reduction in non-aqueous electrolytes. Both electrodes show pronounced variations in discharge behavior with different electrolytes. Again, at this time, we simply seek to describe the phenomena as clearly as possible, without undue interpretation.

We recognize that a number of other cathodes should be examined but believe, for the present, it is more desirable to investigate in some detail only one or two specific cathodes in an attempt to understand the processes occurring.

#### B. Systems Development

It is unrealistic to undertake a detailed examination of electrodes in half-cell studies in excess electrolyte and not consider the modifications that may be required in the type of environment which exists in an operating cell.

In Appendix I we describe what we believe to be a reasonable model for a high energy density non-aqueous cell. This model consists of an anode and a cathode, each with a capacity of  $10 \text{ mA-hr cm}^{-2}$ , capable of discharge at the one-hour rate ( $10 \text{ mA cm}^{-2}$ ). There is yet no apparent reason why such a model is impracticable, but we believe it is essential that the limitations of this model be found to guide future research into those areas which are, indeed, most important.

We use this cell model as a standard against which to measure the performance of electrodes. For this model to operate without excess weight it is also required that the electrolyte be such that ions can effectively be transported from one electrode to the other. Whether there are limitations to the facility with which this process can occur remains to be learned, but it is a process which must be considered in systems development. It is an important environmental restriction which may greatly modify the operation of individual electrodes.

### C. Summary

The results obtained to date in a screening program designed to investigate electrolytes and their effects on electrode performance are described. Electrolyte impurities will, of course, influence electrode behavior and the results obtained for the vacuum distillation of propylene carbonate, dimethylformamide, and acetonitrile and the vapor phase chromatographic analysis of propylene carbonate are described. Cathodic reduction in propylene carbonate and dimethylformamide are described for a number of electrolytes and the phenomena of surface effects and background reduction described. The discharge of  $\text{CuF}_2$  and  $\text{AgCl}$  in various electrolytes is discussed, and significant variations in the different electrolytes noted.

## II. PURIFICATION OF MATERIALS

II-A. Introduction. Impurities present in solvents, solutes, and the materials of electrode construction may seriously affect the validity of data, particularly in any screening examination. The co-reduction of impurities may be the sole source of lithium deposition inefficiency. Chemical compatibility studies may reflect nothing more than the rate of impurity attack, for example, on active metals. The evident solubility of cathode salts may reflect spurious impurity effects.

The procedure we seek to follow is:

- (1) Purify solvents by distillation.
- (2) Determine the nature and quantities of impurities and the efficacy of distillation and molecular sieve treatment in removing these impurities.
- (3) Determine the impurities in the total electrolyte -- solvent plus solute.
- (4) Characterize the systems electrochemically to establish tentative hypotheses relating impurities to electrochemical propensity.
- (5) Investigate other methods of purification.

II-B. Purification by distillation. During this quarter three solvents have been distilled, and the conditions of distillation recorded. These solvents were propylene carbonate, dimethylformamide, and acetonitrile.

As previously described, distillation is conducted using a 90-cm, jacketed, electrically heated column packed with Berl saddles and fitted with a water jacketed receiver. About three liters of solvent are placed in the pot and the still is operated at total reflux until the pressure and temperature become constant at the distilling head. The initial, low-boiling material is collected in a cold trap and discarded. The specific conditions of distillation



for the three solvents are described below.

Propylene carbonate (B.P. =  $241.7^{\circ}\text{C}$ ): In most of our previous work propylene carbonate has been distilled at 1 mm Hg. Under these conditions the temperature at the distilling head is about  $65^{\circ}\text{C}$ ; the pot temperature is maintained at  $130\text{--}150^{\circ}\text{C}$ . During the past quarter distillation has been conducted at a higher pressure and temperature, in the hope that cleaner separation might be effected. The pot temperature was  $130\text{--}150^{\circ}\text{C}$ . The pressure was maintained at 4-5 mm Hg. throughout most of the run. When distillation began, the pressure at the distilling head was 6 mm Hg and the temperature  $76.5\text{--}77^{\circ}\text{C}$ . About 65 ml. of distillate came over under these conditions. Thereafter the temperature rose quite sharply to  $92\text{--}99^{\circ}\text{C}$ , and remained there for the rest of the distillation, the pressure fluctuating between 4 and 5 mm Hg. Successive fractions of distillate were collected and will be analyzed by V.P.C.

Dimethylformamide (B.P. =  $153^{\circ}\text{C}$ ): Total reflux was continued until the temperature at the distilling head remained constant at  $24\text{--}30^{\circ}\text{C}$  at about 4 mm Hg. The pot temperature was about  $65^{\circ}\text{C}$  for the entire distillation. After the first 50 ml. of distillate were collected the pressure was increased to 8-9 mm Hg and the temperature remained at  $39\text{--}50^{\circ}\text{C}$ . for the rest of the distillation. Successive fractions were collected and will be analyzed by V.P.C.

Acetonitrile (B.P. =  $81.6^{\circ}\text{C}$ .): Distillation was conducted at atmospheric pressure. The pot temperature was  $83\text{--}84^{\circ}\text{C}$  and the temperature at the distilling head  $81\text{--}82^{\circ}\text{C}$ . Successive fractions were collected and will be analyzed by V.P.C.

II-C. Testing by Boiling Point Measurements. Apparatus for accurate boiling point determinations has been received, but no data have yet been collected.

II-D. Testing by Vapor Phase Chromatography. During this quarter a Perkin-Elmer Model 801 Gas Chromatograph has been received and put into operation.

A pair of matched, stainless steel columns packed with 80 mesh Chromasorb W coated with 1.5% SE-30 silicon rubber were employed, using helium carrier gas. To establish the capability of the hot wire detector and to test the resolving power of the columns in determining water three solutions were prepared in the propylene carbonate solvent: 0.05, 0.5, and 1.1 M in water. A wide variety of experimental conditions were tried, in which we varied the injection temperature, the detector temperature, the column temperature and programming, and the sample size. The optimum conditions were:

Helium flow	20 ml/min
Hot wire current	200 mA
Injector temperature	250° C
Detector temperature	250° C
Column temperature	100-250° C at 32°/min
Sample size	ca. 2 microliters

Under these conditions for the 1.1 M solution three peaks were obtained having retention times of 20, 33, and 60 sec. The first was an unidentified component of the propylene carbonate, the second was water, and the third, which exhibited an enormous plateau and pre-tailing was the propylene carbonate. In going from the 1.1 M water solution to the 0.05 M solution, the water wave tended to shift to longer retention times and became a shoulder on the front of the propylene carbonate wave. This resolution was unsatisfactory and other types of packing material were examined.

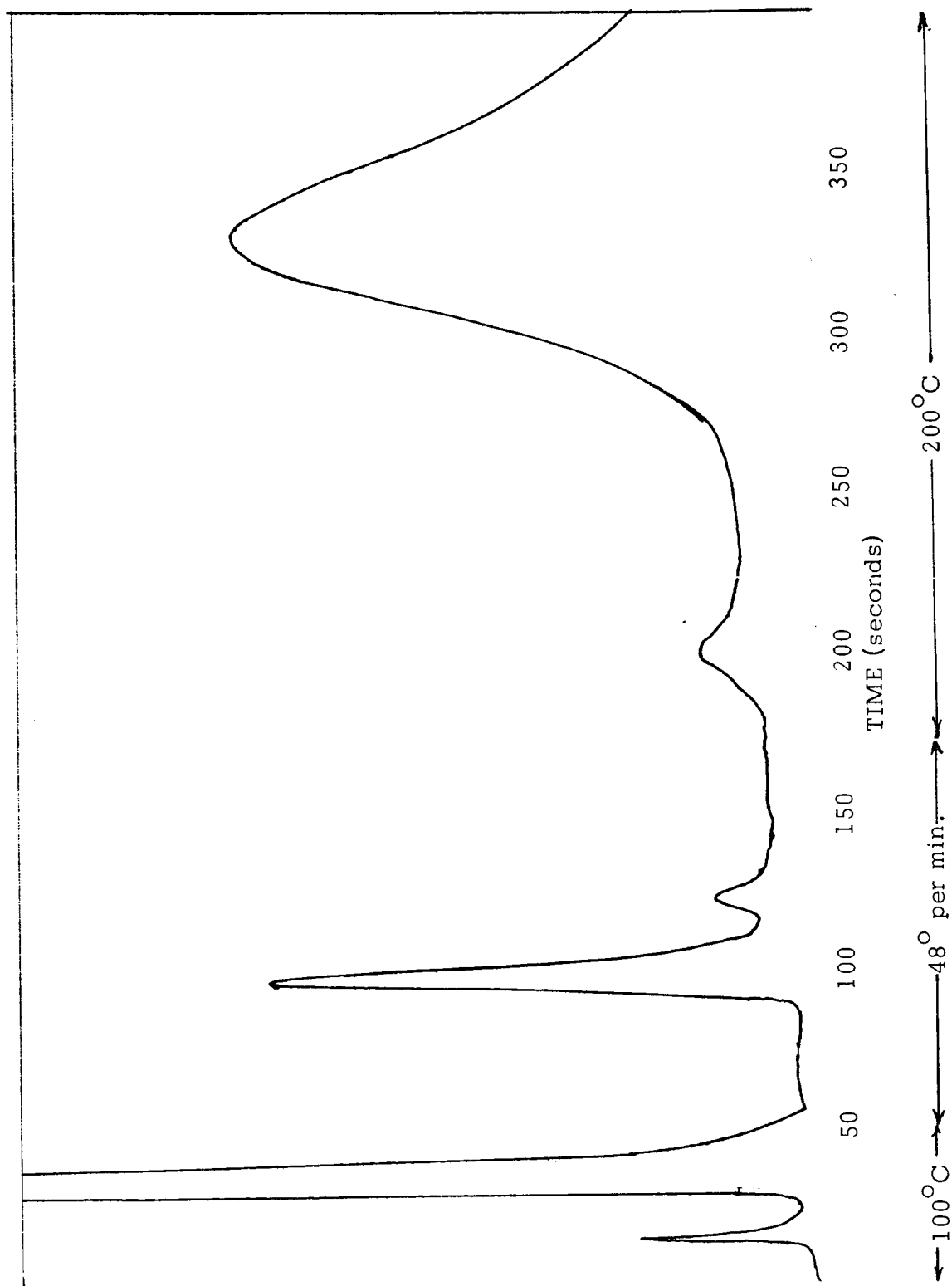
Matched stainless steel tubes pre-packed with 10% carbowax K1540 on No. 6 mesh Teflon powder were used. Initial examination was conducted on unpurified propylene carbonate. This material, received in 3 kg

containers from Matheson Coleman and Bell was described as having a boiling point of 108-110°C at 10 mm; no further designation was applied. Initial examination gave excellent results with good separation and little tailing of the peaks. Two types of procedures were at length accepted: (1) isothermal operation at a column temperature of 200°C for fast, qualitative scans, and (2) isothermal operation at 100°C for 50 sec., followed by a programmed increase of column temperature at 48°/min up to 200°C to obtain maximum resolution of the various components. A typical run is shown in Figure 1. The weight percent is approximately proportional to the area of the wave. In Table 1 below are shown the results obtained on the as-received propylene carbonate.

Table 1  
V.P.C. Analysis of Unpurified Propylene Carbonate

Component No.	Retention Time at 200°C Isothermal	Retention Time for programmed run	Approximate weight percent
1	11	14	0.02%
2	16	31	0.75%
3	21	96	0.1%
4	46	121	0.04%
5	46	197	0.08%
6	93	329	1.0%
7	at foot of 8	--	--
8	270-274	--	98%

The next problem was the identification of the major impurities. The direct addition of CO<sub>2</sub> enhanced the area of peak 1. The direct addition of water enhanced the area of peak 3. The direct addition of propylene oxide enhanced the area of peak 2. Chromatograms were also run using the



VAPOR PHASE CHROMATOGRAPH OF PROPYLENE CARBONATE

Figure 1

hydrogen flame detector, which is not sensitive to water and carbon dioxide. These chromatograms did not show the presence of peaks 1 and 3, thus lending support to their tentative identification as CO<sub>2</sub> and water respectively. Other possible impurities were added and the chromatograms run. Isopropyl alcohol, propionaldehyde, and propiolactone gave new peaks, indicating that their presence in the initial material is improbable. Other materials will be added when received. We are particularly interested in component 6, which is the major impurity.

Calibration curves for the V.P.C. analysis of water in PC were prepared by analyzing synthetic mixtures of water in distilled propylene carbonate. Concentrations of 1, 0.5, 0.1, and 0.05 weight percent were examined at four injection volumes, 0.4, 0.8, 4 and 8 microliters. Linear plots of weight percent water versus peak area were obtained. Calibration curves for propylene oxide were similarly prepared. In Table 2 below are shown the results of the subsequent analyses using these calibration curves and estimating the weight percent of component 6 directly from the area. The "vacuum distilled" propylene carbonate used in obtaining these results had been standing in a closed flask for over a month; thus, we have little confidence that the results are more than tentative.

Table 2

V.P.C. Analysis of Propylene Carbonate  
for Water and Propylene Oxide

Sample	Water	Propylene Oxide	Component 6
P.C. (as delivered)	0.086%	0.50%	0.43%
P.C. (vacuum distilled, stood for one month)	0.04%	0.34%	none
P.C. (as delivered, treated by long standing with Molecular Sieves, Linde 4A)	0.028%	0.45%	0.60%
P.C. (vacuum distilled, stood for one month, then treated briefly with molecular sieves.)	0.049%	0.002%	0.19%

As we acquire more familiarity with this technique, we expect these evident discrepancies to be resolved.

Vapor phase chromatography has proved successful in separating the various impurities in propylene carbonate. It can be used to measure the water content and other impurities. When the identification of all the impurities in propylene carbonate is complete, the technique will be used for the analysis of other solvents and, finally, of solvent-solute systems. To the degree that various impurities are found to be deleterious, vapor phase chromatography will be used to investigate the efficacy of different methods of purification.

## II-E. Testing by Electrochemical Characterization

### II-E-1. Electrochemical Characterization: Introduction

We seek, in our screening program, an answer to the question: "What are the relative abilities of various solvents to allow lithium electrodeposition?"

The orthodox answer would be that if the cathodic decomposition potential of the solvent is more negative than that of the lithium species in solution, lithium deposition will occur. Further, the relative ability of solvents to support lithium deposition should increase as their cathodic decomposition potentials are more negative.

Such an answer is invalid. As has been clearly pointed out by Foley<sup>(1)</sup>, the very term, "decomposition potential", is ambiguous and derives from the nature of the experiments performed in the early days of electrochemistry. The concept of a "minimum decomposition potential"<sup>(1)</sup>,

---

(1) Foley, R. T., Swinehart, J. S., and Schubert L., "Investigation of Electrochemistry of High Energy Compounds in Organic Electrolytes", April 1965, NASA Research Grant NGR 09-003-005

defined as "the potential, anodic or cathodic, required to maintain a current density of the arbitrary value of  $0.1 \text{ mA cm}^{-2}$ " is, we believe, quite useful. Unfortunately, it has been our experience that such a minimum decomposition potential cannot, in fact, be measured. An "effective minimum decomposition potential" may be measured, but this appears to have no correlation with the ability of the electrolyte to tolerate lithium electrodeposition.

The difficulties in solving this problem arise, we believe, from a combination of surface effects, impurities, and the complex nature of the electrode reactions. To date, we have no evidence that at least three solvents, propylene carbonate, butyrolactone, and dimethylformamide, are not equally satisfactory for use with lithium electrodes. Any variations observed are not, we believe, ascribable to inherent solvent characteristics and may, indeed, reflect nothing more than varying impurity contents.

At this time, our specific objective is to present a clear phenomenological description of what actually does happen in various electrolytes during cathodization. Thus, we do not concentrate only on lithium systems, but also on other electrolytes in order to obtain as full a description as possible.

The following propylene carbonate electrolytes have been investigated during this quarter:

PC/LiBF <sub>4</sub> (0.01 - 0.06 M)	PC/KI (0.1 M)
PC/LiBr (0.10 M)	PC/Morpholinium PF <sub>6</sub> (0.25M)
PC/LiI (0.09 M)	DMF/LiBF <sub>4</sub> (0.1 M)
PC/AgClO <sub>4</sub> (0.03 M)	DMF/LiCl (0.1 M)
	DMF/AgClO <sub>4</sub> (0.1 M)

#### II-E-2. Electrochemical Characterization: PC/LiBF<sub>4</sub>

Vacuum distilled propylene carbonate was made 0.01 M in

LiBF<sub>4</sub>. This low concentration was selected as probably being less than the concentration of impurities in the electrolyte. A series of electrochemical measurements were performed, as described below. Thereafter portions of solid LiBF<sub>4</sub> were added to make the solution 0.02, 0.03, 0.04, and 0.06 M in LiBF<sub>4</sub>, and similar electrochemical measurements performed after each addition.

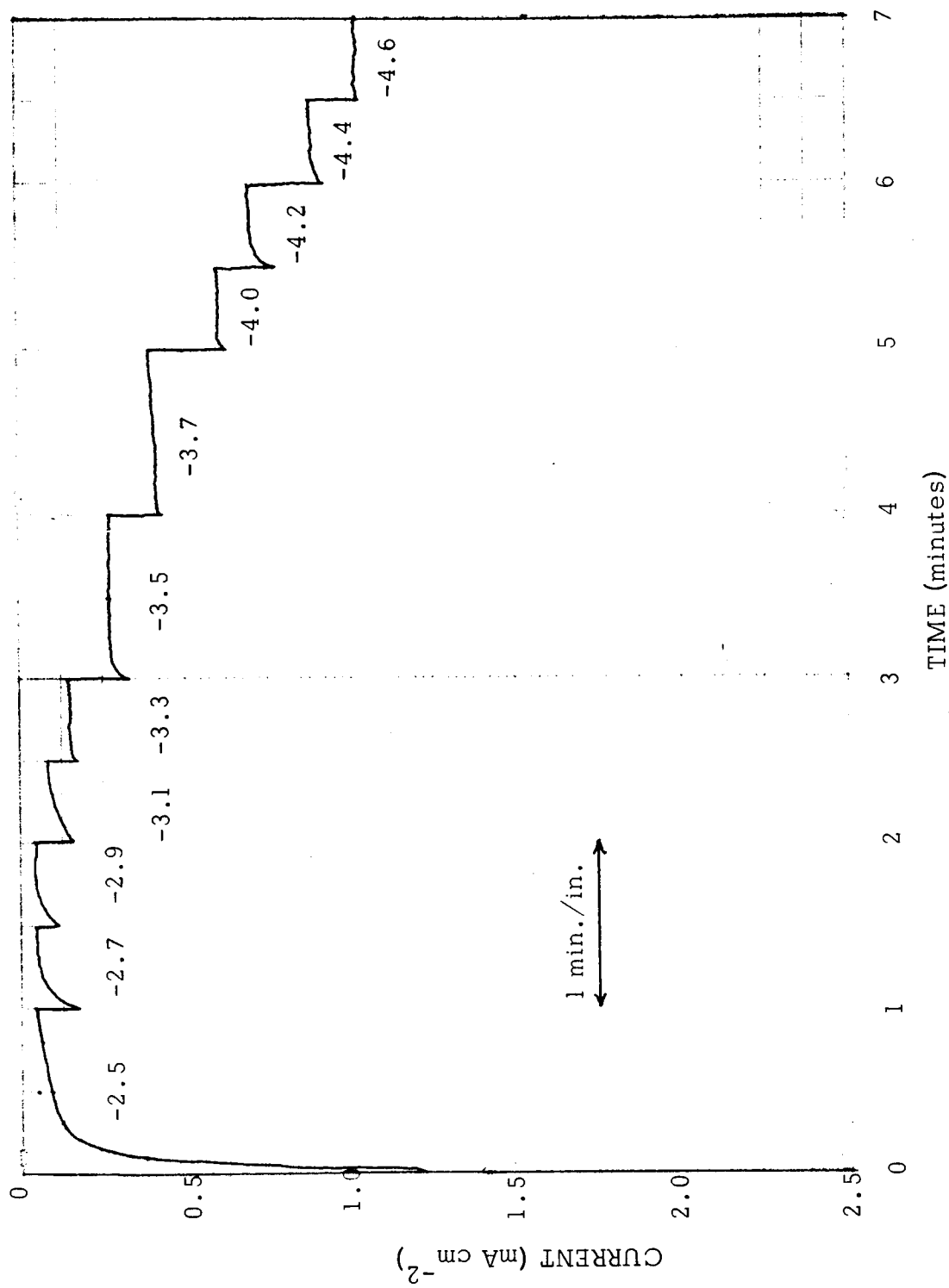
In Figure 2 is shown an actual trace of the results obtained when a freshly polished platinum disc electrode (0.2 cm<sup>2</sup>) was cathodized potentiostatically, using the Wenking Potentiostat, and the resultant current recorded. This is the raw data from which the polarization curve is obtained.

In Figure 3 is shown the polarization curve, a plot of current density versus the corrected potential. The correction for the potential is made as follows. As described in some detail in the First Quarterly Report the iR drop included in the measured potential between the working electrode disc and the silver electrode disc is given by:

$$iR \text{ (V)} = i \text{ (A cm}^{-2}\text{)} \cdot R \text{ (ohm-cm)} \cdot d_L \text{ (cm)}$$

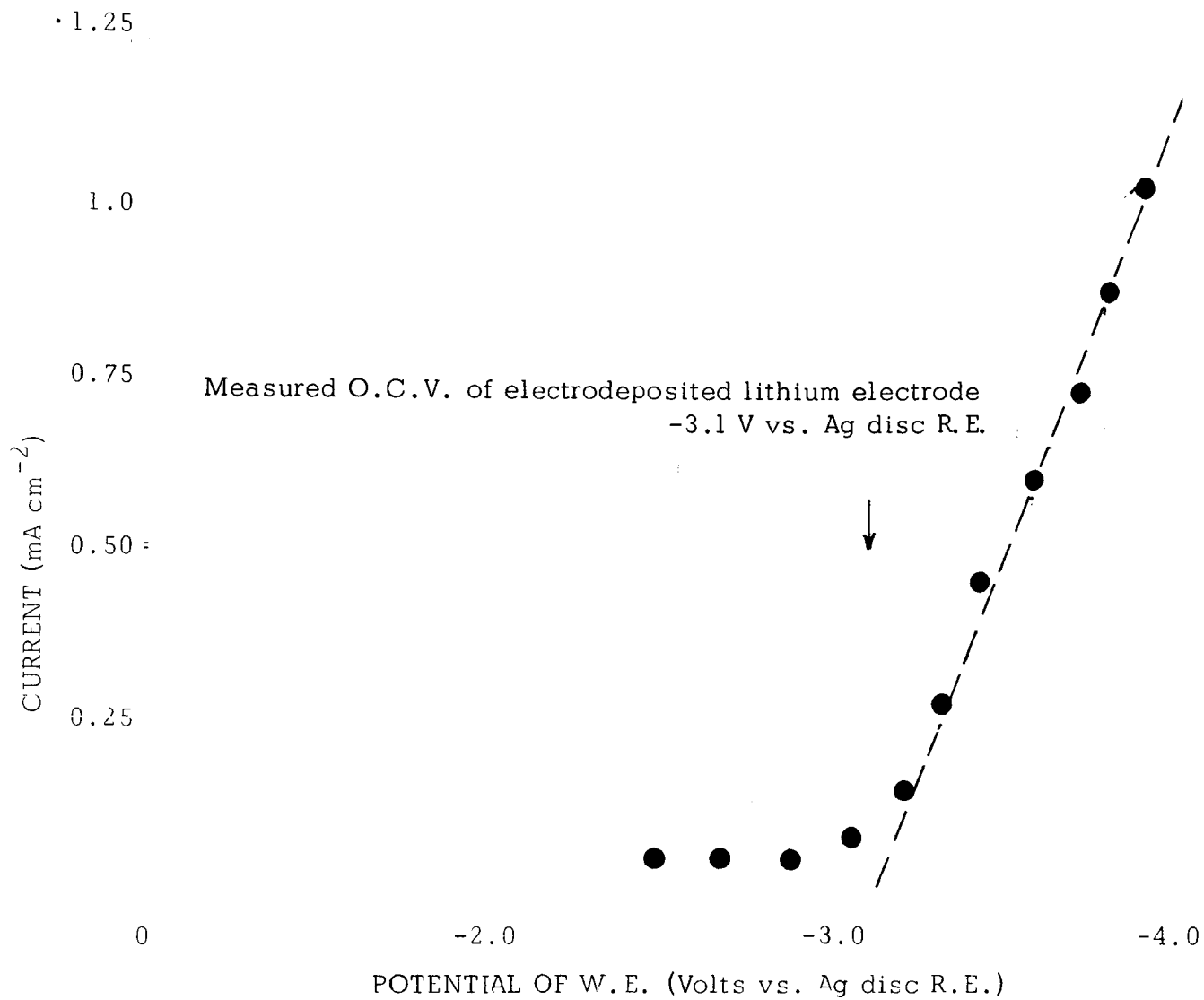
where  $i$  is the measured current density,  $R$  is the measured specific resistance, and  $d_L$  is an effective length corresponding to the distance between the tip of a Luggin capillary and the surface of the working electrode. This effective distance must be measured experimentally and, as discussed in the First Quarterly Report, was found to be 0.157 ( $\pm 5\%$ ) cm for the type of geometry employed in our systems. The data shown in Figure 2 have been corrected in this manner, using the final value of the observed current immediately before going to the next higher potential. As an example, the final measurements made at -4.6 V yield a current density of  $1.05 \times 10^{-3}$  A cm<sup>-2</sup>. The specific resistance was 4340 ohm-cm, thus an iR drop of 0.71 V is calculated and this, subtracted from the measured potential gives the corrected potential of





POTENTIOSTATIC CATHODIZATION IN PROPYLENE CARBONATE

Figure 2



POLARIZATION CURVE FOR 0.01 M  $\text{LiBF}_4$  - PROPYLENE CARBONATE

Figure 3

-3.89 V. The other data in Figure 2 have been similarly corrected to give the results shown in Figure 3.

When the measurements were discontinued, a deposit of lithium was observed on the working electrode. The open circuit potential of the lithium deposited working electrode was -3.1 V versus the silver disc reference electrode.

We do not consider data of the type shown in Figure 3 to be a reliable reflection of the electrochemical properties of the systems. In particular, we focus attention on the "background current", that current observed before lithium deposition (i.e., at potentials more positive than -3.1 V vs. Ag disc R.E.). The observed value, about  $0.05 \text{ mA cm}^{-2}$ , is, we believe, unreasonably low. This conclusion is based on the following reasoning. If the background reduction is that of some soluble, electroreducible, impurity, we may estimate the concentration of this material in the solution. Our previous work in propylene carbonate solutions indicates that, in stirred solution, the limiting current is related to the concentration of reducible material thus:

$$i \text{ (mA cm}^{-2}\text{)} \cong (100) \text{ (Conc. in M l}^{-1}\text{)} (n \text{ electrons})$$

If, for example, this background material were water, undergoing a two-electron reduction, this would correspond to a concentration of water of  $0.05/100 = 5 \times 10^{-4} \text{ M}$ . For propylene carbonate with a density of  $1.2 \text{ g cm}^{-3}$ , this is a concentration of:

$$\text{Wt \% water} = \frac{(5 \times 10^{-7} \text{ M cm}^{-3}) (18 \text{ g M}^{-1})}{1.2 \text{ g cm}^{-3}} = 7.5 \times 10^{-4} \%$$

or 7.5 parts per million, by weight. We believe 100 parts per million to be a more reasonable expectation, and conclude that the background reduction does not correspond to the diffusion limited reduction of water.

Furthermore, we have consistently found that, in propylene carbonate lithium salt solutions, this background current does not remain constant with time, but steadily diminishes. Thus, true steady state conditions are not observed. In those cases where steady state limiting currents are observed, we have found that, in stirred solution, the steady state situation is obtained within seconds after commencing electrolysis. Finally, the oscillations about an average steady state current, customarily observed for reductions on solid electrodes in stirred solution,<sup>(2)</sup> are not observed for the background reduction.

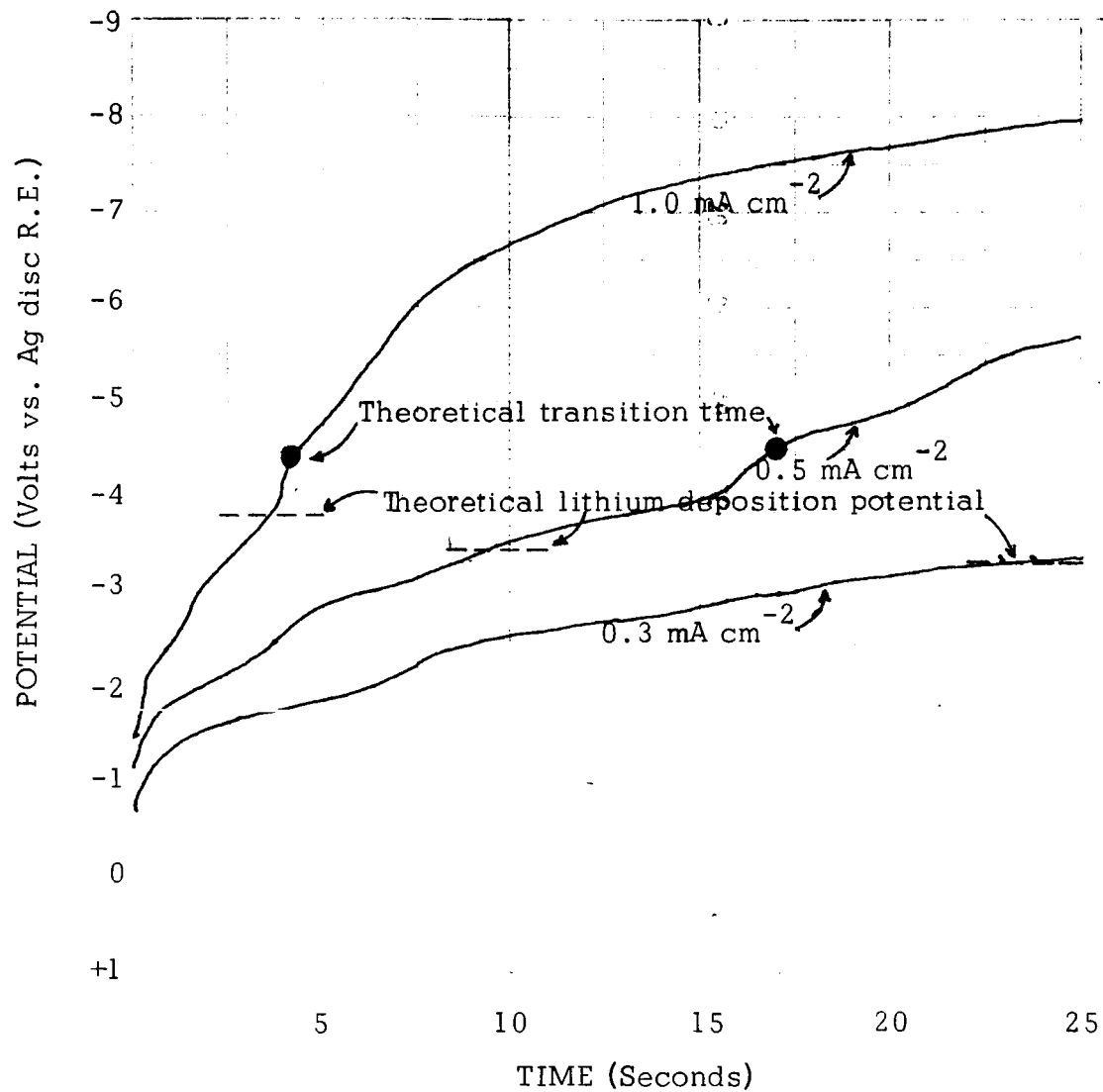
To summarize, though potentiostatic, steady state measurements constitute a classical electrochemical technique, we do not believe the results are interpretable in terms of a diffusion limited process and the observed currents cannot be related to impurity levels. Recourse must be had to alternative electrochemical techniques.

Chronopotentiometry has been extensively used by us in our work. Chronopotentiograms were run on freshly polished platinum disc electrodes at 1, 0.5, and 0.3 mA cm<sup>-2</sup>. Typical results are shown in Figure 4. These are actual traces of the chronopotentiograms and have not been corrected for iR drop, which is calculated to be 0.70, 0.35, and 0.21 V respectively at 1, 0.5, and 0.3 mA cm<sup>-2</sup>.

What information do such chronopotentiograms convey? First, it will be observed that considerable reduction occurs at potentials positive to the lithium deposition potential. The lithium deposition potential has been calculated by adding the iR drop calculated for the separate current densities to the observed open circuit potential of the deposited lithium electrode of -3.1 V. The amount of background reduction is obtained by multiplying

---

(2) Vetter, K. J. *Elektrochemische Kinetik*, Springer-Verlag, Berlin, 1961, pp. 306- 308.

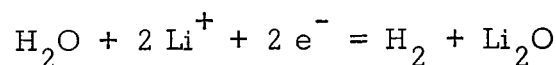
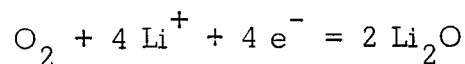


CATHODIC CHRONOPOTENTIOMETRY IN 0.01 M LiBF<sub>4</sub> - PROPYLENE CARBONATE

Figure 4

the current by the time required to reach the lithium deposition potentials and is about 2.5, 4.5, and 6.6 mC cm<sup>-2</sup> respectively for reductions at 1, 0.5, and 0.3 mA cm<sup>-2</sup>. A monomolecular layer of material on an electrode surface (e.g., PtO) has a capacity of about 0.2 mC cm<sup>-2</sup>. Nevertheless, considering the possible surface roughness (Note: the electrodes were polished to a mirror finish with 1 micron alumina) it is quite possible that this background reduction is merely that of an adsorbed layer of oxygen.

Secondly, it is interesting to compare the observed "transition times" with those theoretically anticipated. In the past we have found that, in propylene carbonate-lithium salt solutions, a transition time is always observed for which the product,  $iT^{1/2}$  (in mA cm<sup>-2</sup>), is about 200 times the concentration of the lithium salt (in M l<sup>-1</sup>). For a 0.01 M LiBF<sub>4</sub> solution one would therefore expect a transition time at 4 sec. for reduction at 1 mA cm<sup>-2</sup>, and at 16 sec. for reduction at 0.5 mA cm<sup>-2</sup>. These theoretical transition times are shown by the solid circles in Figure 4. Now, of course, the chronopotentiograms shown in Figure 4 are quite messy, and little significance would be attached to them were there not some theoretical justification for analysis. We believe that the fact that the theoretically anticipated transition times for lithium reduction are consistently observed, even though it is evident that there is extensive background reduction, suggests that lithium ions are, in some way, consumed during background reduction. Suppose there existed a surface film of oxygen or water on the electrode. The following reactions are consistent with the data shown in Figure 4:



Either species, O<sub>2</sub> or H<sub>2</sub>O, could serve as the species S<sub>O</sub> hypothesized on page 13 of the Second Quarterly Report.

The nature and extent of background reduction seems to be about the same, regardless of the concentration of lithium salt. In Figure 5 are shown the results obtained at  $1 \text{ mA cm}^{-2}$  in each of the  $\text{LiBF}_4$  solutions. Although in Fig. 5 we have shown the expected lithium deposition potential in each case by adding the  $iR$  drop to  $3.1 \text{ V}$ , it should be apparent that relatively minor changes in the correction or the zeroing of the recorder would move these points quite a bit from left to right. We do not know whether the evident variations in the extent of background reduction are real or not -- the question may be argued either way.

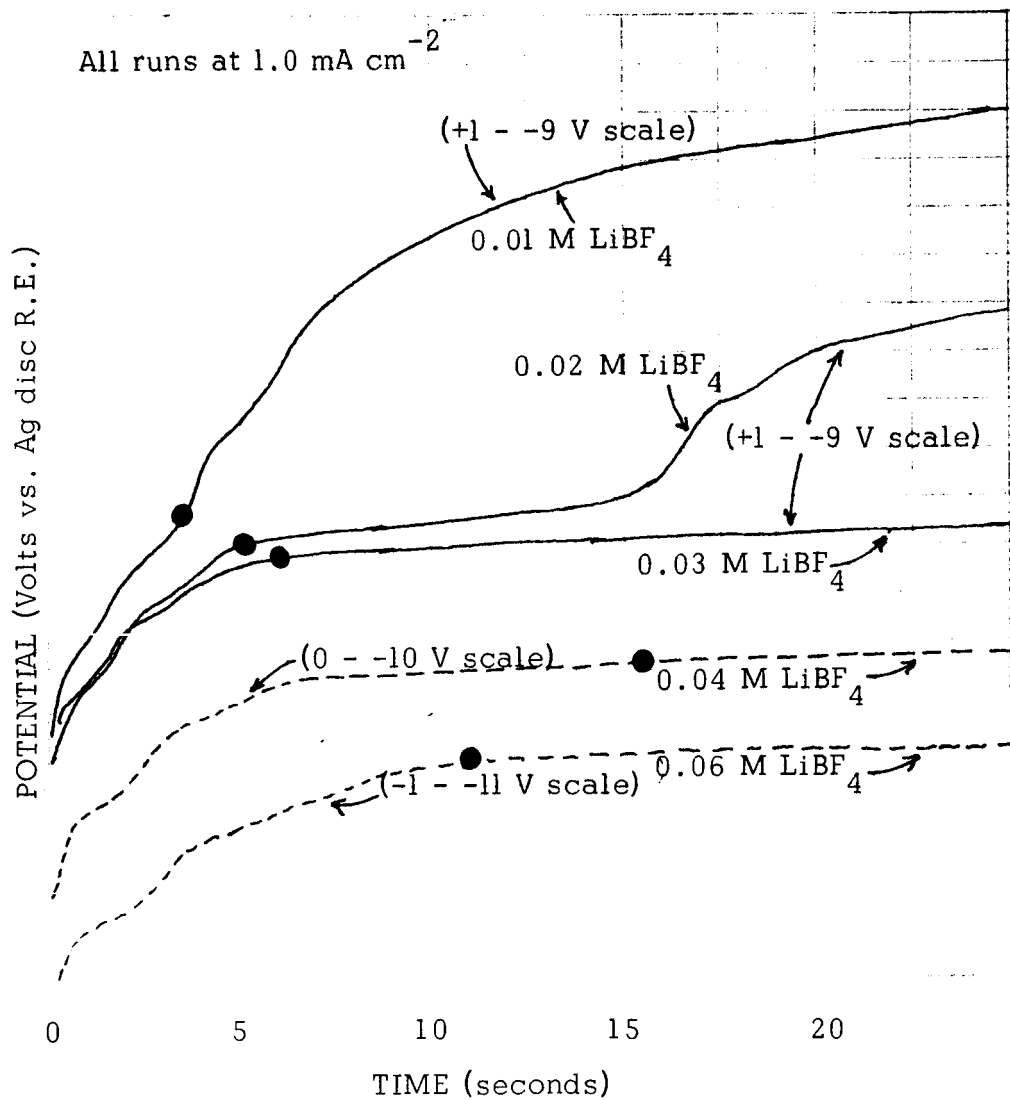
Figure 6 shows a series of chronopotentiograms which display the relationship between the concentration of the lithium salt and  $iT^{1/2}$ . The following values are calculated from the apparent point of inflection on the chronopotentiograms. To demonstrate the proportionality between  $iT^{1/2}$  and concentration, the term  $iT^{1/2}/C$  is also shown below.

Conc. of $\text{LiBF}_4$	$iT^{1/2}$ $\text{mA cm}^{-2} \text{ sec}^{1/2}$	$iT^{1/2}/C$ $\text{mA cm sec}^{1/2} \text{ mM}^{-1}$
0.01	2.0	200
0.02	4.05	202
0.03	*6.15	207
0.04	8.16	204
0.06	12.3	205

The solid circles in Figure 6 represent the calculated lithium deposition potential given by:  $E = -3.1 - iR$ . Again, the  $iR$  drop at the specified current was calculated from the measured specific resistance, as previously discussed.

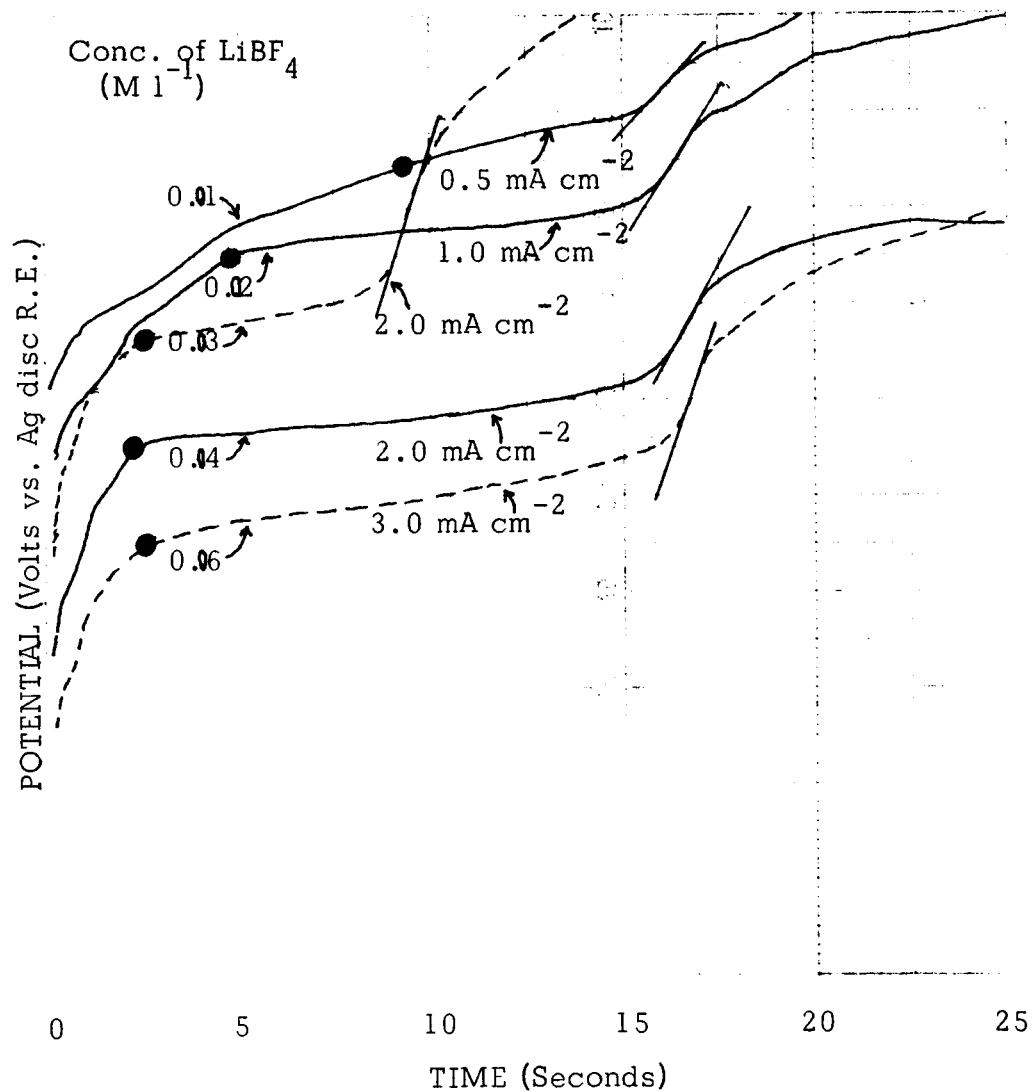
Summary:  $\text{LiBF}_4/\text{PC}$ . The phenomenon of "background reduction" is described in more detail. The following points are noted:

- (a) Background reduction is evidently not a diffusion



CATHODIC CHRONOPOTENTIOMETRY IN  $\text{LiBF}_4$  - PROPYLENE CARBONATE





Voltage Scales:	0.01 M Solution	+5 - -5 V
	0.02 M Solution	+4 - -6 V
	0.03 M Solution	+3 - -7 V
	0.04 M Solution	+2 - -8 V
	0.06 M Solution	+1 - -9 V

CATHODIC CHRONOPOTENTIOMETRY IN  $\text{LiBF}_4$  - PROPYLENE CARBONATE

Figure 6  
- 22 -

limited cathodic reduction of soluble, reducible impurities.

(b) Background reduction evidently results in the consumption of lithium ions, as attested by the constancy of  $iT^{1/2}/C$ .

(c) Although it is presently our objective only to describe the phenomenon, tentative hypotheses may be advanced. One explanation may be the formation of insoluble lithium salts at the electrode surface (See Second Quarterly Report), which deactivate the surface toward further background reduction. Another explanation may be the formation of surface alloy formation, in which the activity of the lithium metal is significantly less than unity, to account for the fact that the potentials at which background reduction occurs are positive to that of a lithium metal electrode in the same solution.

(d) It is still questionable to what degree the "background reduction" here described is relevant to the cyclability of a lithium electrode. However, an appreciation of the phenomenon is relevant to electrolyte evaluation and screening and to the determination of "minimum decomposition potentials."

(e) Further work in the study of the phenomenon of background reduction will be done concurrently with analytical determination of the concentration of water in the electrolyte and, if possible, other impurities found by V.P.C. The deliberate addition of water and, if desirable, other impurities will also be done, to see how the character of background reduction changes.

### II-E-3. Electrochemical Characterization: PC/LiI

A supply of nineteen different lithium salts has been received. Experiments were begun with lithium iodide. Iodide solutions are useful for two primary reasons: (1) silver may be anodically oxidized to AgI, thus providing a stable reference electrode with a thermodynamically

meaningful potential, and (2) the anodic chronopotentiometry of the iodide ion may be investigated, providing additional information concerning the significance of  $iT^{1/2}$  measurements in poorly conductive solutions in the absence of supporting electrolyte.

A variety of measurements were performed on both polished silver and polished platinum electrodes. The results are conveniently summarized by the chronopotentiograms with current reversal shown in Figure 7. The open circuit potential of an electrodeposited lithium electrode versus the silver/silver iodide reference electrode was -2.45 V. The specific resistance of the solution was 590 ohm-cm, from which the  $iR$  correction at the various currents was calculated and added to the open circuit potential to give the theoretical lithium deposition potential shown in Figure 7.

Several conclusions are apparent from the chronopotentiograms shown in Figure 7.

- a. The amount of background reduction on platinum appears to be larger than on silver.
- b. Anodic utilization is about the same on both electrodes but the discharge curves on silver are significantly flatter than on platinum.
- c. Though the observed lithium deposition potential differs somewhat from that theoretically calculated, we do not at this time believe this indicates severe electrokinetic irreversibility. For example, on silver at  $0.8 \text{ mA cm}^{-2}$  the deposition potential, corrected for  $iR$  drop is -2.51 V, and the anodic dissolution potential is -2.38. This gives an overvoltage on cathodization of 0.06 V, and on anodization of 0.07 V. Using the simple expression  $\eta = 0.059 \log i/i_0$ , where  $\eta$  is the activation (electrokinetic) overvoltage,  $i$  is the current density, and  $i_0$  the exchange current density, one calculates an exchange current of about  $0.064 \text{ mA cm}^{-2}$  for  $\eta = 0.065 \text{ V}$ . At present we doubt, however, that the apparent deviation of cathodic and anodic

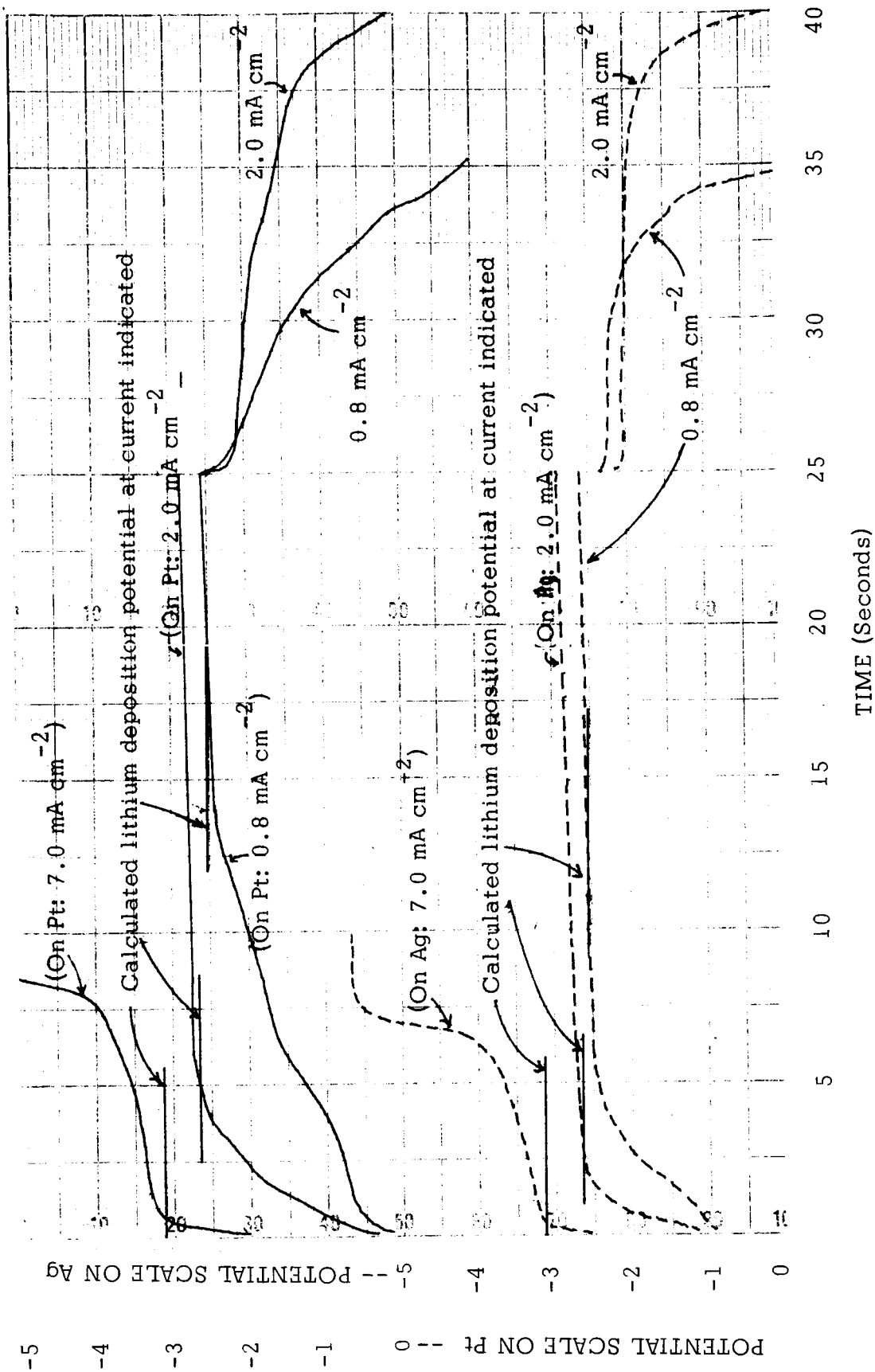


Figure 7

potentials about the open circuit potential is less a reflection of electrokinetic irreversibility than of the concurrent growth of insulating films at the electrode during deposition.

Finally, we consider two other facts observed in this study:

d. The value of  $iT^{1/2}$  on platinum varied from 18.7 to 20.4  $\text{mA cm}^{-2} \text{sec}^{1/2}$  over a range of currents. That on silver varied from 16.4 to 18.1  $\text{mA cm}^{-2} \text{sec}^{1/2}$ . The deviation is not outside the bounds of experimental error and we cannot say whether the deviation is real and significant or not.

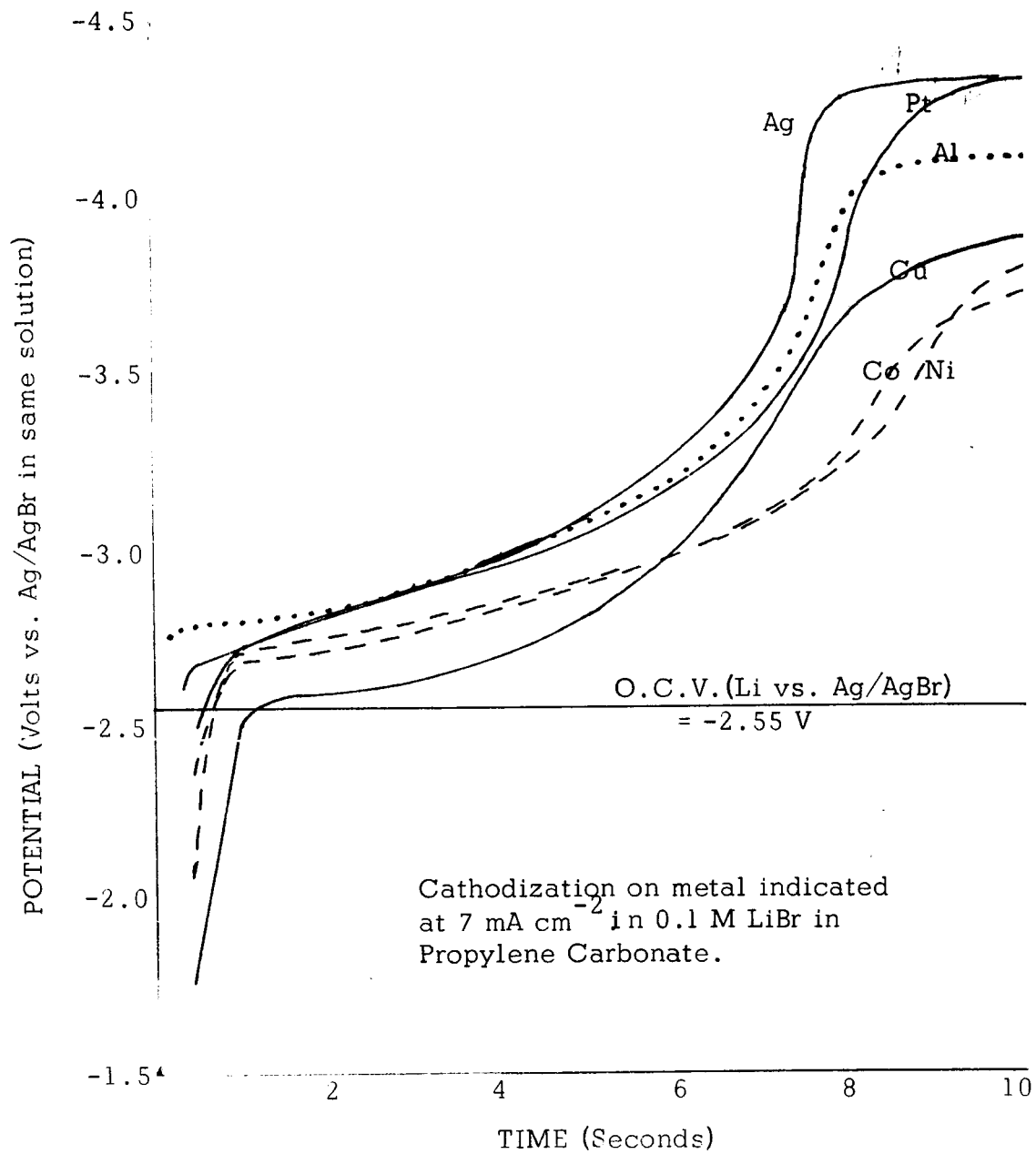
e. The open circuit potential of a lithium electrode in 0.09 M LiI/PC vs. a Ag/AgI electrode in the same solution is -2.45 V. The calculated potential difference between a lithium electrode in an aqueous 0.09 M LiI solution is -3.03 V vs. a Ag/AgI electrode in the same solution. As discussed in Appendix II we ascribe this largely to a difference in the heat of solution of LiI in the two solvents of about  $10 \text{ kcal M}^{-1}$ .

f. Finally, the anodic oxidation of iodide was studied chronopotentiometrically on platinum. Anodic chronopotentiograms showed transition times which gave values for  $iT^{1/2}$  of 16.9 to 17.4  $\text{mA cm}^{-2} \text{sec}^{1/2}$ . These are almost identical to those obtained for the reduction of lithium and indicate the effective transport parameters of the two species to be similar.

#### II-E-4. Electrochemical Characterization: LiBr/PC

A propylene carbonate solution of LiBr, 0.1 M, was prepared and examined chronopotentiometrically. It had, at this time, been found that quite marked differences for lithium deposition existed for various electrodes, and particular attention was directed toward investigating this phenomenon in the LiBr solution.

In Figure 8 are shown chronopotentiograms obtained at  $7 \text{ mA cm}^{-2}$  on the six metals investigated: platinum, silver, cobalt, nickel, aluminum, and copper. The shape of a chronopotentiogram has theoretical



CATHODIC CHRONOPOTENTIOMETRY IN LiBr - PROPYLENE CARBONATE

Figure 8

importance, just as does the shape of a polarogram, and this is discussed in a later section of this report, Kinetic Studies. Observe that the transition times vary from about 7 to 9 seconds on the various metals, giving values for  $iT^{1/2}$  of from 18.5 to 21 mA cm<sup>-2</sup> sec<sup>1/2</sup>. This is a variation of about ±5% about the average. We cannot yet say whether the variation is real or results from experimental error.

In Figure 9 are shown chronopotentiograms with current reversal at 2 mA cm<sup>-2</sup>, and in Figure 10 similar measurements at 0.8 mA cm<sup>-2</sup>. Again, we note without further comment the difference in background reduction on the metals, and also the shape of the subsequent anodic stripping curve.

The open circuit potential of a lithium electrode in the 0.1 M LiBr/PC solutions was -2.55 V vs. the Ag/AgBr reference electrode. The calculated potential in aqueous 0.1 M LiBr vs. the AgBr electrode would be -3.17 V. Again, we ascribe the difference in potentials to a difference in heats of solution of about 10 kcal M<sup>-1</sup>, as discussed in Appendix II.

Attempts to establish anodic  $iT^{1/2}$  values for the oxidation of the bromide ion were not attempted in this study.

#### II-E-5. Electrochemical Characterization: PC/AgClO<sub>4</sub>

The reason we perform measurements on AgClO<sub>4</sub> solutions is to have a reference system for comparison with the results obtained in the lithium salt solutions. The reduction of the silver ion, being a one-electron reduction, is therefore like the reduction of the lithium ion. The equivalent conductance of an AgClO<sub>4</sub> solution is similar to that of a lithium salt solution, hence one expects similar transport parameters for the two species, and, accordingly, similar  $iT^{1/2}$  values.

In Figure 11 are shown a series of chronopotentiograms obtained in propylene carbonate, 0.03 M in AgClO<sub>4</sub>. These

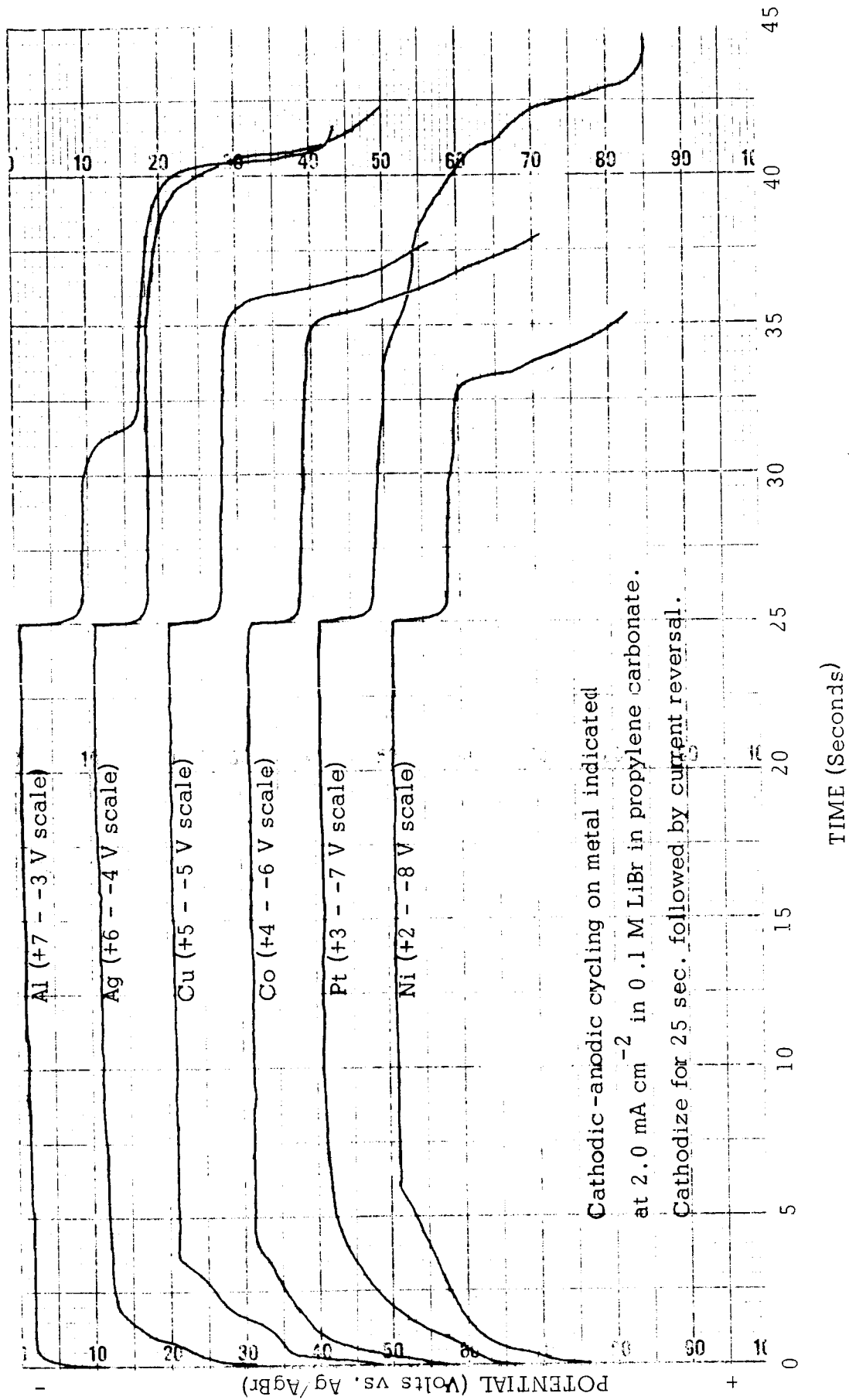


Figure 9

CATHODIC -ANODIC CYCLING IN LiBr - PROPYLENE CARBONATE



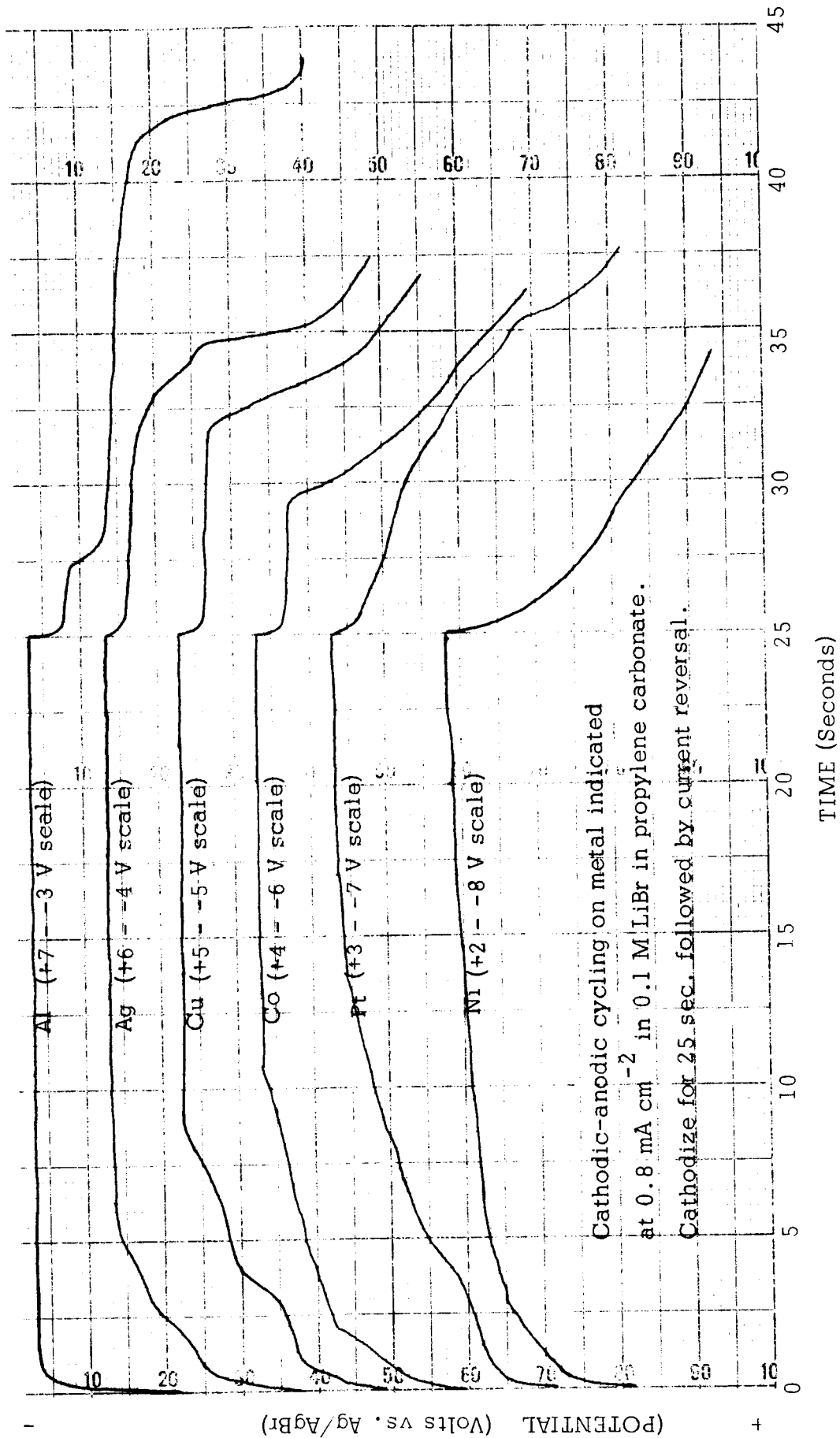
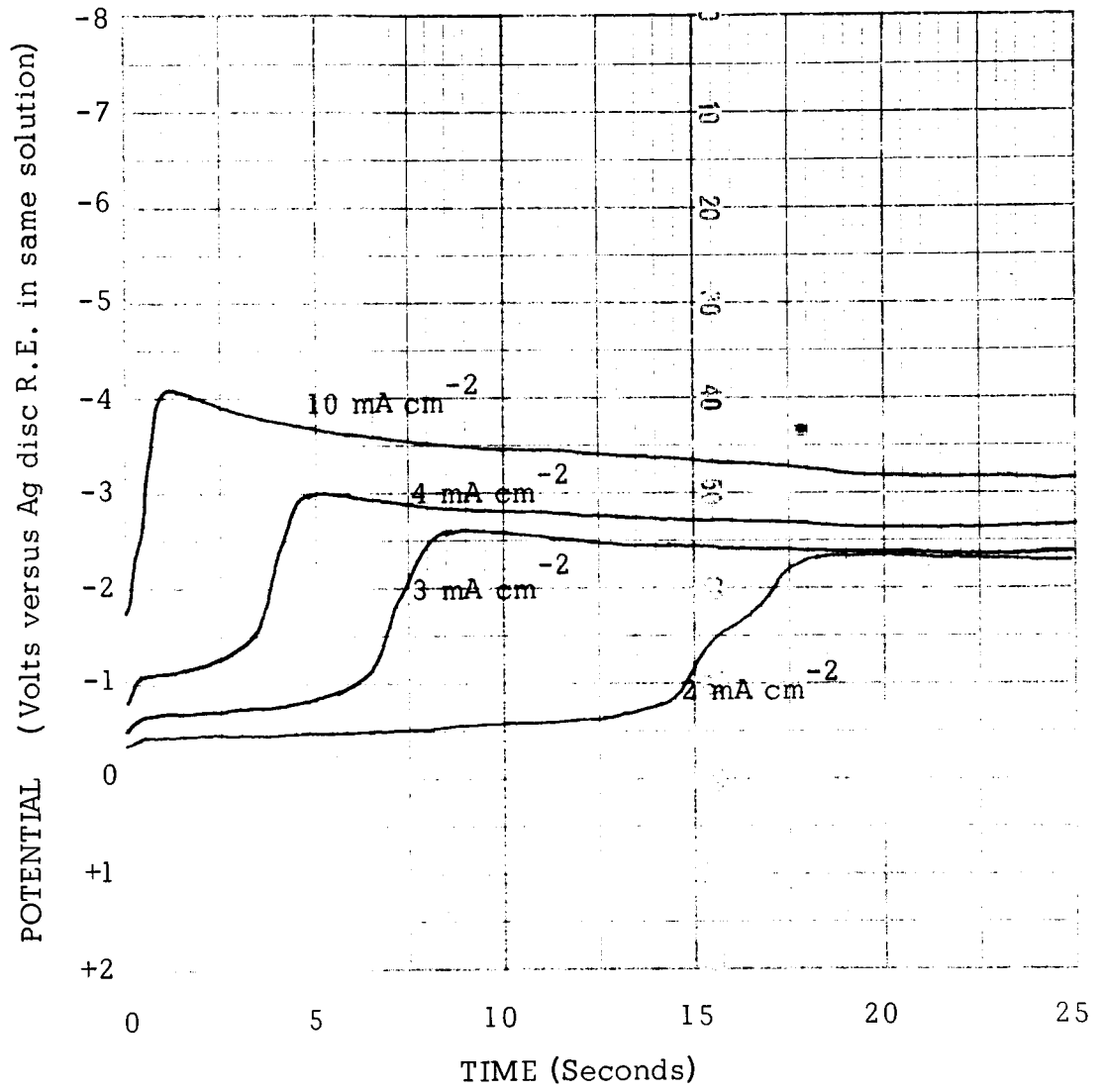


Figure 10

CATHODIC-ANODIC CYCLING IN LiBr - PROPYLENE CARBONATE



CATHODIC CHRONOPOTENTIOMETRY IN  $\text{AgClO}_4$  - PROPYLENE CARBONATE

Figure 11

chronopotentiograms were obtained on silver electrodes. Chronopotentiograms obtained on platinum electrodes were identical. The transport properties of the 0.03 M  $\text{AgClO}_4$  solution are compared with those of the 0.03 M  $\text{LiBF}_4$  solution, reported in Section II-E-2, above:

$$0.03 \text{ M LiBF}_4 = 20 \text{ ohm}^{-1} \text{ cm}^2 \text{ M}^{-1} \quad iT^{1/2} = 6 \text{ mA cm}^{-2} \text{ sec}^{1/2}$$

$$0.03 \text{ M AgClO}_4 = 25 \text{ ohm}^{-1} \text{ cm}^2 \text{ M}^{-1} \quad iT^{1/2} = 7.7 \text{ mA cm}^{-2} \text{ sec}$$

The similarity further establishes the validity of  $iT^{1/2}$  values for the lithium reduction.

Finally, in the  $\text{AgClO}_4$  solutions, we are interested in the second reduction which occurs following that of the silver ions. The maximum potential at which this reduction occurs is given below:

<u>Current</u>	<u>Observed Potential</u>	<u>iR Correction</u>	<u>Corrected Potential</u>
10 mA cm <sup>-2</sup>	-4.10 V	2.15 V	-1.95 V
4 mA cm <sup>-2</sup>	-3.00 V	0.86 V	-2.14 V
3 mA cm <sup>-2</sup>	-2.60 V	0.65 V	-1.95 V
2 mA cm <sup>-2</sup>	-2.35 V	0.43 V	-1.92 V

These potentials, it must be noted, are with respect to a silver electrode in a solution of silver ions. The potential of such an electrode is not the same as that of a silver disc R.E. in a solution in which silver ions are absent. These potential relationships are clarified below:

E of Li electrode in Li salt/PC vs.

$$\text{Ag disc R.E. in Li salt/PC} = -3.1 \text{ V}$$

E of Ag electrode in Ag salt/PC vs.

$$\text{Ag disc R.E. in Li salt/PC} = +0.7 \text{ V}$$

E of Li electrode in Li salt/PC vs.

$$\text{Ag disc R.E. in Ag salt/PC} = -3.8 \text{ V}$$

E of second reduction in Ag salt/PC vs.

Ag disc R.E. in Ag salt/PC = ca. -2.0 V (see above)

Thus, the second reduction observed in Figure 11 occurs about 1.8 V in advance of the reduction of lithium to the metal.

The reason why the potential for this second reduction goes through a maximum and then decreases to less negative values may possibly be ascribed to the fact that, on reduction, silver dendrites were observed to form which penetrated into the solution. This may have decreased the  $iR$  drop between the reference and working electrodes, thus resulting in an apparent decrease in the potential difference.

We do not know what this second reduction might be. It may even be reduction of solvent itself on the fresh, silver surface presented during deposition, whereon one might expect the overvoltage for solvent reduction to be significantly decreased. Similar phenomena are observed during chronopotentiometric measurements in aqueous solution. For example, if one observes the cathodic behavior on polished platinum electrodes in aqueous perchloric acid, the overvoltage for the reduction of hydrogen ions is significantly greater than is observed when a silver salt is dissolved in the solution, and cathodization performed. In the latter case the reduction of silver will proceed before the reduction of hydrogen ions, and a fresh, catalytically active silver surface is thus presented for subsequent hydrogen ion reduction.

#### II-E-6. Electrochemical Characterization: PC/KI

The previously described results for lithium and silver salt solutions in propylene carbonate indicate what should be expected when a 1:1 univalent electrolyte is subjected to cathodization. It was of interest to examine another active metal salt, and KI was chosen, since the results could be conveniently compared with those for the LiI solution.

We consider first the cathodic behavior on freshly polished platinum. Chronopotentiograms were performed at six currents between 0.5 to 7 mA cm<sup>-2</sup>. Two runs were made at each current. The results were not reproducible and this is shown by the two examples in Figure 12 by the dotted lines. These are two chronopotentiograms run at 2 mA cm<sup>-2</sup> on freshly polished platinum (not repeated on the same electrode). The correction for iR drop at this current was calculated to be 0.15 V. Violet deposits formed during deposition along with significant gassing. This is contrasted with the behavior of the lithium salt solutions, where a fine gray deposit forms and no significant gassing is observed at the currents normally employed. Furthermore, on reversing the current, there was no significant anodic oxidation of potassium.

The results on silver electrodes were more similar to those obtained for the reduction of lithium. In Figure 12 are shown the two best examples. We consider first the run performed at 8 mA cm<sup>-2</sup>, for which the calculated iR drop is 0.57 V. Thus, correcting the measured potential of reduction, ca. -3.45 V, for iR drop gives a deposition potential of -2.88 V. An approximate  $iT^{1/2}$  of about 30 mA cm<sup>-2</sup> sec<sup>1/2</sup> is compared with the equivalent conductance of 21 ohm<sup>-1</sup> cm<sup>2</sup> M<sup>-1</sup>. Comparing these results with those described in the previous section II-E-5 indicates such an  $iT^{1/2}$  is not wildly different from that expected. The current was stopped after 18.5 sec. and the O.C.V. recorded. After about 5 sec. the drop in O.C.V. indicated, we believe, the loss of potassium through chemical reaction with the electrolyte.

In Figure 12 is also shown a chronopotentiogram obtained on silver at 7 mA cm<sup>-2</sup> followed by current reversal. The calculated iR drop is 0.49 V, giving a corrected cathodic deposition of -3.40 + 0.49 = -2.91 V. The anodic dissolution potential is similarly corrected giving -1.70 - 0.49 = -2.19 V. If we take the average of the corrected cathodic deposition potential and the anodic dissolution potential as the true open circuit potential for potassium deposition we obtain -2.55 V. This, it will be observed is almost

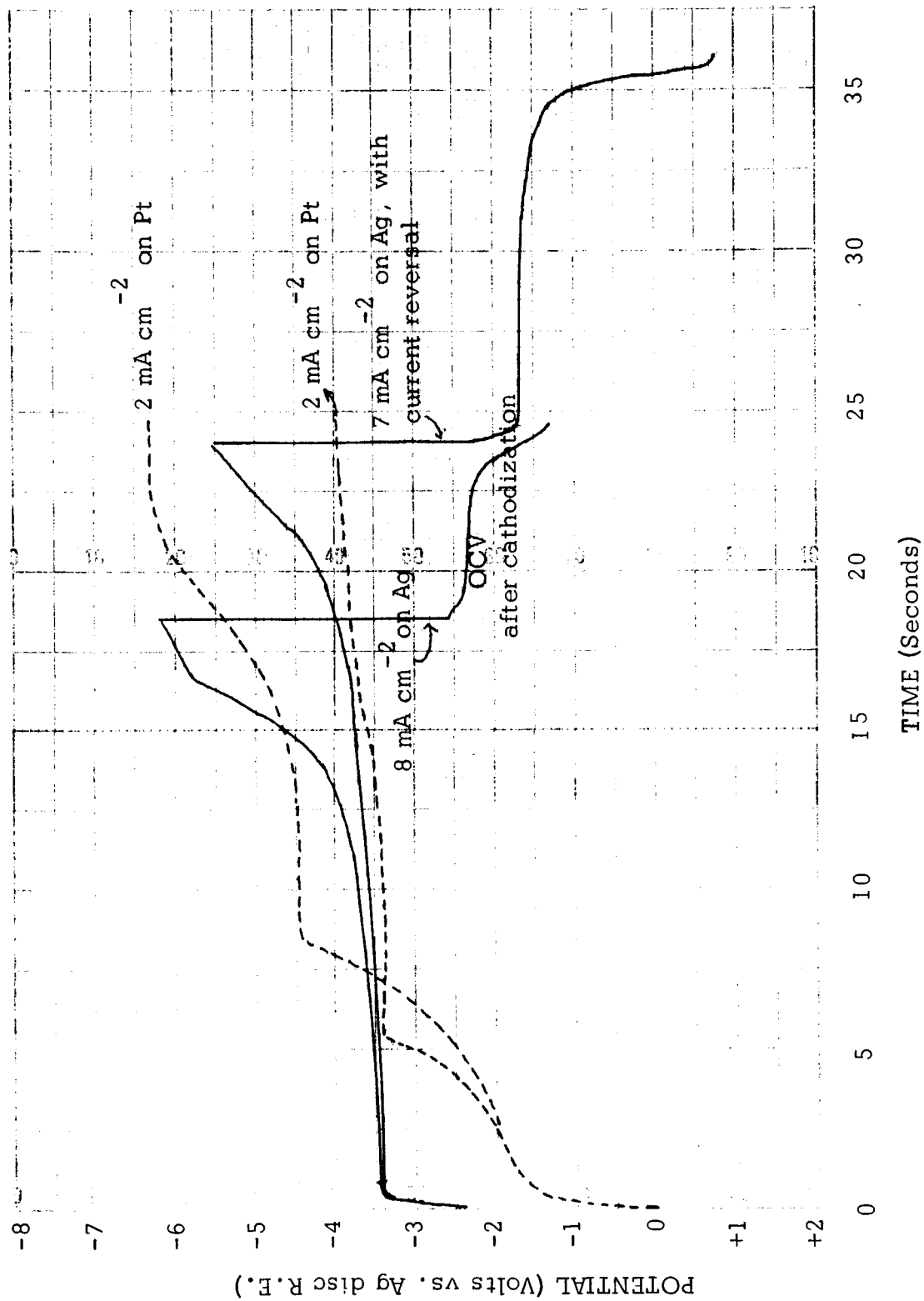


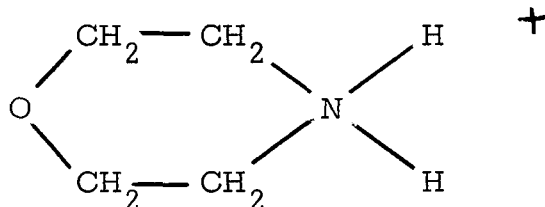
Figure 12

identical with the initial O.C.V. obtained for the run performed at  $8 \text{ mA cm}^{-2}$ , shown in Figure 12. This should also be compared with the potential of  $-2.45 \text{ V}$  for the lithium electrode in the LiI solution.

The behavior of potassium in these relatively cursory experiments is so inferior to that of lithium in similar electrolytes that we eliminate potassium from further consideration. Since both potassium and lithium have about the same theoretical deposition potential, and are both monovalent ions, the differences in behavior are somewhat surprising and attest, we believe, to the uniqueness of the lithium ion.

#### II-E-7. Electrochemical Characterization: Morpholinium $\text{PF}_6/\text{PC}$

We anticipate further investigations into the use of alkyl ammonium salts. We have begun this work with preliminary electrochemical characterization of propylene carbonate solutions of Morpholinium hexafluorophosphate ( $\text{MoPF}_6$ ). The morpholinium ion has the structure:



and thus has two active hydrogens. Morpholinium salts have been reported to have quite high conductivities, and it was of interest to see whether the electrochemical activity of the ion was sufficiently great to prevent incorporation in lithium cells.

Propylene carbonate solutions,  $0.25 \text{ M}$  in  $\text{MoPF}_6$ , were examined. Constant cathodic current was applied to platinum disc working electrodes. The results are shown below. In each case the potential rapidly rose to the initial value indicated within  $0.2 \text{ sec.}$  after the commencement of cathodization. Thereafter there was a slow increase in potential with time

to the final value indicated. No transition times or other irregularities in the chronopotentiograms were observed. The specific resistance of the solution was 206 ohm-cm, and the potentials given below, with reference to the silver disc R.E., have been corrected for  $iR$  drop. It will be recalled the potential of lithium deposition is -3.1 V versus the silver disc R.E.

Current	Potential after 0.2 sec	Potential after 25 sec
2.4 mA cm <sup>-2</sup>	-0.68 V	-0.76 V
6.0 mA cm <sup>-2</sup>	-0.78 V	-0.80 V
15 mA cm <sup>-2</sup>	-0.7 V	-0.80 V
37.5 mA cm <sup>-2</sup>	-0.68	-0.98 V

The largest  $iT^{1/2}$  was  $37.5 \times (25)^{1/2} = 188 \text{ mA cm}^{-2} \text{ sec}^{1/2}$ . If reduction were of the morpholinium ion, if both active hydrogen were reducible, and if the diffusion coefficient of the ion were the same as that of the lithium ion, one would calculate an  $iT^{1/2}$  for reduction of  $0.25 \times 200 \times 2 = 100 \text{ mA cm}^{-2}$ . However, vigorous gassing was observed at all reductions and this would so disturb the diffusion layer that one would not be surprised at the inability to obtain transition times.

It would appear that the severe background reduction occurring in morpholinium solutions would preclude the use of such salts in lithium cells.

#### II-E-8. Electrochemical Characterization: DMF/AgClO<sub>4</sub>

A DMF solution of AgClO<sub>4</sub>, 0.106 M, was initially examined by performing chronopotentiograms at several current densities. The chronopotentiograms were so similar to those shown in Figure 11, displaying well-defined transition times and a second reduction peak, that they are not here presented. The data are presented below. The potentials have been corrected for  $iR$  drop, calculated from the measured specific resistance of 144 ohm-cm.



<u>Current</u> (mA cm <sup>-2</sup> )	<u>Transition Time</u> (sec)	<u>iT<sup>1/2</sup></u> (mA cm <sup>-2</sup> sec <sup>1/2</sup> )	<u>Potential of Ag+reduction</u>	<u>Potential of Second reduction</u>
10	--	--	-0.17	--
15	--	--	-0.26	--
20	12.2	70	-0.24	-1.25
25	4.8	55	-0.33	-1.54
50	1.08 (CRO)	52	-0.35	-1.6
75	0.54 (CRO)	55	--	-1.7

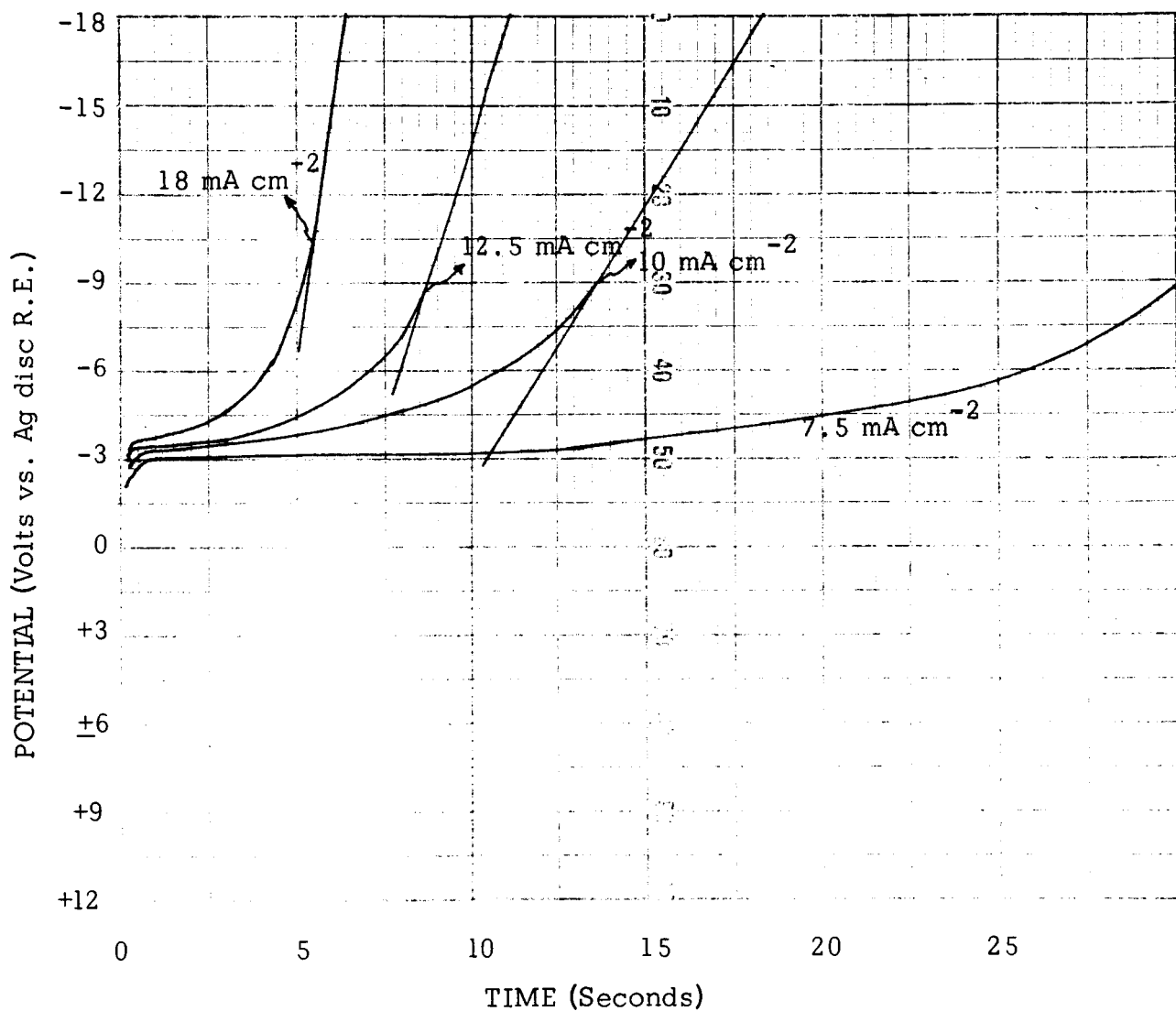
The gaps in the above data indicate that electrolysis was not continued long enough to give a transition time, or that the data were not measured.

We believe the larger iT<sup>1/2</sup> of 70 mA cm<sup>-2</sup> sec<sup>1/2</sup> reflects the effect of pronounced dendritic silver growth, which disturbs the diffusion layer and enhances the transition time. This is the type of phenomena often encountered in aqueous solution chronopotentiometry. We use the value iT<sup>1/2</sup> of 53 to calculate iT<sup>1/2</sup>/C, which is 500 mA cm sec<sup>1/2</sup> mM<sup>-1</sup>. We compare the data with that obtained in propylene carbonate solutions:

<u>Solution</u>	<u>Equivalent Conductance</u>	<u>iT<sup>1/2</sup>/C</u>
0.03 AgClO <sub>4</sub> /PC	25 ohm <sup>-1</sup> cm <sup>2</sup> M <sup>-1</sup>	260 mA cm sec <sup>1/2</sup> mM <sup>-1</sup>
0.106 M AgClO <sub>4</sub> /DMF	66 ohm <sup>-1</sup> cm <sup>2</sup> M <sup>-1</sup>	500 mA cm sec <sup>1/2</sup> mM <sup>-1</sup>

#### II-E-9. Electrochemical Characterization: LiCl/DMF, LiBF<sub>4</sub>/DMF

Figure 13 shows a series of chronopotentiograms obtained in DMF, 0.11 M in LiBF<sub>4</sub>. Such chronopotentiograms we consider "ill-defined" because it is difficult to unambiguously determine a specific transition time. We take the transition time as the point where the linear extrapolation of the chronopotentiogram begins to deviate from the actual curve. For the



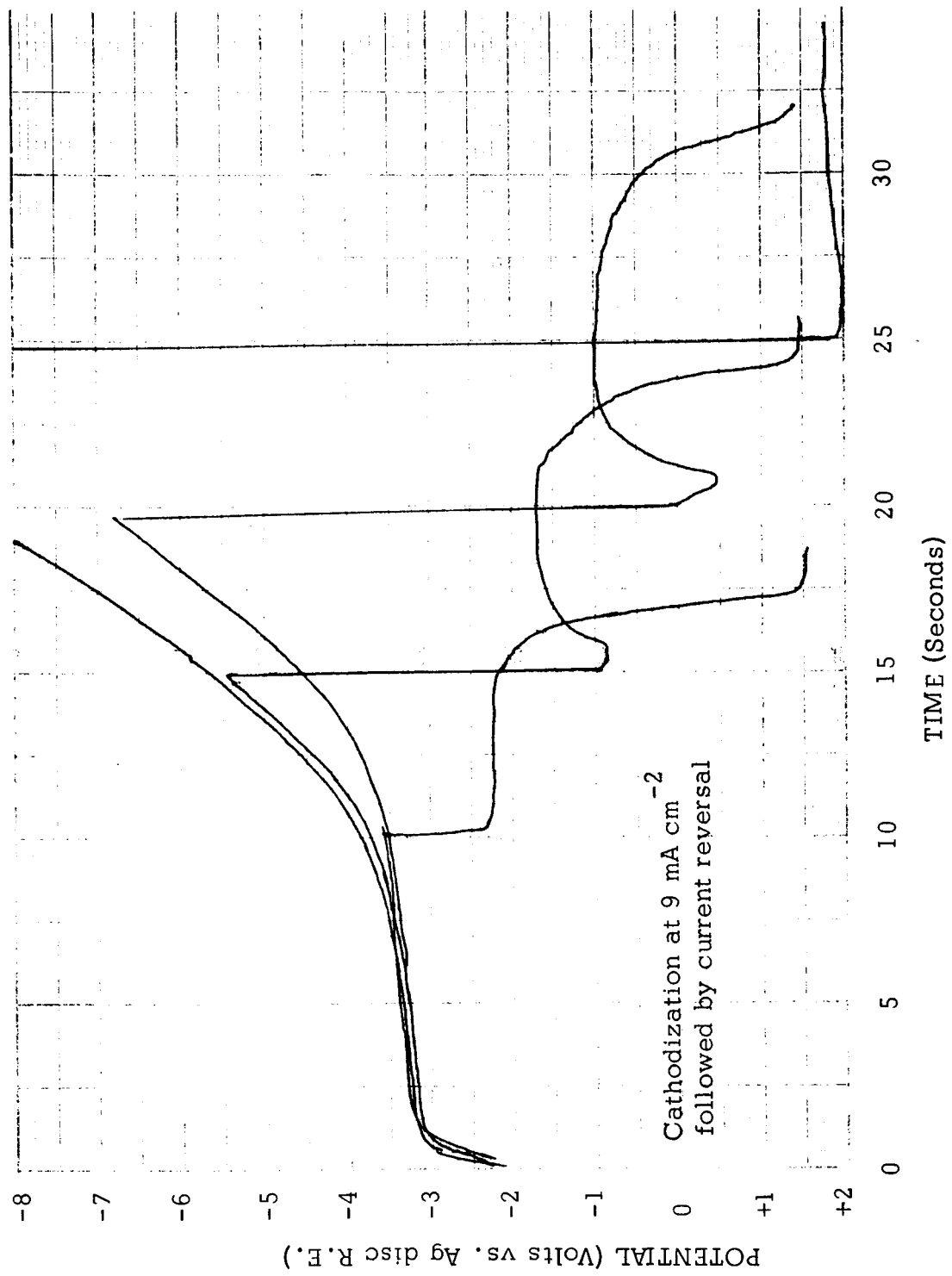
CATHODIC CHRONOPOTENTIOMETRY IN  $\text{LiBF}_4$  - DIMETHYLFORMAMIDE

Figure 13

chronopotentiograms in Figure 13 we select an average value for  $iT^{1/2}$  of  $37.5 \text{ mA cm}^{-2} \text{ sec}^{1/2}$ . This gives a value for  $iT^{1/2}/C$  of  $340 \text{ mA cm sec}^{1/2} \text{ mM}^{-1}$ . The measured specific conductance was  $174 \text{ ohm-cm}$ , giving an equivalent conductance of  $52 \text{ ohm}^{-1} \text{ cm}^2 \text{ M}^{-1}$ . If the proportionality between  $iT^{1/2}/C$  and equivalent conductance were the same for the  $\text{AgClO}_4$  and the  $\text{LiBF}_4$  solutions, one would calculate an  $iT^{1/2}/C$  of  $(55/66) (500) = 420 \text{ mA cm sec}^{1/2} \text{ mM}^{-1}$ . Thus, the results indicate that the transition time is probably the result of diffusion limited concentration polarization of the lithium ion.

Note also the extremely negative potentials observed during the course of cathodization. This was believed to be due to the formation of a resistive film during deposition, and these conclusions tended to be confirmed by subsequent results obtained in a  $0.137 \text{ M LiCl/DMF}$  solution. The results are shown in Figure 14. These chronopotentiograms were obtained by cathodizing a platinum electrode at  $9 \text{ mA cm}^{-2}$  for 10, 15, 20, and 25 sec., followed by immediate current reversal. The  $iR$  drop correction at this current is calculated to be  $0.22 \text{ V}$ . Below we calculate the difference between the potential at the end of cathodization and the deposition potential ( $-3.0 \text{ V}$ ), and the difference between the potential peak observed during anodization and the deposition potential.

	Time of cathodization			
	10 sec	15 sec	20 sec	25 sec
Corrected Potential at end of Cathodization	-3.4	-5.2	-6.6	--
Deposition Potential	-3.0	-3.0	-3.0	--
$iR$ drop	<u>0.4</u>	<u>1.2</u>	<u>3.6</u>	--
Corrected Potential at beginning of anodization	-2.4	-1.1	+0.3	+1.8
Deposition Potential	-3.0	-3.0	-3.0	-3.0
$iR$ drop	<u>0.6</u>	<u>1.9</u>	<u>3.3</u>	<u>4.8</u>



CATHODIC CHRONOPOTENTIOMETRY IN LiCl - DIMETHYLFORMAMIDE

Figure 14  
- 41 -

At lower currents the evident build-up of a resistive film does not occur. The best results showing this were obtained in the LiCl/DMF solution when cathodization was continued at  $5 \text{ mA cm}^{-2}$  for 25 sec. followed by immediate current reversal, with 75% anodic utilization. The potential during cathodic deposition and subsequent anodic dissolution did not differ by more than 0.2 V from the theoretical deposition potential.

Only one long term experiment was performed. Lithium was deposited from the 0.137 M LiCl/DMF solution at  $0.75 \text{ mA cm}^{-2}$  for 670 sec ( $500 \text{ mC cm}^{-2}$ ). The potential of deposition was  $-3.0 \text{ V}$  vs. the Ag disc R.E. On subsequent current reversal 84% anodic utilization was obtained. These results are comparable with those obtained in propylene carbonate, and one cannot conclude that either solvent is superior to the other with respect to their relative abilities to support lithium deposition.

It is apparent that, though the chronopotentiograms for lithium reduction reflect diffusion limited concentration polarization in both propylene carbonate and dimethylformamide solutions, their shapes are quite different, implying the existence of important differences in the deposition process. Yet, even though the chronopotentiograms display important differences, this cannot be correlated with the efficiency for lithium deposition in the two solvents, which is about the same.

#### II-E-10. Electrochemical Characterization: Conclusions

The electrodeposition of lithium metal from non-aqueous lithium salt solutions, while remarkably efficient, is not a simple process. The chronopotentiograms do not have the shape characteristic of a reversible one-electron reduction. This will be discussed in a later section, Kinetic Studies. However, transition times are observed which, when compared with similar measurements performed on the reasonably well-behaved  $\text{AgClO}_4$  solutions, indicate that the processes are limited by the mobility of the lithium ion.

Background reduction, defined as the sum of all reduction processes which occur at potentials positive to the theoretical lithium deposition potential, is a phenomenon of importance. Furthermore, background reduction is sensitive to the nature of the electrode metal. While we do not know what processes constitute background reduction, the fact that transition times are apparently independent of the extent of preceding background reduction suggests that background reduction must, in some way consume lithium ions. Two tentative hypotheses are advanced to explain this fact. First, background reduction may consist of the formation of surface alloys of lithium metal with the electrode substrate; this would account for the positive potentials at which background reduction occurs, since the activity of lithium metal in the alloy would be less than unity. Secondly, background reduction may consist of the electro-reduction of solvent or impurities, in which a reaction product is an insoluble lithium salt. It is important to re-emphasize that, if impurities constitute the electro-reducible material, the extent of background reduction is far less than would correspond to the diffusion limited reduction of what we believe to be the actual amount of reducible impurities. This suggests that the product of background reduction deactivates the electrode toward further reduction.

Potassium solutions, which would be expected to display behavior similar to that of lithium solutions, do not, in fact, do so. The behavior is quite different in all respects and testifies, we believe, to the uniqueness of the lithium ion.

Finally, while it had been our original objective to perform experiments which reflect the relative ability of various solvents to support high energy density electrodes, we must conclude that this cannot, at present, be done. No data thus far obtained can be assumed to reflect solvent properties, except the transport parameters reflected in the  $iT^{1/2}$  values. Whether a solvent is electrochemically "inert" or not, cannot be deduced from the

presently available data.

We shall continue to perform experiments of the type outlined in this section. It will be our primary objective only to describe the phenomena as clearly as possible without undue interpretation. It is our hope, that with the accumulation of sufficient data for a variety of electrolytes, one may deduce certain patterns of behavior which will allow a less ambiguous assessment of the relative virtues of the various solvents.

#### II-F. Effect of Impurities: Molecular Sieve Treatment

One would predict water to be the most serious impurity. The effect of various treatments with Molecular sieves (Linde 4A) has been studied, since these materials are effective water scavengers.

Four systems were prepared as described below:

a. Solution 1: 0.1 M  $\text{LiBF}_4$  in "impure" propylene carbonate. Solid  $\text{LiBF}_4$ , was added to an amount of propylene carbonate. This propylene carbonate had been standing in a glass stoppered flask for over two months. As described in an earlier section on V.P.C. analysis, a sample of propylene carbonate which had stood for one-month had a water content of 0.04% by weight. For this reason we describe the sample of propylene carbonate used in these experiments as "impure".

b. Solution 2: To Solution 1, above, was added about 2 g. of molecular sieve and the mixture stirred for 20 min.

c. Solution 3: 0.1 M  $\text{LiBF}_4$  in "pure" propylene carbonate. Solid  $\text{LiBF}_4$  was placed in a 100-ml. cell. A stream of argon was played over the cell while 60 ml. of propylene carbonate were passed through a column of molecular sieves at about one drop per second. The column consisted of a standard 50-ml. buret containing 30 ml. of molecular sieves. The first 10 ml.

of propylene carbonate were discarded. The remaining 50 ml., passed into the cell, gave a 0.1 M  $\text{LiBF}_4$  solution.

d. Solution 4: 0.1 M  $\text{LiBF}_4$  in "impure" propylene carbonate. The entire solution was passed through a column of molecular sieves into the cell under the same conditions as described for Solution 3.

The solutions were examined in two ways. Chronopotentiograms were run at  $6.5 \text{ mA cm}^{-2}$ . Several runs were made in each solution to establish the reproducibility, which was, indeed, excellent in all cases. The results are shown in Figure 15. Note that the runs made in Solutions 1 and 3, wherein the solute had not been in contact with molecular sieves are similar in that both solutions give transition times of about 8.5 sec. However, the shape of the chronopotentiograms are radically different. Evidently, the better the chronopotentiogram, the less the amount of water.

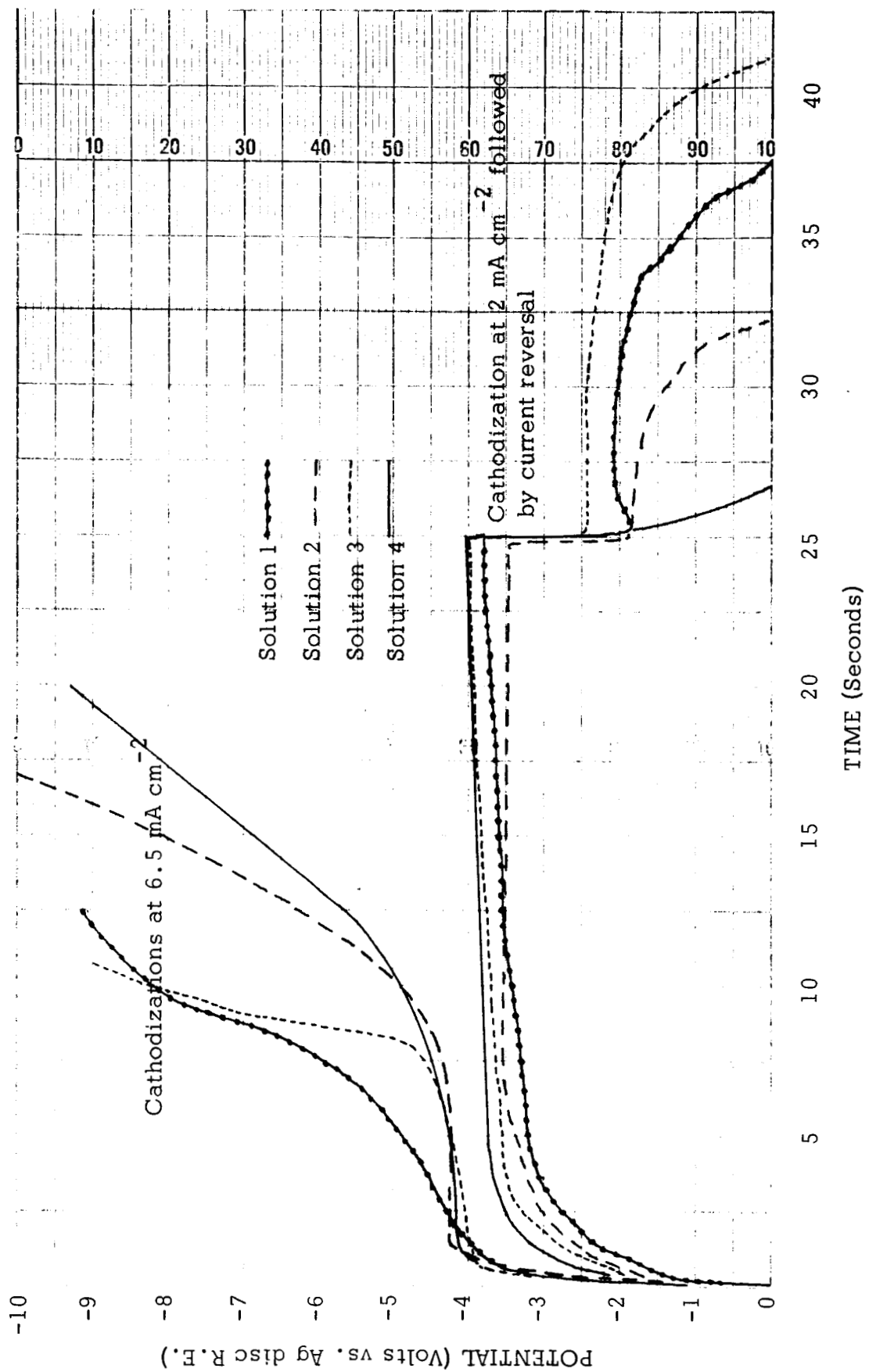
Note in the runs made in solutions wherein the solute had been in contact with molecular sieves that the chronopotentiograms look quite different. They more resemble those obtained in the KI solutions, described earlier, than the typical lithium chronopotentiograms.

The solutions were examined by performing a series of cathodic-anodic cycling experiments at various currents. The best results were obtained at currents between 2 and  $3 \text{ mA cm}^{-2}$ . The runs made at  $2 \text{ mA cm}^{-2}$  are shown in Figure 15.

Note the difference in anodic utilization in solutions 1 and 2. The utilization was about 50% in solution 1,  $\text{LiBF}_4$  in "impure" propylene carbonate, and decreased to 30% when the solution was added molecular sieves. Anodic utilization apparently decreased to 0% when the solution was treated by passing through a column of molecular sieves.

It should be further noted that in Solution 4 a shiny,





CATHODIC CHRONOPOTENTIOMETRY IN  $\text{LiBF}_4$  - PROPYLENE CARBONATE (MOLECULAR SIEVE TREATMENT)

Figure 15

black-violet deposit formed during cathodization, and this was attended by significant gassing.

The difference between Solutions 1 and 3 indicate the efficacy of molecular sieves in removing water from the solvent and enhancing the anodic utilization. The poorer results obtained when the entire solution was treated with molecular sieves results, we believe, from the exchange of sodium ions in the sieve with lithium ions in solution. Solution 4 is doubtless a solution of  $\text{NaBF}_4$  rather than  $\text{LiBF}_4$ .

Other types of molecular sieves may be used. We anticipate the complete exchange of sodium ions in the sieve by lithium or silver ions, and then treating the complete electrolyte with this material. Silver ions are most tenaciously held by the sieve, and the exchange with lithium ions should be small.

#### II-G. Time Stability Tests.

No time stability tests have yet been performed. We believe that such tests, at present, are more likely to reflect the effects of atmospheric contamination through leaks in the systems, rather than inherent stability.

### III. SCREENING PROGRAM

III-A. Chemical Compatibility. Of particular interest is the extent of possible chemical reaction between electrode materials and solvents. At present, we suspect that the cathode materials available through normal channels, such as  $\text{CuF}_2$  and  $\text{CoF}_3$ , are so impure as to make meaningful tests difficult. Preliminary studies have begun as discussed in Section III-C, Solubility Studies. We shall examine these materials more carefully by chemical analysis and X-ray diffraction before proceeding to a study of chemical compatibility. We expect to perform such studies in conjunction with vapor phase chromatographic analysis.

The question of chemical compatibility is particularly important with respect to active anode materials. Unfortunately, it is difficult to obtain meaningful data for two reasons. First, the extent of reactivity is doubtless critically dependent on the nature of surface pre-treatment. Secondly, long term experiments may reflect reaction with solvent impurities rather than with solvent itself. It is doubtless true that various active anode materials will react to some degree with all useful solvents. It is most essential that the nature of the reaction be established, and we anticipate performing such experiments in conjunction with V.P.C. analysis, to determine the nature of the reaction products, and thus elucidate the reaction.

#### III-B. Electrochemical Reversibility

##### III-B-1. Electrochemical Reversibility: Anodes

a. Bulk Metal Anodes. Preliminary work in the study of the discharge of bulk lithium metal was attempted, using the electrode support structure described in Appendix II. Lithium metal was cut from ribbon, 1/2" wide and 1/16" thick, and pressed into the recess of the electrode support structure.

It was necessary that the electrode surface next to the platinum substrate be scraped clean, otherwise stable open circuit potentials did not obtain. When these conditions were met the potential of the bulk lithium electrode in 1 M  $\text{LiBF}_4$  was  $-3.1$  V versus the silver disc R.E. This is the same value obtained when lithium is electrodeposited on platinum or other metals.

It was also necessary that the electrode surface in contact with the solution be scraped clean, otherwise, during the passage of current, polarization was extensive, as will be later described.

We were particularly concerned whether there was any evidence that the anodic dissolution of bulk lithium does not proceed with electrokinetic irreversibility. Constant current pulses were applied for 30 sec. in quiet solution. After each pulse the O.C.V. immediately returned to the initial O.C.V. value of  $-3.1$  V. After one minute of quiet stand the next higher current pulse was applied. The results are shown by the solid circles in Figure 16.

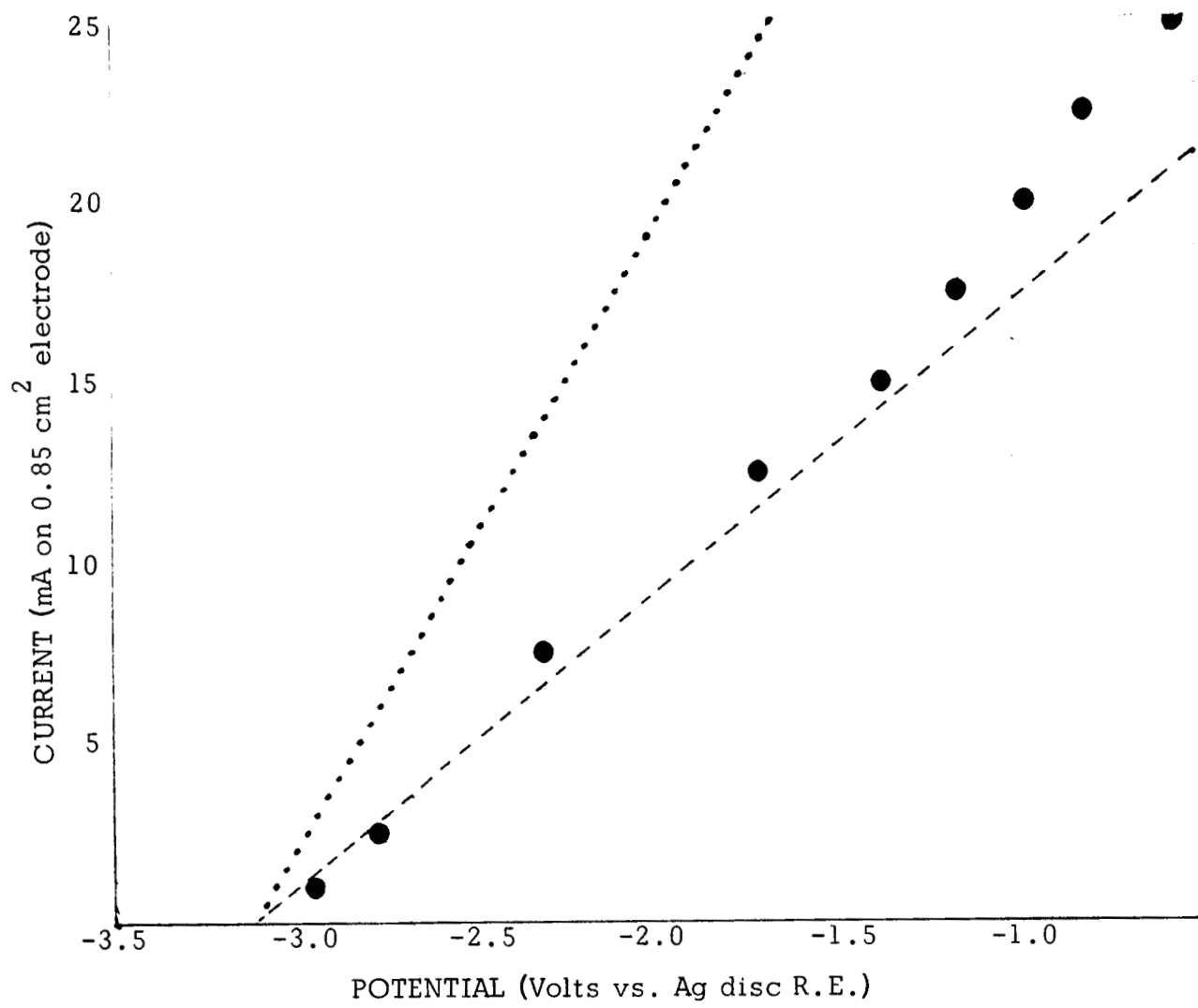
The correction for  $iR$  drop was calculated, as described in Appendix II. For the reversible, anodic dissolution of lithium the measured potential should be given by:

$$E = -3.1 + (i \text{ A cm}^{-2}) (265 \text{ ohm-cm}) (0.39 \text{ cm})$$

The specific resistance was 265 ohm-cm, and the effective  $d_L$ , as discussed in Appendix II, was 0.39 cm. This calculated potential is shown by the dashed line in Figure 16.

The dotted line in Figure 16 shows what the measured potential would be for the reversible, anodic dissolution of bulk lithium if the effective  $d_L$  were 0.1 cm. That is, if the potential were measured via a Luggin capillary, 0.1 cm from the surface of the working electrode.

The measured potential, given by the solid circles in Figure 16, is, indeed, closer to the calculated value than would be expected. This



ANODIC DISCHARGE OF BULK LITHIUM IN PROPYLENE CARBONATE

Figure 16

probably results from a cancellation of errors. First, since the lithium metal in the recess is comparatively thick (ca. 0.07 cm when pressed into the recess), this should lower the effective  $d_L$  and give an  $iR$  correction less than that calculated. The measured potentials should lie to the left of the dashed line.

Secondly, in the absence of supporting electrolyte, a back EMF is set up in the diffusion layer as discussed in the First Quarterly Report. This should put the observed values to the right of the dashed line.

Thirdly, the true active surface area is not known, since one cannot be sure the electrode surface is uniformly cleaned. This may affect the homogeneity of the current flux and give errors in the measured potential.

We have also investigated the time dependent behavior during anodic dissolution. The results are shown below for anodizations performed in quiet solution:

<u>Current</u>	<u>Time</u>	<u>Potential</u>
25 mA	0	-0.75
	0.5 min	-0.65
	1.0 min	-0.40
	1.5 min	-0.10
	2.0 min	+0.40
10 mA	0	-1.95
	5 min	-1.86
	10 min	-1.80
	15 min	-1.75
5 mA	0	-2.55
	30 min	-2.54

It is not surprising that a serious potential drift is observed at 25 mA ( $30 \text{ mA cm}^{-2}$ ) since this is close to what one would expect the limiting current to be in a 1 M propylene carbonate solution. Thus, for example, the calculated  $iT^{1/2}$  would be  $200 \text{ mA cm sec}^{1/2} \text{ mM}^{-1}$ , the value for  $iT^{1/2}/C$  in propylene carbonate solutions of lithium salts, times the concentration,

$1 \text{ mM cm}^{-3}$ , or  $200 \text{ mA cm}^{-2} \text{ sec}^{1/2}$ . It has been experimentally observed that, in propylene carbonate solutions where transition time measurements can be made, the limiting current for the process in quiet solution is about one-fifth the magnitude of  $iT^{1/2}$ , or, in this case,  $40 \text{ mA cm}^{-2}$ .

We believe the results of this series of, admittedly, rather crude measurements, rather strongly suggests the inherent electrokinetic reversibility of the lithium electrode. It seems likely that apparent polarization may reflect  $iR$  drop or concentration polarization rather than electrokinetic irreversibility.

Further studies on the discharge of bulk lithium metal will not be made until the necessary experimental refinements can be made. We anticipate making such measurements in starved electrolyte configurations and will be particularly interested in observing the effects of concentration polarization in limiting the maximum discharge rate of lithium and other active metals.

b. Lithium Deposition. It is our objective to be able to deposit coherent, stable lithium electrodeposits with a capacity of  $10 \text{ mA-hr cm}^{-2}$  ( $36,000 \text{ mC cm}^{-2}$ ) at a current of  $10 \text{ mA cm}^{-2}$ . To our knowledge, no one has yet reached this goal. It is apparent that a more detailed examination of the deposition process must be undertaken. It is desirable that a number of systems receive preliminary study, and the more detailed work then be done only with those systems which seem most like to be successful.

In an earlier section of this report, II-E (Electrochemical Characterization), important variations between different electrolytes were discussed. It was further noted that the electrochemical behavior was quite markedly dependent on the nature of the electrode substrate.

In this section of the report we shall discuss in more detail the effect of electrode substrate on deposition efficiency, a topic which was only cursorily examined in Section II-E. In effect, this work then

constitutes a preliminary screening of electrode substrates.

It would appear that the most desirable type of experiment to be performed would simply be an attempt to examine different systems with respect to the degree to which the objectives outlined in the first paragraph above are realized. That is, simply cathodize an electrode at  $10 \text{ mA cm}^{-2}$  for 1 hr, and then reverse the current and see how much lithium can be recovered. Long term experiments of this type are especially sensitive to the morphology of the lithium deposit. Thus, in some cases, the lithium may deposit in the form of fine black dendrites (as in  $\text{LiAlCl}_4/\text{PC}$  solutions) which, in excess electrolyte, become physically detached from the electrode. In other cases (as in  $\text{LiClO}_4/\text{PC}$  solutions), a fine, adherent gray deposit forms. Since it is likely that the morphology of the deposit will be sensitive to the actual operating cell environment, it would appear that long term experiments in excess electrolyte do not truly reflect the relative merits of different solvents. Thus we have avoided long term experiments, not only because such phenomena as deposit morphology may obscure more important basic electrochemical differences between systems, but also to conserve time. Given a certain amount of time for examination of each system, it is, we believe, more instructive to perform a series of short-term experiments, rather than one or two long term experiments.

Three types of screening experiments are performed, as described below. Needless to say, the particular type of experiment to be performed is somewhat arbitrary. However, it is our experience that the experiments described below do establish, quite clearly, a pattern of behavior and emphasize the important variations between different systems. This is, of course, the objective of initial screening.

Procedure 1: Anodic utilization vs. current (Q constant).

These experiments are performed in stirred solution. The current at which



deposition is performed is different for each run, but the total time elapsed is such that the total amount of deposition,  $Q$  ( $\text{mC cm}^{-2}$ ), is the same for each run. Anodic utilization is determined by reversing the current and is plotted vs.  $i$  ( $\text{mA cm}^{-2}$ ), the current of deposition. As will be observed from the data, we normally do such runs for depositions of only about  $500 \text{ mC cm}^{-2}$ , which is only a little more than 1% of the desired objective.

Procedure 2: Anodic Utilization vs.  $Q$  ( $i$  constant). These experiments are also performed in stirred solution. The current is the same for each run, but the time of deposition is varied to give different amounts of deposition. Anodic utilization is determined by subsequent current reversal and plotted vs.  $Q$  ( $\text{mC cm}^{-2}$ ).

Procedure 3: Anodic Utilization vs.  $it^{1/2}$ . The significance of this type of experiment is most open to debate. While the experiments constitute only the most preliminary type of screening there does exist a logical rationale for their performance. This will be discussed later in connection with the actual data. In the experiments current between  $0.6$  and  $10 \text{ mA cm}^{-2}$  are applied to the electrode in successive runs. The cathodizations are done in quiet solution and the current interrupted at varying periods of time between  $4$  and  $36 \text{ sec}$ . In this procedure we are only interested in the product,  $it^{1/2}$ , the current time the square root of the elapsed time of cathodization. Anodic utilization is determined by current reversal, and is plotted vs.  $it^{1/2}$ .

In Table 3 below, are shown the specific experiments performed. The experiment no. is given for convenience in subsequent discussion, and does not reflect the chronology of the experiments. The number given in parentheses after the symbol for the metal used as the electrode, gives the maximum anodic utilization obtained for the system. The number given after this is the number of experiments actually performed.

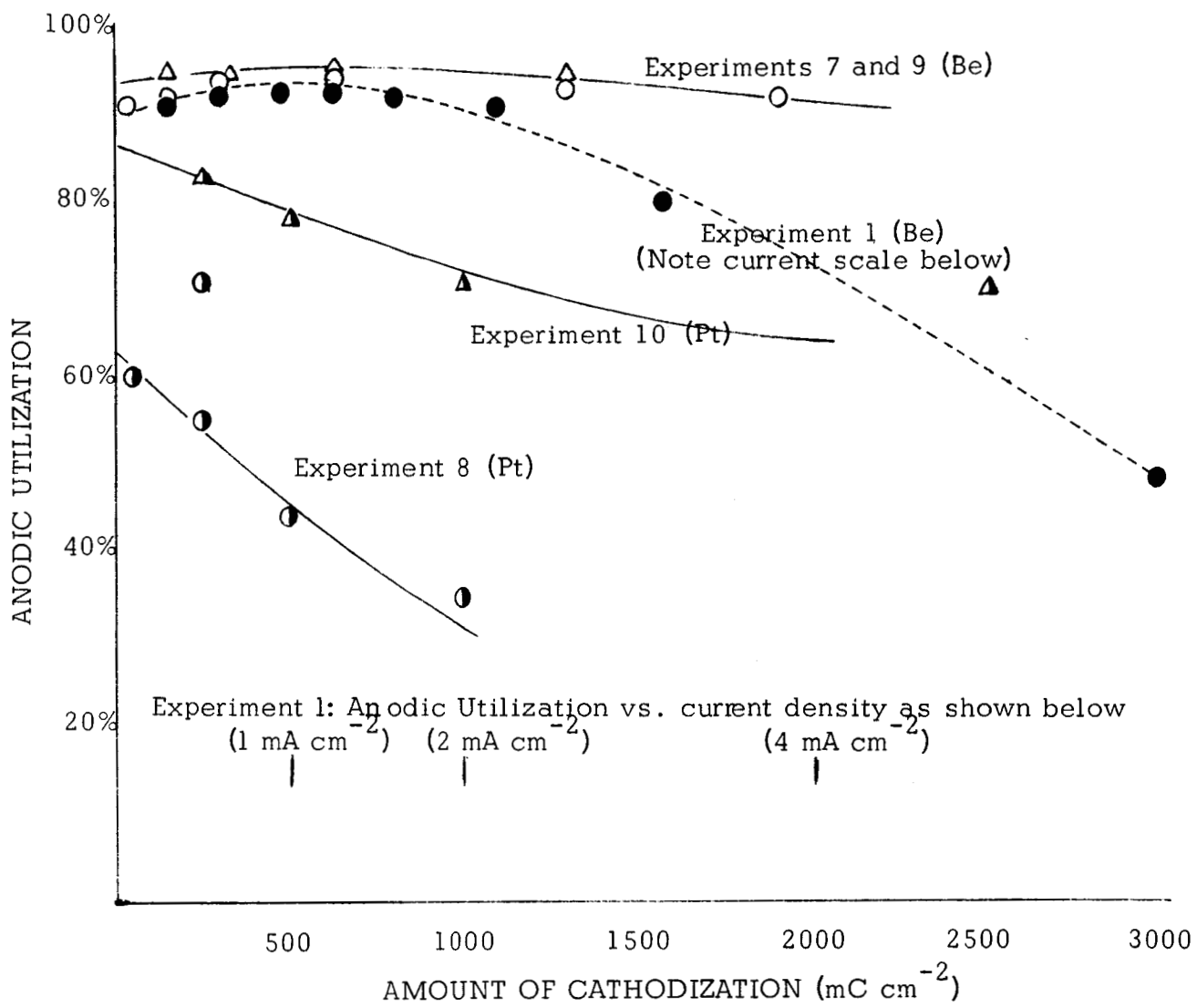
Table 3  
Lithium Anodic Utilization: Substrate Effects

Solution	Procedure 1 (Util. vs. i)	Procedure 2 (Util. vs. Q)	Procedure 3 (Util. vs. it <sup>1/2</sup> )
0.1 M LiBF <sub>4</sub> /PC <sup>a</sup>	1-Be (93%)-8	7-Be (95%)-6 8-Pt (70%)-5	
0.1 M LiBF <sub>4</sub> /PC <sup>b</sup>		9-Be (95%)-4 10-Pt (83%)-4	
0.1 M LiBF <sub>4</sub> /PC <sup>c</sup>	2-Be (95%)-6 3-Al (86%)-6 4-Pt (88%)-6 5-Cu (45%)-10		
0.1 M LiClO <sub>4</sub> /PC <sup>b</sup>	6-Be (70%)-6	11-Be (78%)-7	
0.1 M LiBF <sub>4</sub> /BL		12-Be (94%)-13	15-Be (88%)-17
LiCl (sat'd)/PC <sup>b</sup>			16-Be (58%)-6
0.1 M LiAlCl <sub>4</sub> /PC <sup>b</sup>		13-Be (38%)-5 14-Pt (53%)-5	17-Be (72%)-6 18-Pt (72%)-6

a, b, and c were successive 1000-ml. fractions of PC obtained on vacuum distillation.

Figure 17 shows the results of experiments 1, 7, 8, 9, and 10. The limiting current in this 0.1 M LiBF<sub>4</sub> solution should be 10-20 mA cm<sup>-2</sup>. Note the reduction in efficiency on beryllium at currents substantially below this value. Note, also, that at capacities up to 2000 mC cm<sup>-2</sup> anodization utilization on beryllium remains at 90-95%, whereas, on platinum a marked decrease is observed with increasing capacity but that, with platinum there is also a pronounced difference with the two samples of propylene carbonate used.

Experiments 2, 3, 4, and 5 compare four electrode materials and the results are shown in Figure 18. Note the markedly lower



DEPOSITION OF LITHIUM ON BERYLLIUM AND PLATINUM

Figure 17

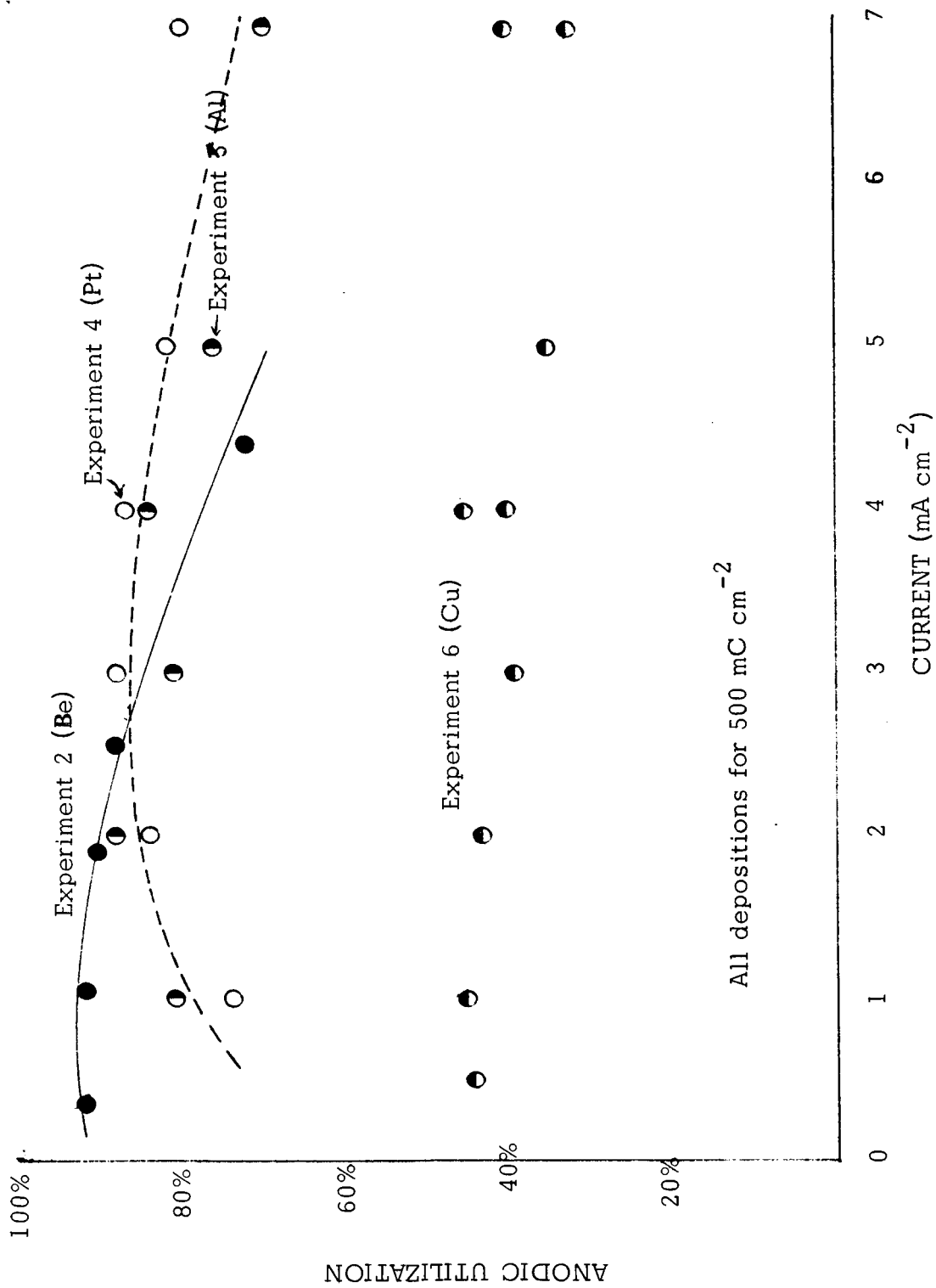


Figure 18

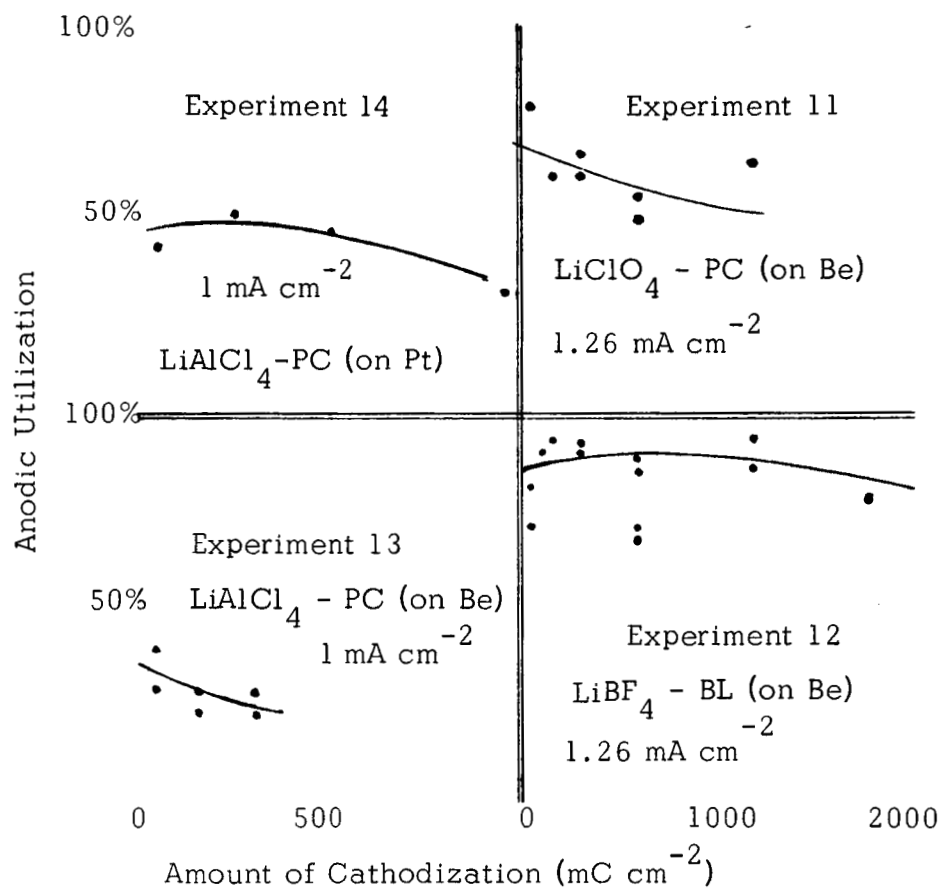
efficiency on copper. Note, also, that an apparent difference between beryllium on one hand and aluminum and platinum on the other seems to be in the increased efficiency at lower currents on beryllium.

Experiments 11, 12, 13, and 14 are shown in Figure 19. Clearly, the results of experiments 11, 12, and 13 are not very good in that the scatter of data is too great to allow a reasonable curve to be drawn.

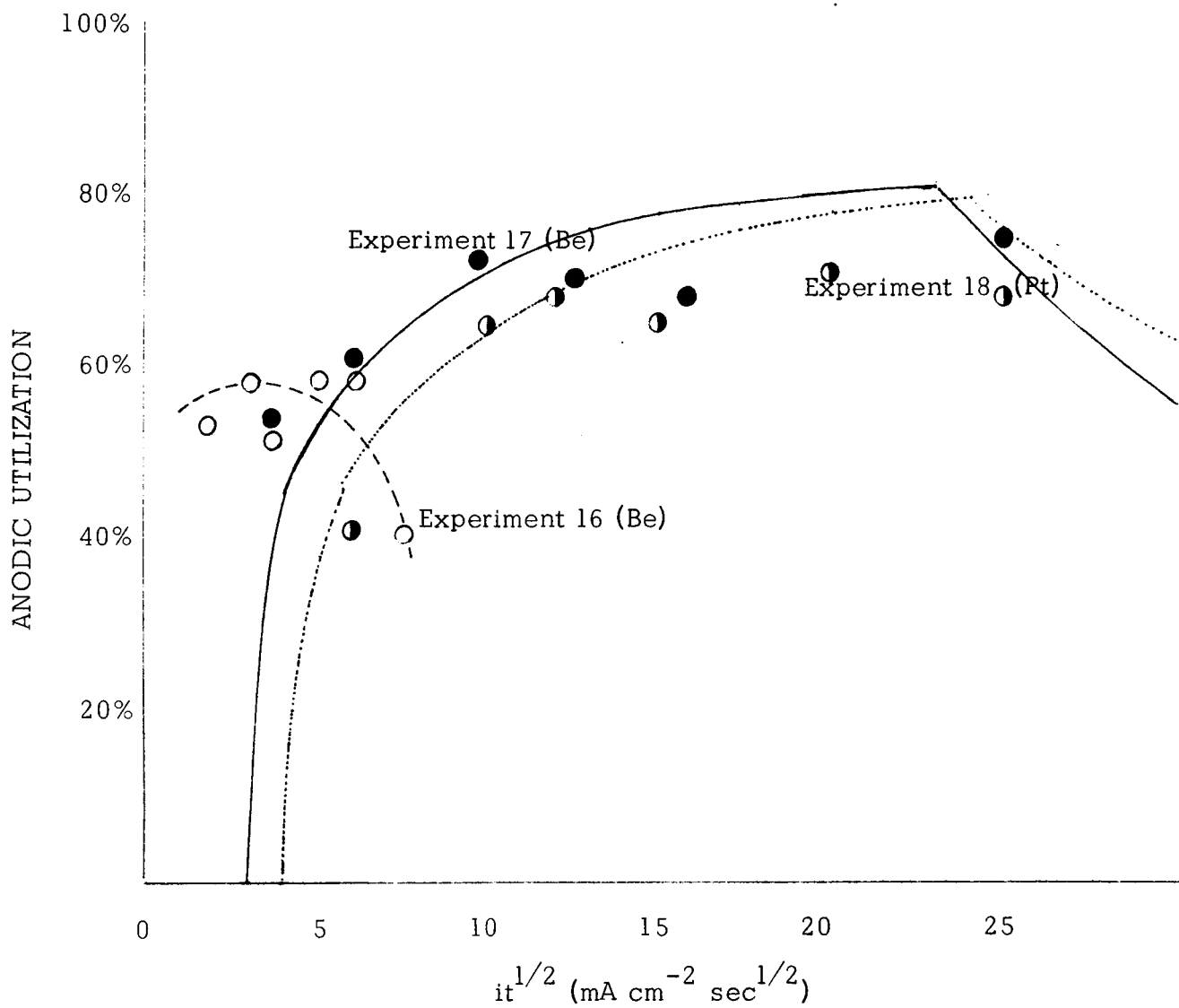
The results of experiments 16, 17, and 18 are shown in Figure 20. These are the anodic utilization vs.  $it^{1/2}$  experiments and further comment is necessary concerning the significance of such experiments. We focus attention on experiments 17 and 18. Of concern is the fact that during lithium deposition there may be concurrent parasitic reductions. For clarity we consider a 0.1 M lithium salt solution in propylene carbonate. The value for  $iT^{1/2}$  will be  $20 \text{ mA cm}^{-2} \text{ sec}^{1/2}$ . Now suppose there is present in solution impurity, such as water, which is reduced more easily than lithium. Let it be further supposed that the concentration of this impurity is such that if a chronopotentiogram could be obtained,  $iT^{1/2}$  would be  $3 \text{ mA cm}^{-2} \text{ sec}^{1/2}$ . If the effective diffusion coefficient were the same as for the lithium ion, this would correspond to a concentration of 0.015 M if the reduction involved only one electron. The solid line in Figure 20 shows what the anodic utilization vs.  $it^{1/2}$  curve should look like. At values of  $it^{1/2}$  less than  $3 \text{ mA cm}^{-2} \text{ sec}^{1/2}$ , no lithium will be deposited, regardless of the current density. At values of  $it^{1/2}$  larger than this amount an increasing fraction of the current will be consumed by lithium reduction. The dotted line in Figure 20 shows the theoretical predictions if the  $iT^{1/2}$  for the reducible impurity were 4 instead of  $3 \text{ mA cm}^{-2} \text{ sec}^{1/2}$ . The theoretical predications are based on theory<sup>(3)</sup>. While such an analysis is, of course, subject to many qualifications, it may offer some

---

(3) P. Delahay, New Instrumental Methods in Electrochemistry, Interscience N. Y. 1954, pp. 189-191.



DEPOSITION OF LITHIUM ON BERYLLIUM AND PLATINUM



LITHIUM DEPOSITION ON BERYLLIUM AND PLATINUM

Figure 20

insight into what actually does happen during cathodization. At any rate, our knowledge of the processes occurring during cathodization of lithium salt solutions will not be complete until the phenomena represented by the appearance of the  $it^{1/2}$  vs. anodic utilization are ascertained.

c. Conclusions.

It will be apparent, from the preceding discussion, that the cyclability of the lithium electrode is sensitive to the environment -- the electrolyte and the electrode substrate. The cycling behavior in the starved electrolyte environment characteristic of operating cells may be quite different. It is essential that the cycling behavior of the lithium electrode be studied under such conditions. We anticipate the performance of such experiments in the near future, using appropriately constructed laboratory cells. These will approximate the conditions extant in an operating cell, in that only a minimal amount of electrolyte will be used.

III-B-2. Electrochemical Reversibility: Cathodes

a. Cycling of Copper and Cobalt Metals.

These experiments are to consist in performing anodic-cathodic cycling on metallic copper and cobalt electrodes. Previous data were reported in the Second Quarterly Report. No new data have been obtained during the third quarter.

b. Discharge of Cathode Salts.

It was our objective to screen various electrolytes with respect to their relative propensity to enhance or inhibit the discharge of  $CuF_2$ . We intended to perform such screening experiments by observing the complete discharge of  $CuF_2$  at various current densities.

It was first necessary to develop a satisfactory "screening electrode". It was essential that such an electrode be inherently



capable of discharge at moderate rates ( $1 - 10 \text{ mA cm}^{-2}$ ), and that the electrode be easily and reproducibly constructed. We anticipated the use of an electrode support structure of the kind described in Appendix III, in which one could simply compress a mix of conductor and active material. Since nothing is yet known about the inherent electrochemical behavior of  $\text{CuF}_2$ , we anticipated that the data obtained might be subject to question unless certain preliminary points were considered. We attempted to anticipate some of these problems by concurrently studying the discharge of  $\text{AgCl}$ . The essential question is: To what degree does a discharge curve obtained for uncharacterized active materials, operating in largely uncharacterized electrolytes, actually reflect any useful electrochemical information?

(1) Discharge of  $\text{AgCl}$ . Discharge of  $\text{AgCl}$  electrodes was undertaken because of our doubts concerning:

(a) The basic validity of the measurements. That is, may simple corrections for  $iR$  drop be applied, as was true for the flat, lollipop electrodes, or does the electrode itself contribute seriously to the total resistance?

(b) Structural problems. That is, is the inherent structure of the electrode sufficiently sound that one may be reasonably confident that low efficiencies are not simply due to structural collapse with resultant loss of electrical contact?

(c) Conductivity problems. That is, to what degree is it likely that the evident loss in efficiency results from the failure of ions to move sufficiently rapidly through the electrode to neutralize the ionic charge produced on discharge of the active material?

(d) Parasitic reductions. That is, to what degree is it likely that, at low current densities, apparently high efficiencies reflect

concurrent parasitic reduction of impurities in the electrolyte and impurities imbedded in the electrode?

Ag-Cl electrodes were prepared by evenly distributing over the platinum substrate in the recess of the electrode support a mix of silver powder and silver chloride. The material was pressed at 1500 lb. Initial discharges were conducted in aqueous solution. The results are shown in Table 4 below:

Table 4  
Discharge of AgCl in Aqueous Solution

<u>Electrode Number</u>	<u>Solution</u>	<u>Weight Ratio Ag:AgCl</u>	<u>Theoretical Electrode Capacity (mA-hr cm<sup>-2</sup>)</u>	<u>Discharge Current (mA cm<sup>-2</sup>)</u>	<u>Efficiency</u>
Ag-1	H <sub>2</sub> O/HCl <sup>(1)</sup>	1:3	17	61	99%
Ag-2	"	1:1	17	61	102%
Ag-3	"	0:1	17	61	98%
Ag-4	"	1:9	17	61	96%
Ag-5	"	1:50	17	61	98%
Ag-6	"	1:20	17	61	98%
Ag-7	"	(2)	17	61	42% electrode lifted off
Ag-8	"	"	17	61	99%
Ag-9	"	1:20 <sup>(3)</sup>	17	61	96%
Ag-10	"	1:20 <sup>(4)</sup>	17	61	97%
Ag-11	"	1:20 <sup>(5)</sup>	17	17	77%
Ag-14	"	1:20	17	17	102%

- (1) Aqueous, 1 M HCl
- (2) About 1% by weight of graphite, instead of silver powder
- (3) Added 4% by weight of Teflon molding powder as a binder
- (4) Added 8% by weight of Teflon molding powder as a binder
- (5) Pressed nickel screen into the mix. Evident loss of AgCl through reaction with the nickel screen.

Table 4 (continued)

Electrode Number	Solution	Weight Ratio Ag:AgCl	Theoretical Electrode Capacity (mA-hr cm <sup>-2</sup> )	Discharge Current (mA cm <sup>-2</sup> )	Efficiency
Ag-12	H <sub>2</sub> O/LiCl <sup>(1)</sup>	1:20 <sup>(2)</sup>	17	61	0% (gassing)
Ag-13	"	1:20 <sup>(2)</sup>	17	1.1	60%
Ag-22	"	1:1	17	17	88%
Ag-40	"	1:10	34	34	75%
Ag-42	"	1:10	37	34	67%
Ag-38	"	1:10	8.5	34	80%
Ag-41	"	1:10	34	17	95%
Ag-43	"	1:10	17	17	93%
Ag-37	"	1:10	8.5	17	88%
Ag-39	"	1:10	34	8.5	97%
Ag-44	"	1:10	17	8.5	99%
Ag-36	"	1:10	8.5	8.5	97%
Ag-35	"	1:10	8.5	4.3	97%

- (1) Dilute aqueous LiCl solution, ca. 0.04 M. The measured specific resistance was 290-ohm cm. This gives a conductivity commensurate with those which obtain in non-aqueous electrolytes.
- (2) Nickel screen pressed into the mix.

---

The high rate discharges in aqueous HCl would seem to attest to the basic structural integrity of the electrode. The somewhat lower efficiencies at high currents in the dilute LiCl solution probably reflect concentration polarization within the electrode.

Similar AgCl electrodes were then discharged in propylene carbonate, 1 M in LiBF<sub>4</sub>, the measured conductivity of which, 290-ohm-cm was identical to that of the dilute LiCl solution. Transport properties may differ. The results are shown in Table 5 below. As observed in the Table, attempts to vary the mix ratio and the pressure did not effect significant improvement in efficiency.

Table 5

## Discharge of AgCl in Propylene Carbonate

<u>Electrode Number</u>	<u>Weight Ratio Ag:AgCl</u>	<u>Theoretical Capacity (mA-hr cm<sup>-2</sup>)</u>	<u>Discharge Current (mA cm<sup>-2</sup>)</u>	<u>Efficiency</u>	<u>Pressure</u>
Ag-17	1:20	17	17	3%	1500 lb
Ag-18	1:20	17	17	3%	400 lb
Ag-19	1:20	17	17	5%	150 lb
Ag-20	1:10	17	17	2%	1500 lb
Ag-23	1:10	17	17	2%	"
Ag-21	1:1	17	17	2%	"
Ag-24	1:1	17	17	2%	"

In order to get sufficiently large efficiencies to justify screening it was necessary to go to lower loading and lower discharge currents. The results of such discharges in various propylene carbonate solutions are shown in Table 6, below:

Table 6

Discharge of AgCl in Propylene Carbonate  
(Electrode Capacity = 8.5 mA-hr cm<sup>-2</sup>)

<u>Electrode Number</u>	<u>Solution</u>	<u>Weight Ratio Ag:AgCl:LiClO<sub>4</sub></u>	<u>Discharge Current (mA cm<sup>-2</sup>)</u>	<u>Efficiency</u>	<u>Comments</u>
Ag-25	LiBF <sub>4</sub>	1:20	8.5	10%	
Ag-26	"	1:20	1.4	80%	
Ag-37	"	1:10	8.5	10%	
Ag-45	"	1:10:1	8.5	20%	
Ag-48	LiAlCl <sub>4</sub>	1:10:1	8.5	13%	
Ag-27	LiBF <sub>4</sub>	1:10	4.2	27%	
Ag-46	"	1:10:1	4.2	35%	
Ag-49	LiAlCl <sub>4</sub>	1:10:1	4.2	24%	
Ag-59	MoPF <sub>6</sub>	1:10	4.2	10%	
Ag-50-51	KPF <sub>6</sub>	1:10	4.2	none	

Table 6 (Cont'd)

<u>Electrode Number</u>	<u>Solution</u>	<u>Weight Ratio</u> <u>Ag:AgCl:LiClO<sub>4</sub></u>	<u>Discharge Current</u> <u>mA Cm<sup>-2</sup></u>	<u>Efficiency</u> <u>Comments</u>
Ag-32	LiBF <sub>4</sub>	1:10	2.1	25%
Ag-60	MoPF <sub>6</sub>	1:10	2.1	45%
Ag-29	LiBF <sub>4</sub>	1:10	1.4	44%
Ag-28	LiBF <sub>4</sub>	1:10	1.0	48%
Ag-35	LiBF <sub>4</sub>	1:10	0.53	64%
Ag-47	"	1:10:1	0.53	87%
Ag-50	LiAlCl <sub>4</sub>	1:10:1	0.53	ca. 52% ill-defined
Ag-61	MoPF <sub>6</sub>	1:10	0.53	93%
Ag-34	LiBF <sub>4</sub>	1:10	0.18	91%
Ag-52	KPF <sub>6</sub>	1:10	0.1	38%

Table 7

Discharge of AgCl in BL, DMF, and AN

<u>Electrode Number</u>	<u>Solution</u>	<u>Weight Ratio</u> <u>Ag:AgCl</u>	<u>Theoretical Capacity</u> <u>(mA-hr cm<sup>-2</sup>)</u>	<u>Discharge Current</u> <u>(mA cm<sup>-2</sup>)</u>	<u>Efficiency</u>
Ag-67	DMF/LiBF <sub>4</sub> <sup>(1)</sup>	1:10	8.5	17	58%
Ag-66	"	1:10	8.5	8.5	58%
Ag-65	"	1:10	8.5	4.3	56%
Ag-58	BL/LiBF <sub>4</sub> <sup>(1)</sup>	1:10	8.5	17	60%
Ag-57	BL/LiBF <sub>4</sub>	1:10	8.5	8.5	63%
Ag-55	BL/LiBF <sub>4</sub>	1:10	8.5	4.3	60%
Ag-56	"	1:10	8.5	0.53	95%
Ag-69	AN/LiClO <sub>4</sub> <sup>(1)</sup>	1:10	8.5	8.5	23%
Ag-70	"	1:10	8.5	6.0	37%
Ag-68	"	1:10	8.5	4.3	56%
Ag-71	"	1:10	8.5	2.1	36%
Ag-62	BL/MoPF <sub>6</sub> <sup>(2)</sup>	1:10	8.5	4.3	18%
Ag-64	"	1:10	8.5	2.1	52%
Ag-63	"	1:10	8.5	0.53	87%

Table 7 (Cont'd)

<u>Electrode Number</u>	<u>Solution</u>	<u>Weight Ratio Ag:AgCl</u>	<u>Theoretical Capacity (mA-hr cm<sup>-2</sup>)</u>	<u>Discharge Current (mA cm<sup>-2</sup>)</u>	<u>Efficiency</u>
Ag-77	AN/MoPF <sub>6</sub> <sup>(2)</sup>	1:10	8.5	8.5	8%
Ag-75	"	1:10	8.5	8.5	11%
Ag-76	"	1:10	8.5	4.3	63%
Ag-78	"	1:10	8.5	6.0	12%
Ag-53	BL/KPF <sub>6</sub> <sup>(1)</sup>	1:10	8.5	4.3	negligible
Ag-54	"	1:10	8.5	0.2	14%
Ag-72	AN/KPF <sub>6</sub> <sup>(1)</sup>	1:10	8.5	0.53	8%

(1) Enough salt was added to make the solutions 1 M if totally soluble.

(2) Enough salt was added to make the solutions 0.25 M if totally soluble.

The results show a considerably more marked dependence on electrolyte than we had anticipated. We know of no simple explanation which will summarize the data in Tables 6 and 7. We believe a variety of specific interactions are indicated. One of the simplest considerations is the volume of products formed. In the reaction  $\text{AgX} + \text{Li}^{\bar{}} = \text{Ag} + \text{LiX}$  the volume of products, when  $\text{X} = \text{Cl}^{\bar{}}$ , is almost 20% greater than the volume of  $\text{AgCl}$ . However, if  $\text{X} = \text{NO}_3^{\bar{}}$ , the calculated volume of products is only a fraction of a percent larger than the volume of  $\text{AgNO}_3$ . Electrodes of  $\text{AgNO}_3$  were prepared in similar fashion and discharged in butyrolactone, 1 M in  $\text{LiBF}_4$ , with the results shown in Table 8 below:

Table 8

Discharge of  $\text{AgNO}_3$  in Butyrolactone

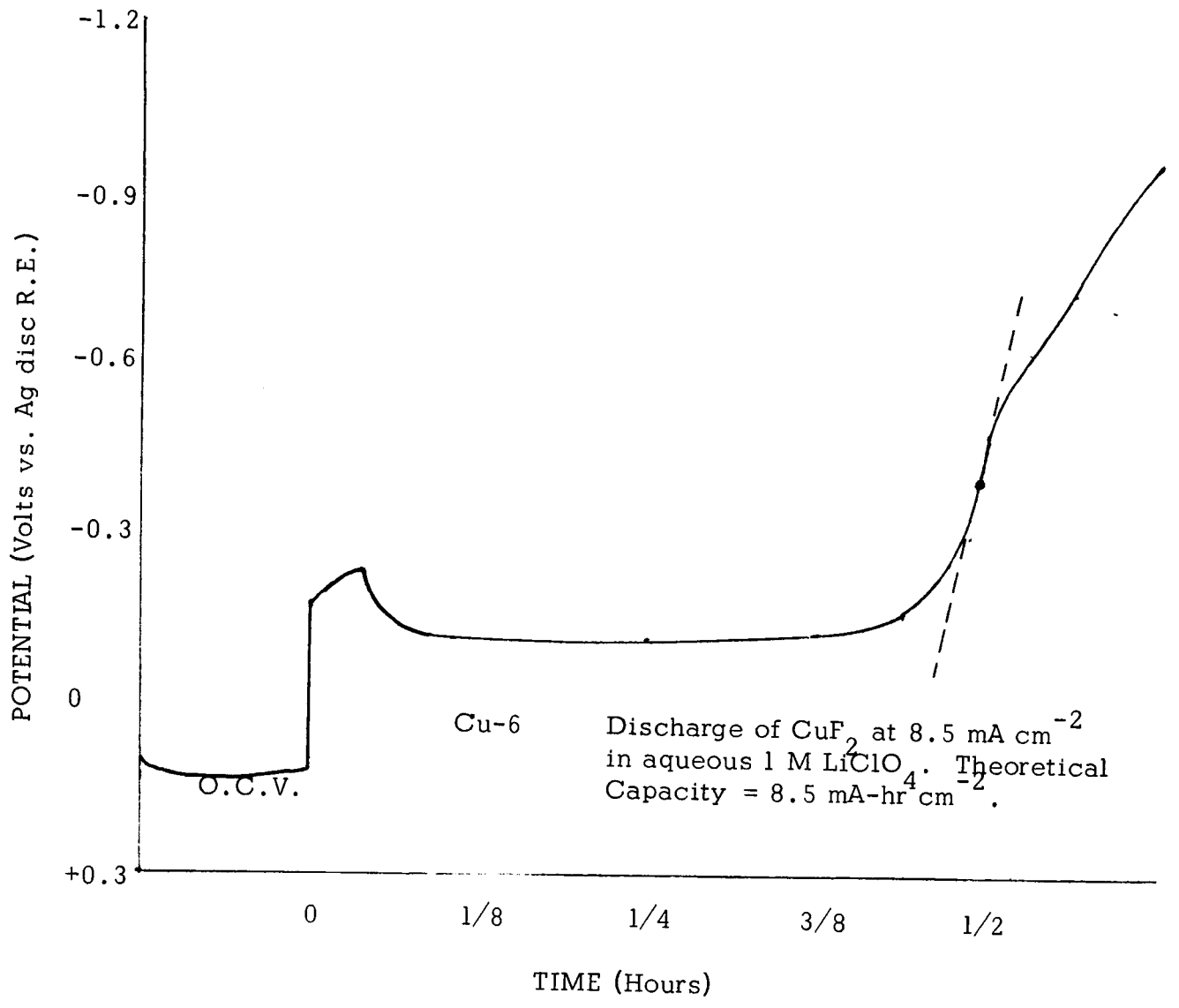
<u>Electrode Number</u>	<u>Weight Ratio Ag:AgNO<sub>3</sub></u>	<u>Theoretical Capacity (mA-hr cm<sup>-2</sup>)</u>	<u>Discharge Current (mA cm<sup>-2</sup>)</u>	<u>Efficiency</u>
Ag-81	1:20	8.5	8.5	90%
Ag-80	1:20	17	4.3	89%
Ag-79	1:20	17	1.0	86%

Discharge of AgCl: Conclusions. We are satisfied that the relatively simple method of electrode construction employed is at least adequate for a preliminary screening of electrolytes. The differences in performance noted are summarized below, where we consider the efficiency at only two current densities, 8.5 and 4.3 mA cm<sup>-2</sup> for the 1:10 mixes with 8.5 mA-hr cm<sup>-2</sup> theoretical capacity:

	Solvent			
	P.C.	B.L.	DMF	AN
Efficiency at:	8.5/ 4.3	8.5/4.3	8.5/4.3	8.5/4.3
<u>Solute</u>	<u>(mA cm<sup>-2</sup>)</u>	<u>(mA cm<sup>-2</sup>)</u>	<u>(mA cm<sup>-2</sup>)</u>	<u>(mA cm<sup>-2</sup>)</u>
LiBF <sub>4</sub>	10%/27%	63%/60%	58%/56%	--
LiClO <sub>4</sub>	--	--	--	23%/56%
KPF <sub>6</sub>	0%/0%	0%/0%	--	-- /3%
MoPF <sub>6</sub>	--/10%	--/18%	--	11%/63%

We believe the marked differences with different electrolytes indicates specific interactions rather than variations in the electrode fabrication. For example, the low efficiencies in KPF<sub>6</sub> solution may reflect the formation of passivating KCl films during discharge, and this phenomena may not occur as seriously with the lithium salt solutions.

(2) Discharge of CuF<sub>2</sub>. The same procedure was followed with CuF<sub>2</sub> as had proved successful with AgCl. Initial attempts were made to discharge a mix of CuF<sub>2</sub> and copper powder, pressed into the recess of the electrode support at 1500 lb, in an aqueous solution, 1 M in LiClO<sub>4</sub>. The solution was saturated with CuF<sub>2</sub> and the measured concentration of copper (II) in solution was about 0.01 M, which would correspond to a limiting current, in quiet solution, of about 1-2 mA cm<sup>-2</sup>. Various mix ratios were used, and it was found that a large excess of conducting material was required. This, of course, is completely unsatisfactory for an operating battery electrode, but it is allowable for a screening electrode. Most discharge curves had an appearance similar to that shown in Figure 21. The initial potential jump, we presume, represents the establishment



DISCHARGE OF  $\text{CuF}_2$

Figure 21



of uniform electrical contact throughout the electrode. The results are shown in Table 9, below. The potential along the level plateau is given when the discharge curve was sufficiently well-defined to give an unambiguous value.

Table 9  
Discharge of  $\text{CuF}_2$  in Aqueous  $\text{LiClO}_4$

<u>Electrode Number</u>	<u>Mix Ratio Cu:CuF<sub>2</sub></u>	<u>Capacity (mA-hr cm<sup>-2</sup>)</u>	<u>Discharge Current (mA cm<sup>-2</sup>)</u>	<u>Efficiency</u>	<u>Potential</u>
Cu-1	0:1	17	17	13%	
Cu-2	1:1	17	17	9%	
Cu-3	3:1	8.5	8.5	30%	
Cu-4	9:1	8.5	8.5	52%	-0.17 V
Cu-5	9:1	8.5	8.5	56%	-0.14 V
Cu-6(Fig 21)	9:1	8.5	8.5	50%	-0.12 V
Cu-12	9:1	8.5	8.5	61%	-0.09 V
Cu-14	9:1	8.5	8.5	61%	-0.1 V
Cu-15	9:1	8.5	8.5	47%	-0.06
Cu-16	9:1	8.5	8.5	43%	-0.06
Cu-20	9:1	8.5	4.3	40%	-0.01
Cu-20(1)	9:1	8.5	4.3	33%(1)	0.00
Cu-19	9:1	8.5	2.1	24%	+0.01
Cu-17	9:1	8.5	0.53	no potential break observed	
Cu-11	14:1	8.5	8.5	44%	-0.09
Cu-13	6:1	8.5	8.5	37%	-0.06
Cu-8	19:1	4.3	4.3	31%	-0.03
Cu-9	19:1	4.3	4.3	32%	-0.02
Cu-10	19:1	6.4	6.4	48%	-0.06
Cu-7	1:0 (no CuF <sub>2</sub> )	0	8.5	0	-0.75

(1) in  $\text{LiClO}_4$  solution without  $\text{CuF}_2$  saturation

The results were sufficiently consistent to justify use of the 9:1 mix for preliminary screening of non-aqueous electrolytes. The results shown in Table 10, below, were obtained in propylene carbonate, 1 M in  $\text{LiBF}_4$ .

Table 10

Discharge of  $\text{CuF}_2$  in Propylene Carbonate (1 M  $\text{LiBF}_4$ )

Electrode Number	Mix Ratio $\text{Cu}:\text{CuF}_2:\text{LiClO}_4$	Theoretical Capacity ( $\text{mA-hr cm}^{-2}$ )	Discharge Current ( $\text{mA cm}^{-2}$ )	Efficiency	Potential of Discharge Plateau
Cu-21	9:1:0	8.5	4.3	13%	
Cu-22(Fig 22)	9:1	8.5	4.3	13%	
Cu-23	9:1	4.3	4.3	23%	
Cu-24	9:1	8.5	0.53	no break observed	
Cu-25(Fig 22)	9:1	12.7	4.3	11%	-0.5 V
Cu-26	9:1	6.3	4.3	19%	-0.5 V
Cu-27	9:1:3	8.5	4.3	6% most of mix fell off	
Cu-28(Fig 23)	9:1:1	8.5	4.3	50%	-0.33 V
Cu-40	9:1:1	8.5	4.3	51%	
Cu-41	9:1:1	8.5	4.3	21% (1 drop of water added to mix)	
Cu-29	9:1:1	4.3	4.3	53%	-0.42 V
Cu-34	9:1:1	4.3	4.3	51%	-0.45 V
Cu-33	9:1:1	4.3	4.3	32%	(leached in P.C.)
Cu-32	9:1:1	4.3	8.5	47%	
Cu-31	9:1:1	4.3	0.35	17%	

Electrodes incorporating silver powder instead of copper, as the conducting additive, were discharged with the results shown in Table 11 below. These discharges were performed in propylene carbonate, 1 M in  $\text{LiBF}_4$ .

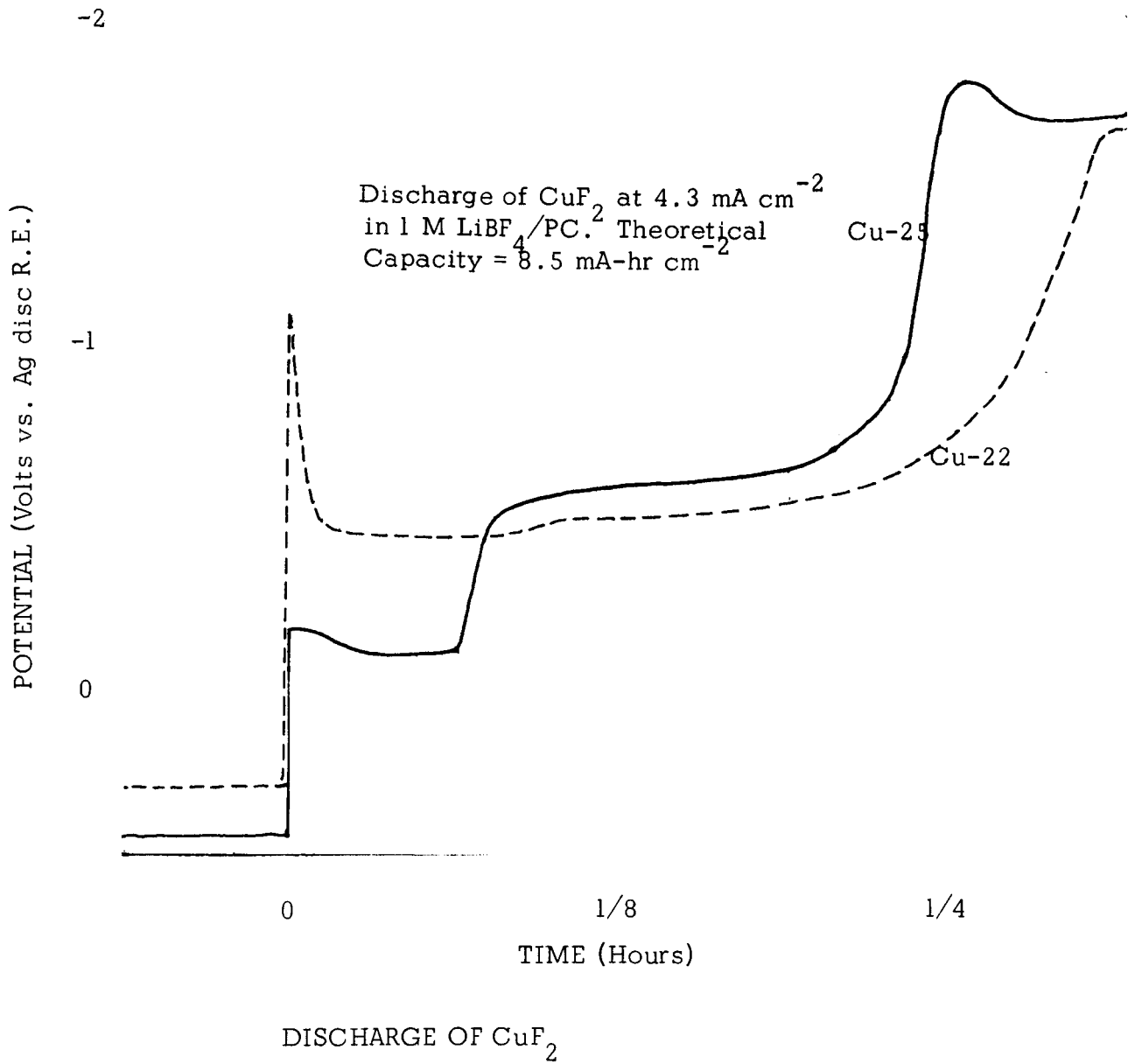
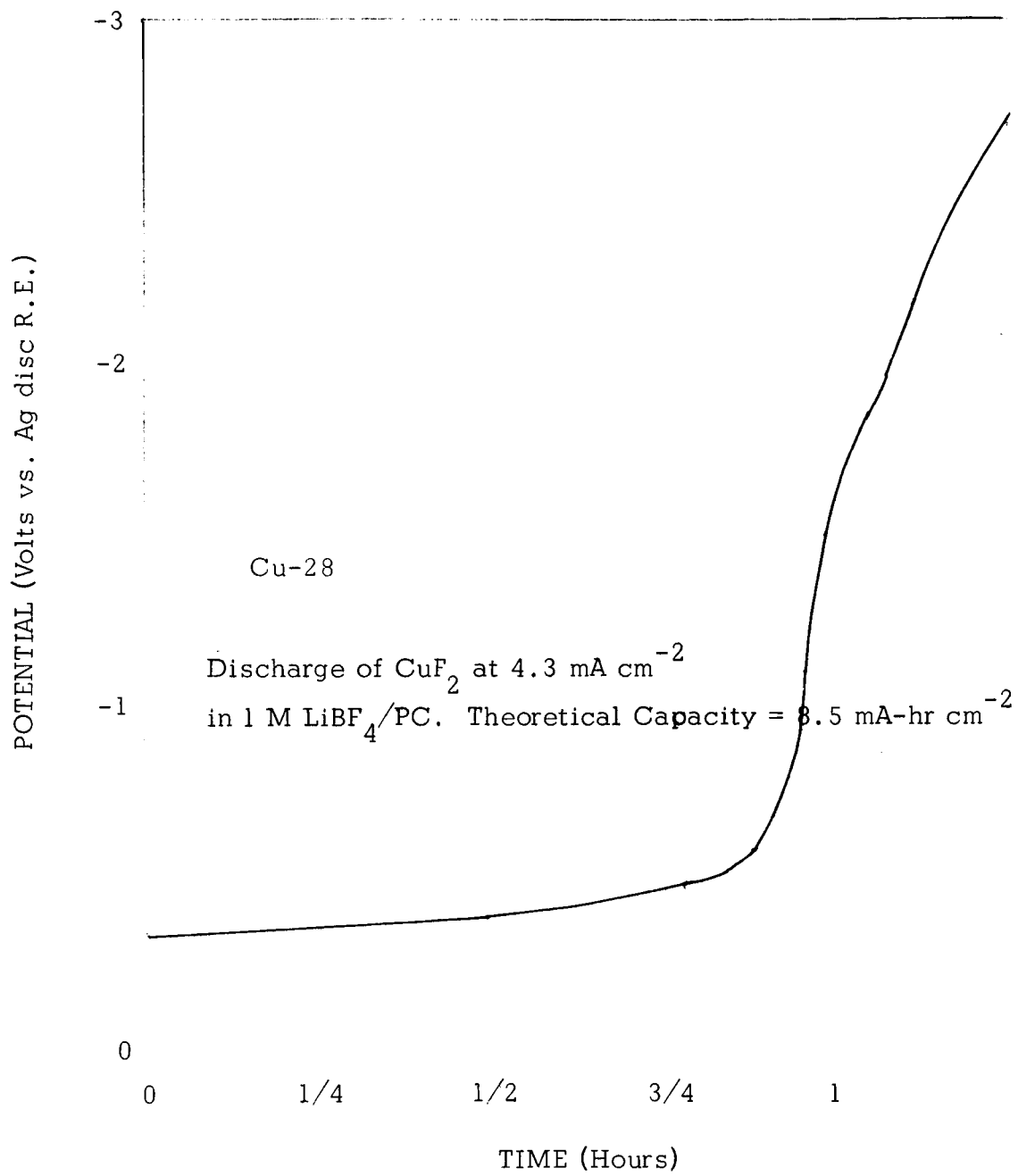


Figure 22



DISCHARGE OF  $\text{CuF}_2$

Figure 23

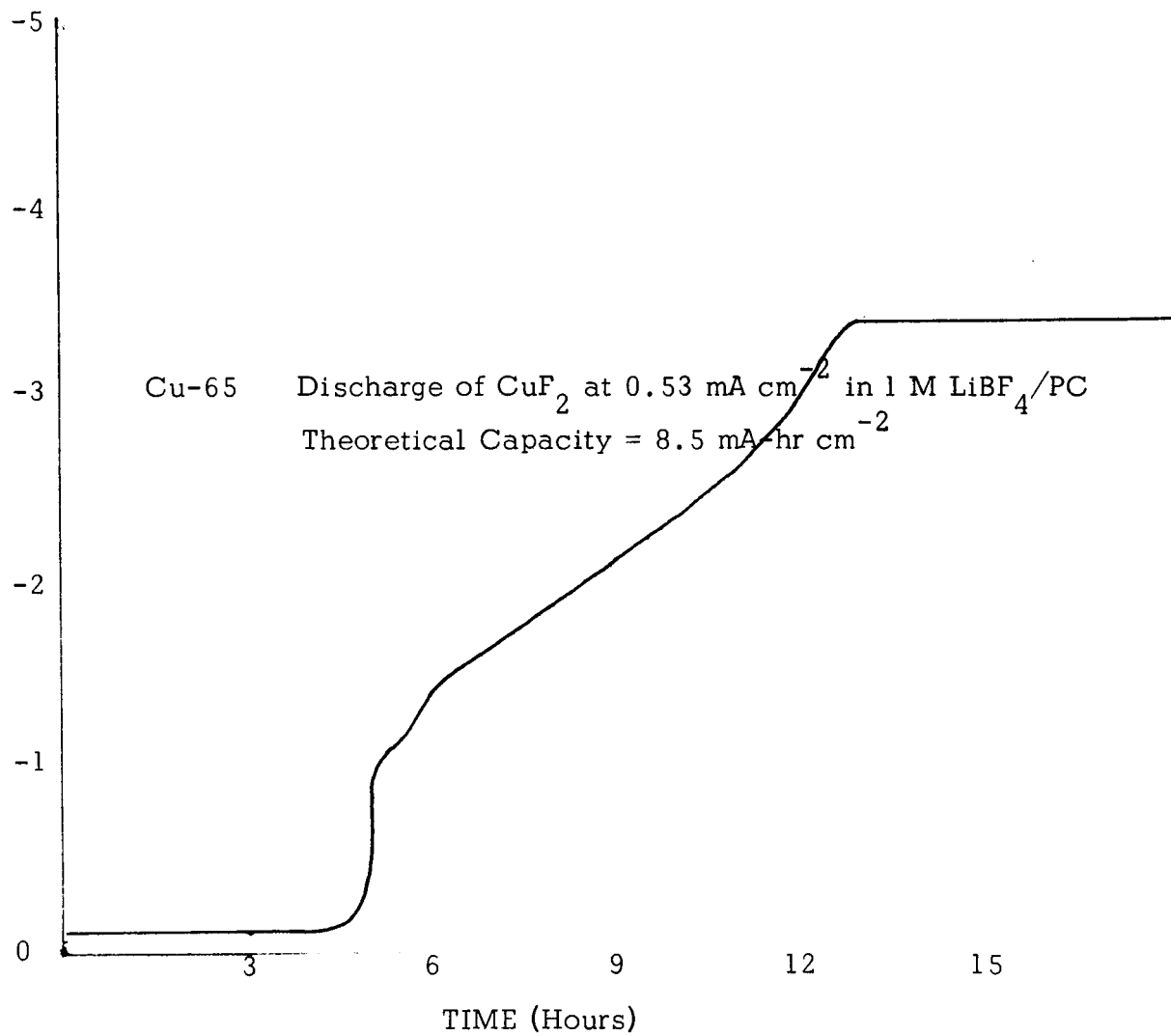
Table 11

Discharge of  $\text{CuF}_2$  (Ag Additive) in Propylene Carbonate

Electrode Number	Mix Ratio $\text{Ag}:\text{CuF}_2:\text{LiClO}_4$	Theoretical Capacity ( $\text{mA-hr cm}^{-2}$ )	Discharge Current ( $\text{mA cm}^{-2}$ )	Efficiency	Potential of Discharge Plateau
Cu-42	1:2:2	8.5	4.3	22%	
Cu-43	2:7:1	17	4.3	13%	(Cu screen pressed into mix)
Cu-44	2:7:1	17	4.3	23%	
Cu-45	1:8:1	17	4.3	7%	
Cu-46	1:8:1	17	4.3	4%	
Cu-47	3:6:1	17	4.3	21%	-0.45 - -0.55
Cu-48	2:7:1	17	8.5	10%	-0.85
Cu-49	2:7:1	17	4.3	22%	-0.5
Cu-50	2:7:1	17	1.0	17%	
Cu-51	2:7:1	34	8.5	11%	
Cu-54	6:3:1	8.5	8.5	22%	-0.8
Cu-52	6:3:1	8.5	4.3	29%	-0.5
Cu-56	6:3:1	8.5	4.3	26%	-0.45
Cu-53	6:3:1	8.5	2.1	31%	-0.35
Cu-55	6:3:1	8.5	2.1	26%	-0.35
Cu-57	6:3:1	8.5	1.0	24%	
Cu-63	6:3:1*	8.5	4.3	29%	-0.45
Cu-66(Fig 25)	6:3:1*	8.5	4.3	31%	-0.4
Cu-64	6:3:1*	8.5	1.0	37%	-0.1 - -0.2 V
Cu-67	6:3:1*	8.5	1.0	39%	-0.2 V
Cu-65(Fig 24)	6:3:1*	8.5	0.53	29%	-0.1 V
Cu-68	8:1:1*	4.3	4.3	47%	
Cu-69	8:1:1*	4.3	0.53	28%	

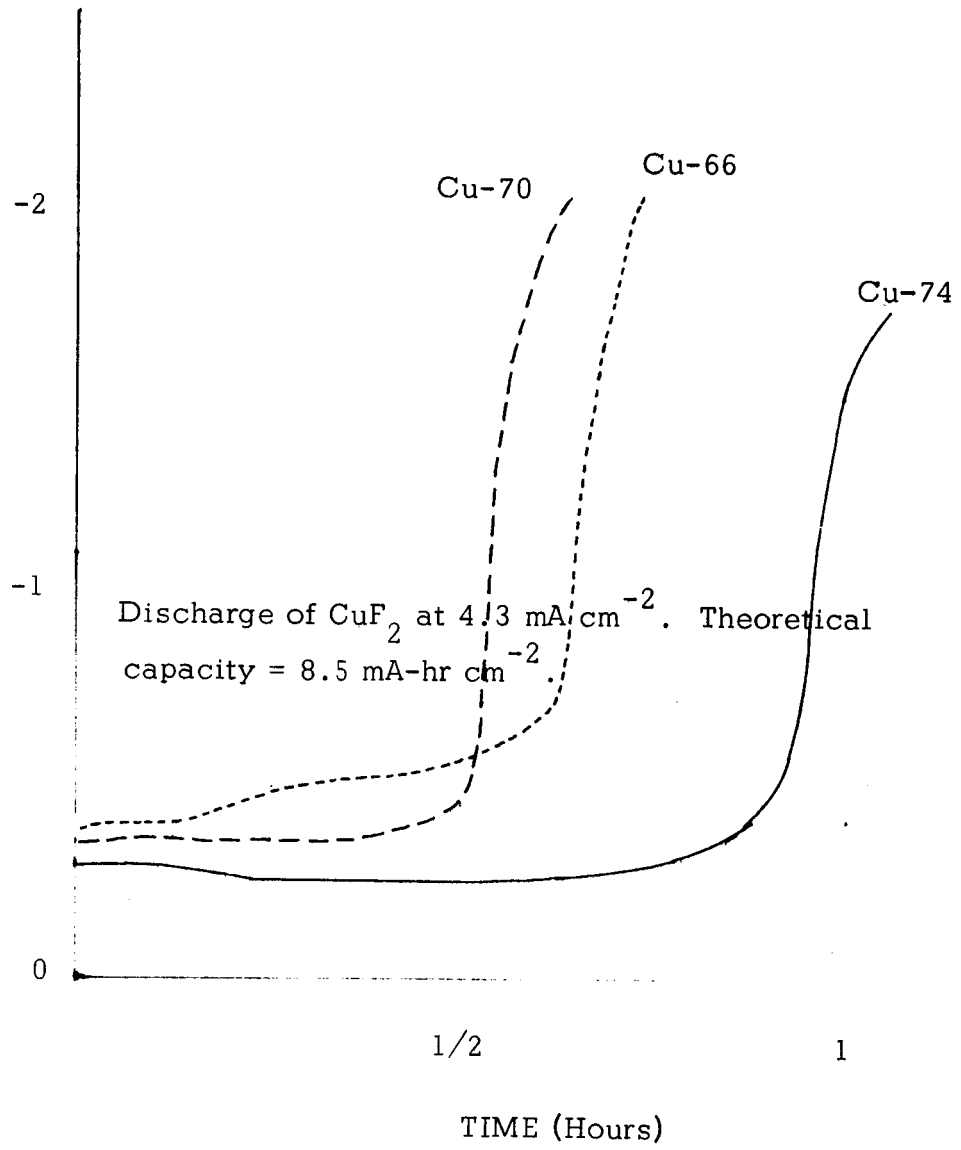
\* Pressed platinum screen into mix

The same type of electrode was used for an examination of other electrolytes as shown in Table 12, below.



DISCHARGE OF  $\text{CuF}_2$

Figure 24



DISCHARGE OF  $\text{CuF}_2$

Figure 25

Table 12  
Discharge of  $\text{CuF}_2$  in Other Electrolytes

Electrode Number	Solution	Mix Ratio $\text{Ag}:\text{CuF}_2:\text{LiClO}_4$	Theoretical Capacity ( $\text{mA cm}^{-2}$ )	Discharge Current ( $\text{mA cm}^{-2}$ )	Efficiency
Cu-61	PC/KPF <sub>6</sub>	2:7:1	17	0.53	5%
Cu-62	PC/KPF <sub>6</sub>	2:7:1	17	1.0	4%
Cu-72	BL/LiBF <sub>4</sub>	6:3:1	8.5	17	22%
Cu-71	"	6:3:1	8.5	8.5	23%
Cu-70(Fig 25)	"	6:3:1	8.5	4.3	26%
Cu-73	"	(1)	8.5	4.3	24%
Cu-75	"	(2)	17	4.3	49%
Cu-76	"	(2)	17	1.0	39%
Cu-74(Fig 25)	"	(2)	8.5	4.3	45%
<p>(1) Graphite instead of silver in mix. Ratio = 0.5:3:1  (2) Acetylene black instead of silver in mix. Ratio = .5:3:1</p>					
Cu-77	PC/MoPF <sub>6</sub>	6:3:1	8.5	2.1	32%
Cu-78	"	6:3:1	8.5	4.3	24%
Cu-79	AN/LiClO <sub>4</sub>	6:3:1	8.5	17	45%
Cu-78	"	6:3:1	8.5	8.5	46%
Cu-77	"	6:3:1	8.5	4.3	45%
Cu-81	"	6:3:1	8.5	2.1	49%
Cu-82	AN/KPF <sub>6</sub>	6:3:1	8.5	4.3 negligible	
Cu-83	"	6:3:1	8.5	0.5 negligible	
Cu-84	AN/MoPF <sub>6</sub>	6:3:1	8.5	4.3	11%
Cu-85	"	6:3:1	8.5	8.5	8%

Discharge of  $\text{CuF}_2$ : Conclusions. As with the  $\text{AgCl}$ , differences in efficiency obtained in the different electrolytes. This is summarized below; for the  $8.5 \text{ mA-hr cm}^{-2}$ , 6:3:1 electrodes.

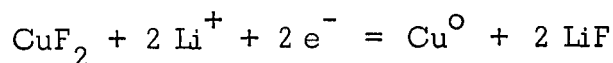


	Solvent			
	P.C.	B.L.	DMF	AN
Efficiency at:	8.5 / 4.3	8.5 / 4.3	8.5 / 4.3	8.5 / 4.3
<u>Solute</u>	<u>(mA cm<sup>-2</sup>)</u>	<u>(mA cm<sup>-2</sup>)</u>	<u>(mA cm<sup>-2</sup>)</u>	<u>(mA cm<sup>-2</sup>)</u>
LiBF <sub>4</sub>	22% / 29%	23% / 26%	--	--
LiClO <sub>4</sub>	--	--	--	46% / 45%
KPF <sub>6</sub>	negligible	--	--	negligible
MoPF <sub>6</sub>	-- / 24%	--	--	8% / 11%

An important difference between the discharge of CuF<sub>2</sub> and AgCl is that the efficiencies for discharge of CuF<sub>2</sub>, in general, seem independent of the current. This is surprising and suggests inherent structural limitations. It is reassuring that CuF<sub>2</sub> may be discharged with quite reasonable efficiency at such high current densities. This suggests, we believe, that there are no inherent problems in discharging a cathode salt in these relatively poorly conducting non-aqueous media, due to the inability of ions to leave or enter the porous electrode at a sufficiently rapid rate.

Much more work remains to be done with the CuF<sub>2</sub> electrode. The nature of the discharge products must be ascertained. The potential observed during discharge must be examined more critically for evidence of activation and concentration polarization. Finally, the discharge must be examined in starved electrolyte.

The question of cyclability remains unanswered. However, knowing that LiF is relatively insoluble, one expects this salt to precipitate during discharge within the pores of the electrode by the reaction:



On subsequent charge one may consider the simplest reaction to be simply the formation of Cu<sup>++</sup>. Now, if CuF<sub>2</sub> is more insoluble than LiF, the lithium

should be displaced from the insoluble fluoride, leaving  $\text{CuF}_2$  as the final product of charge. Efficient cycling, based on this process, will, of course, involve a rather subtle balance of many factors. However, it must be considered to be a reasonable phenomena and one which, indeed, must be induced. Far too little is yet known about the nature of the processes and the properties of the materials to indicate what should be done to induce the phenomenon. We consider it a major objective in our work to find out to what degree this phenomenon may be used to develop cyclable cathodes.

### III-C. Solubility Studies

Four solvents, butyrolactone, propylene carbonate, dimethylformamide, and acetonitrile, have been used to prepare mixtures of solvent and one of the following salts:  $\text{AgCl}$ ,  $\text{CuF}_2$ ,  $\text{CoF}_3$ ,  $\text{MgCl}_2$ ,  $\text{MgCl}_2$ ,  $\text{MgF}_2$ ,  $\text{LiCl}$ , and  $\text{KCl}$ . An amount of salt was added to make the solution 0.1 M in the salt if totally soluble.

To date only the  $\text{LiCl}$ ,  $\text{KCl}$ ,  $\text{MgCl}_2$ , and  $\text{MgF}_2$  solutions have been examined. The specific conductance was measured. The  $\text{LiCl}$  and  $\text{MgCl}_2$  solutions were further examined for the concentration of total chloride. This was done by conductimetric titration with a dilute  $\text{AgClO}_4$  solution. The concentrations of salt shown below are based on the measured concentration of chloride. The concentration of the  $\text{KCl}$  solutions was determined by diluting 5 ml. of the non-aqueous solution to 100 ml. with water. The conductance of this solution was used to calculate the concentration of  $\text{KCl}$ , using the literature value for the equivalent conductance of  $\text{KCl}$  in aqueous solution. It was assumed that the effect of the non-aqueous solvent in the diluted solution did not significantly affect the measured conductance. The results are shown below:

Table 13  
Solubility Studies

System	Conductance (ohm <sup>-1</sup> cm <sup>-1</sup> )	Concentration (M l <sup>-1</sup> )
LiCl/PC	2.17 x 10 <sup>-4</sup>	0.055
LiCl/BL	--	soluble
LiCl/DMF	--	soluble
LiCl/AN	4.3 x 10 <sup>-4</sup>	0.027
KCl/PC	9.5 x 10 <sup>-6</sup>	0.00058
KCl/BL	1.4 x 10 <sup>-5</sup>	0.00063
KCl/DMF	1.5 x 10 <sup>-4</sup>	0.0018
KCl/AN	2.1 x 10 <sup>-5</sup>	0.000124
MgCl <sub>2</sub> /PC	9.1 x 10 <sup>-4</sup>	0.088
MgCl <sub>2</sub> /BL	7.2 x 10 <sup>-4</sup>	0.091
MgCl <sub>2</sub> /DMF	4.3 x 10 <sup>-3</sup>	0.0925
MgCl <sub>2</sub> /AN	5.9 x 10 <sup>-4</sup>	0.0118
MgF <sub>2</sub> /PC	2.4 x 10 <sup>-7</sup>	--
MgF <sub>2</sub> /BL	2.2 x 10 <sup>-7</sup>	--
MgF <sub>2</sub> /DMF	8.3 x 10 <sup>-7</sup>	--
MgF <sub>2</sub> /AN	3.2 x 10 <sup>-6</sup>	--

---

III-D. Electrolyte Conductivity. When electrochemical measurements are performed, the specific conductance is routinely measured so appropriate corrections for iR drop can be made. This data, collected since the beginning of work under the current contract, has been examined for propylene carbonate solutions and is shown in Table 14, below.

We show only the equivalent conductance since this is the transport parameter of major importance.

Table 14  
 Equivalent Conductance in Propylene Carbonate  
 Equivalent Conductance ( $\text{ohm}^{-1} \text{cm}^2 \text{equiv.}^{-1}$ )  
 at concentration indicated:

Solute	1.0 M	0.2 M	0.15 M	0.10 M	0.05 M	0.02 M
LiClO <sub>4</sub>	5.5	15.4	16.4	17.5	20.7	23
LiBF <sub>4</sub>	3.8	--	--	16.2	19	19.5
LiAlCl <sub>4</sub>	--	--	--	20.2	--	--
LiI	--	--	--	18.8	--	--
LiBr	--	--	--	12.4	--	--
LiCl	--	--	--	--	3.9	--
AgClO <sub>4</sub>	--	--	--	21.5	--	25
KI	--	--	--	21	--	--
MoPF <sub>6</sub> <sup>*</sup>	--	20	--	--	--	--
Pr <sub>4</sub> NBF <sub>4</sub> <sup>**</sup>	--	--	--	24.4	--	--
Pr <sub>4</sub> NPF <sub>6</sub>	--	--	--	13.3	--	--
Pr <sub>4</sub> NI	--	--	--	12.2	--	--
MgCl <sub>2</sub>	--	--	--	--	20.6	--

\* Morpholinium hexafluorophosphate

\*\* n-propyl ammonium salts

It is of some interest to compare these values with the calculated limiting equivalent conductance, using Walden's rule, whereby  $\Lambda_{\infty}(\text{P.C.}) = (\eta(\text{H}_2\text{O}) / \eta(\text{P.C.})) \cdot (\Lambda_{\infty}(\text{H}_2\text{O}))$

which, at 25° C is; for LiClO<sub>4</sub>.

$$\Lambda_{\infty}(\text{P.C.}) = (0.8937/1.75) \cdot (104) = 52 \text{ ohm}^{-1} \text{ cm}^2 \text{ equiv}^{-1}.$$

III-E Kinetic Studies. There is, as yet, very little that can be said about the electrokinetics of the electrode processes. For the cathodes, such as  $\text{CuF}_2$ , the electrodes are not sufficiently well-characterized to allow separation of the various polarization terms.

The lithium anode also presents problems. As discussed in an earlier section of this report, standard steady state current-potential measurements do not give a valid representation of electrokinetic parameters. The shape of a chronopotentiogram has some significance in reflecting electrokinetic parameters. We consider two cases, Case I: The reversible, one-electron reduction of lithium ions to the metal, and Case II: The totally irreversible one-electron reduction of lithium ions.

For each case we consider the observed potential,  $E$ , as a function of the concentration of lithium ions at the electrode surface,  $C$ , and the bulk concentration,  $C^0$ .

$$\text{Case I: } E = E_{\text{OCV}} + \frac{RT}{F} \ln (C/C^0), \text{ the Nernst expression} \quad (1)$$

$$\text{Case II: from } i = i_0 \frac{C}{C^0} e^{-\frac{\alpha F}{RT}(E - E_{\text{OCV}})}$$

where  $i_0$  is the exchange current density, and  $\alpha$ , the transfer coefficient; we write:

$$E = E_{\text{OCV}} + \frac{RT}{\alpha F} \ln (C/C^0) - \frac{RT}{\alpha F} \ln (i/i_0) \quad (2)$$

In the absence of supporting electrolyte, the observed potential will be more negative by an additional amount,  $\frac{RT}{F} \ln (C/C^0)$ , which, as discussed in the First Quarterly Report, may be conveniently considered to be the  $iR$  drop generated across the diffusion layer, through the decreasing ionic concentration and resultant decreased conductance.

The important term,  $C/C^0$ , is, for chronopotentiometric measurements, given by:

$$C/C^0 = 1 - t^{1/2}/T^{1/2} \quad (3)$$

where  $t$  is the elapsed time and  $T$  is the transition time.

It is apparent that a plot of the measured potential,  $E$ , vs. the logarithm of the term,  $1 - t^{1/2}/T^{1/2}$  will provide useful information. We consider the slope of  $\log_{10}(1 - t^{1/2}/T^{1/2})$  vs.  $E$ , and the extrapolation to  $t = 0$ , for the two cases; and we include the correction for  $iR$  drop across the diffusion layer discussed above:

$$\text{Case I: Slope} = \frac{(2)(2.303)(RT)}{F} = 0.118 \text{ V} \quad (4)$$

$$\text{Extrapolation to } t = 0: E = E_{\text{OCV}} \quad (5)$$

$$\text{Case II: Slope} = \frac{(2.303)(RT)}{F} + \frac{(2.303)(RT)}{\alpha F} = 0.059(1 + 1/\alpha) \quad (6)$$

$$\text{Extrapolation to } t = 0: E = E_{\text{OCV}} - \frac{0.059}{\alpha} \log\left(\frac{i}{i_c}\right) \quad (7)$$

Naturally, such measurements are, in fact, invalid for reactions taking place on solid electrodes, since the character of the electrode surface changes so markedly during the course of the chronopotentiometric run. It is, however, of interest to note that, for the lithium deposition, we consistently observe that the extrapolation normally results in  $E = E_{\text{OCV}}$  (at  $t = 0$ ), which suggests that the exchange current must be quite large. However, the slopes are always much larger than 0.118 V, as would be predicted for a reversible, one-electron reduction. Values for the slope of 0.4 to 1 V are obtained, which, according to Equation 6, would correspond to transfer coefficients of from 0.17 down to 0.06. These clearly are unreasonably small.

In fact, we believe that the apparent large slopes arise from the growth of resistive films at the electrode which increase the  $iR$  term during the

course of the chronopotentiometric run. It would be of interest to perform chronopotentiometric measurements using mercury pool electrodes, where surface effects might be expected to be less marked.

In conclusion, while we believe detailed kinetic studies of the lithium deposition are of interest, one must not anticipate easy interpretation of experimental results. At present we believe more useful information would be obtained by X-ray or electron microscopic examination of the electrode during cathodization and by consideration of the electrical double layer and the effects on electrode processes in a solvent such as propylene carbonate, where excess electrolyte is not present. In our work we shall continue to be interested in the more practical aspects of the lithium electrode, and in particular, with the cyclability.

#### IV. SUMMARY AND CONCLUSIONS. FUTURE WORK

Reduction behavior is most complex and electrochemical measurements may likely reflect surface effects and impurities rather than the inherent potentialities of the system. This will be investigated in more detail concurrently with vapor phase chromatographic analysis of the total electrolyte.

The study of cathode materials is even more complex. There are marked differences observed in the cathodic discharge of  $\text{AgCl}$  and  $\text{CuF}_2$  in different electrolytes. In the absence of sufficient structural definition for porous electrodes it is presently impossible to give a meaningful explanation for these differences. Further discharge studies will be performed in an attempt to determine just what interactions are involved that prevent efficient discharge at satisfactorily high current densities. We believe that a primary electrode which discharges with electrokinetic reversibility will inherently be cyclable, and are, at present, less concerned with the possibility or, indeed, even the necessity for the cathode anion to be soluble.

The effect of impurities has, to date, been given little attention by any of the several groups working in the field of high energy density non-aqueous cells. We have begun to concentrate more on this area since we believe that impurities often are solely responsible for both bad and good results obtained in different studies. We have characterized the essential electrochemical behavior of the system sufficiently well so that the development of meaningful correlations between impurities and the observed electrochemical behavior can be expected.

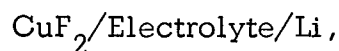
Finally, more serious consideration must be given to ultimate cell construction parameters in order to have some guideline by which the results of screening experiments may be evaluated. Cell construction is also a necessary by-product of basic theoretical work. We are interested in the effects observed in "starved" electrolytes, and do not believe that results obtained



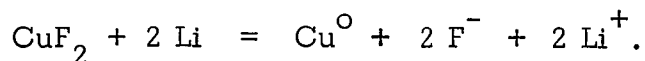
on single electrodes, operating in a large excess of electrolyte, can necessarily be used to predict with any accuracy the results expected in starved electrolytes. Our future work in cell development will continue to be oriented towards an understanding of the basic problems.

## APPENDIX I: Hypothetical Cell Model

In order to provide some focus for screening studies and to insure that the experiments will be performed under relevant conditions, it is desirable to consider possible cells. In this discussion we consider the following cell:



which is assumed to discharge by the reaction:



We consider a miniature cell employing two  $1 \text{ cm}^2$  electrodes facing each other across the electrolyte. Alkaline secondary cell electrodes have capacities of 10 to 100 mA-hr  $\text{cm}^{-2}$ . It is then reasonable to assume that one may construct a  $\text{CuF}_2$  electrode with 10 mA-hr  $\text{cm}^{-2}$  capacity. If the lithium electrode has an equal capacity we may calculate the total weight of active material:

$$\text{Weight} = \frac{(0.01 \text{ A-hr cm}^{-2}) (3600 \text{ sec hr}^{-1}) (116 \text{ g M}^{-1})}{(2 \times 10^5 \text{ C M}^{-1})} = 0.0208 \text{ g cm}^{-2}$$

The term,  $116 \text{ g M}^{-1}$ , is the weight of one mole of  $\text{CuF}_2$  and the requisite two moles of lithium. The term  $2 \times 10^5 \text{ CM}^{-1}$ , is twice the Faraday, since two electrons pass per mole of  $\text{CuF}_2$ .

Let it be assumed that these two  $1 \text{ cm}^2$  electrodes are separated by an amount of electrolyte equal weight, 0.0208 g, and that this electrolyte has a density of  $2 \text{ g cm}^{-3}$ . The thickness of the electrolyte separating the two electrodes is then:

$$\text{Distance} = \frac{(0.0208 \text{ g})}{(2 \text{ g cm}^{-3}) (1 \text{ cm}^2)} = 0.0104 \text{ cm (4 mils)}$$

This is very thin, but not unreasonable.

Finally, we calculate the resistance through this film of electrolyte, assuming a specific resistance of  $10^2 \text{ ohm-cm}$ .

$$\text{Resistance} = \frac{(10^2 \text{ ohm-cm}) (0.0104 \text{ cm})}{(1 \text{ cm}^2)} = 1.04 \text{ ohm.}$$

At the one hour rate,  $10 \text{ mA cm}^{-2}$ , which would be realized for the discharge of a 3 V cell through a 300 ohm load, the  $iR$  drop in the cell is only about 0.01 V.

It is of further interest to consider the number of ions in the electrolyte. We assume a 5 M, 1:1, univalent electrolyte. The volume,  $0.0104 \text{ cm}^3$ , times the concentration,  $5 \times 10^{-3} \text{ M cm}^{-3}$ , gives  $5.2 \times 10^{-5}$  moles of each ion. When the cell discharges by the above reaction the number of moles of ions formed at each electrode may be calculated:

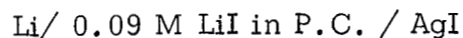
$$\begin{array}{l} \text{Moles of ions} \\ \text{released at} \\ \text{each electrode} \end{array} = \frac{(0.01 \text{ A-hr}) (3600 \text{ sec hr}^{-1})}{(1 \times 10^{-5} \text{ C M}^{-1})} = 36 \times 10^{-5} \text{ moles.}$$

Since ions produced at each electrode must be neutralized as they are formed, and since the number of ions initially present in the electrolyte is not sufficient to provide complete neutralization of all the ions produced on discharge, it is apparent that there must be effective ionic transport from one electrode to the other. Clearly, increasing the volume of electrolyte to the point where enough ions are initially present to neutralize the ions formed at each electrode, will result in too high a weight of electrolyte and resultant decrease in energy density. The necessity for ionic transport between the two electrodes to occur is, apparently, not usually a problem in aqueous cells.

It is, we believe, most desirable that the limitations of such a model be explored. The degree to which such limitations are understood is, in fact, an index to the state of the art of non-aqueous cell construction.

## APPENDIX II: EMF Measurements in Propylene Carbonate

We consider the cell:



The potential of this cell is related to the free energy for the reaction:

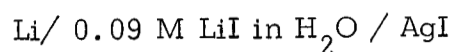


by:

$$-nFE_1 = G_{\text{LiI(P.C.)}}^{\circ} + RT \ln a_{\text{LiI(P.C., 0.09 M)}} - G_{\text{AgI(c)}}^{\circ} \quad (2)$$

where  $G_{\text{LiI(P.C.)}}^{\circ}$  is the free energy of formation of a solution of LiI in propylene carbonate at unit activity,  $a_{\text{LiI(P.C., 0.09 M)}}$  is the activity of the 0.09 M solution, and  $G_{\text{AgI(c)}}^{\circ}$  is the free energy of formation of crystalline silver iodide.

We next consider the potential of the cell:



which is given by:

$$-nFE_2 = G_{\text{LiI(H}_2\text{O)}}^{\circ} + RT \ln a_{\text{LiI(H}_2\text{O, 0.09 M)}} - G_{\text{AgI(c)}}^{\circ} \quad (3)$$

We subtract equation 3 from equation 2; and express the activity,  $a$ , as the product of an activity coefficient,  $\gamma$ , and the concentration,  $C$ , in moles per liter:

$$nF(E_2 - E_1) = G_{\text{LiI(P.C.)}}^{\circ} - G_{\text{LiI(H}_2\text{O)}}^{\circ} + RT \ln(\gamma_{\text{P.C.}} / \gamma_{\text{H}_2\text{O}}) \quad (4)$$

We express the free energy in terms of enthalpy and entropy, obtaining:

$$\begin{aligned} nF(E_2 - E_1) = & H_{\text{LiI(P.C.)}}^{\circ} - H_{\text{LiI(H}_2\text{O)}}^{\circ} \\ & + T(S_{\text{LiI(H}_2\text{O)}}^{\circ} - S_{\text{LiI(P.C.)}}^{\circ}) + RT \ln(\gamma_{\text{P.C.}} / \gamma_{\text{H}_2\text{O}}) \end{aligned} \quad (5)$$

The measured potential,  $E_1$ , in 0.09 M LiI in P.C. was +2.45 V. The calculated value of  $E_2$  in 0.09 M LiI in water is +3.03 V. Thus the left hand term is  $13.3 \text{ kcal M}^{-1}$ . It is, we believe, reasonable to assume that the contribution of the last two terms in the right hand side of equation 5 is sufficiently less than the differences in enthalpies of formation, that one may approximate:

$$H^{\circ}_{\text{LiI(P.C.)}} = H^{\circ}_{\text{LiI(H}_2\text{O)}} + 13.3 \text{ kcal M}^{-1}. \quad (6)$$

The same expression will obtain for the differences in the heats of solution:

$$\begin{aligned} \Delta H_{\text{LiI(P.C.)}} &= \Delta H_{\text{LiI(H}_2\text{O)}} + 13.3 \text{ kcal M}^{-1} & (7) \\ &= -18.57 \quad + 13.3 \quad = -5.6 \text{ kcal M}^{-1}. \end{aligned}$$

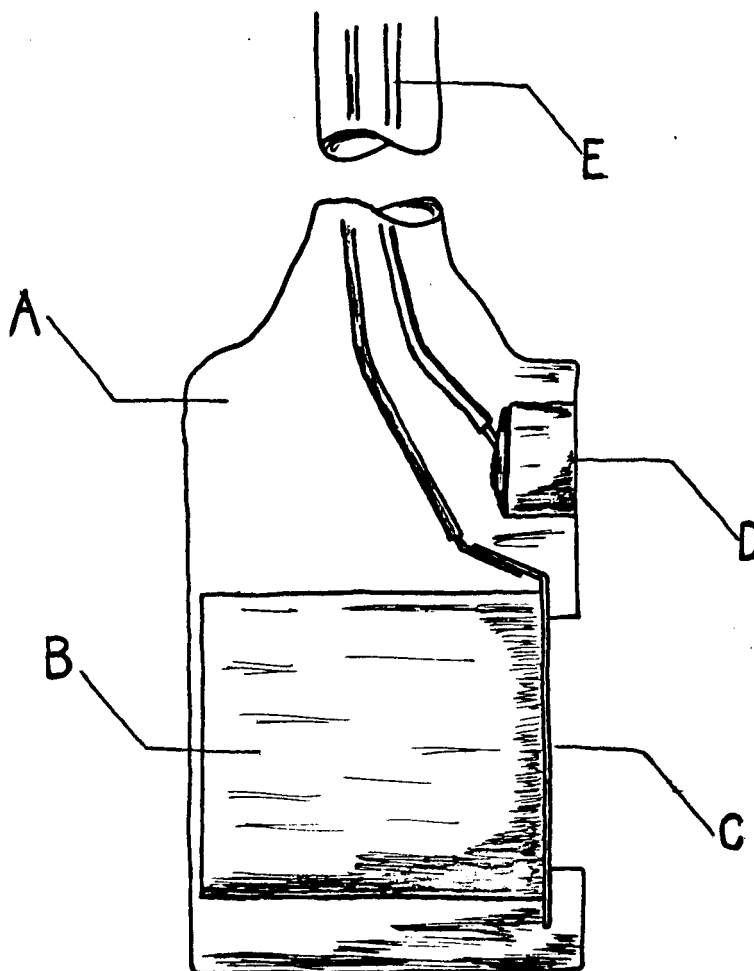
### APPENDIX III: Cathode Support Structure

The electrode support structure used in our work is shown in Figure 26. This is a side view of the structure. The stainless steel rod, to which has been attached a piece of platinum foil, as well as the silver disc reference electrode are sealed in epoxy. The depth of the recessed cavity is controlled by sealing a disc of zinc on top of the platinum. When the matrix has hardened the zinc is dissolved in dilute hydrochloric acid, forming the cavity, into which is pressed the electrode mix.

The electrodes were "calibrated", following the procedure outlined in the First Quarterly Report. A 0.01 M aqueous silver nitrate solution with a specific resistance of 769 ohm-cm was used for the measurements. The completed electrode structure was placed in the solution and the platinum substrate cathodized at various currents (1 - 5 mA). The potential was recorded oscillographically. Plots of current versus potential were linear, and the effective resistance determined from the slope of potential versus current. For example, in a typical calibration a plot of potential versus current gave an effective resistance of 331 ohm. Since the effective resistance is related to the specific resistance of the solution by:

$$R_{\text{effective}} = \frac{R_{\text{specific}} \text{ (ohm-cm)} \cdot d_L \text{ (cm)}}{A \text{ (cm}^2\text{)}}$$

And the calculated ratio of  $d_L/A$  is thus  $331/769 = 0.43$ . This factor may then be used directly to calculate the effective resistance for other solutions when the specific resistance is known.



- A = epoxy matrix
- B = stainless steel rod
- C = platinum foil
- D = silver disc reference electrode
- E = electrical leads

Epoxy matrix is about 1" in diameter and 1/2 " thick. Recessed cavity area is about 0.8 - 0.85 cm<sup>2</sup>.

Figure 26